

AD A089962

FAA-EE-80-09A

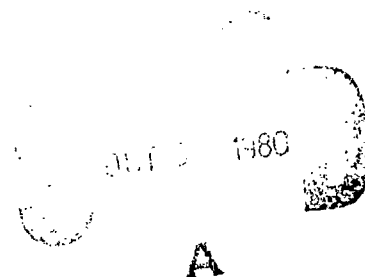


U.S. Department
of Transportation
**Federal Aviation
Administration**

IMPACT OF AIRCRAFT EMISSIONS ON AIR QUALITY IN THE VICINITY OF AIRPORTS

Volume I: Recent Airport Measurement Programs,
Data Analyses, and Sub-Model Development

Office of Environment
and Energy
Washington, D.C. 20591



July 1980

R.J. Yamartino
D.G. Smith
S.A. Bremer
D. Heinold
D. Lamich
B. Taylor

Document is available to the public through
the National Technical Information Service,
Springfield, Virginia 22161

DDC FILE COPY

1. Report No. FAA-EE-80-09A	2. Government Accession No. AD-A089 962	3. Recipient's Catalog No. 11
4. Title and Subtitle Impact of Aircraft Emissions on Air Quality in the Vicinity of Airports, Volume I: Recent Airport Measurement Programs, Data and Sub-Model Development.		5. Report Date July 1980
7. Author(s) R.J. Yamartino, D.G. Smith*, S.A. Bremer, D. Heindol*, D. Lamich, and B. Taylor*		6. Performing Organization Code 41
9. Performing Organization Name and Address Argonne National Laboratory Energy and Environmental Systems Division 9700 S. Cass Avenue Argonne, Illinois 60439		8. Performing Organization Report No. 11-111
12. Sponsoring Agency Name and Address U.S. Department of Transportation Federal Aviation Administration Office of Environment and Energy Washington, D.C. 20591		10. Work Unit No. (TRAIS) 11. Contract or Grant No. DOT-FA77WAI-736
15. Supplementary Notes *Affiliated with Environmental Research and Technology, Inc. 696 Virginia Road Concord, Massachusetts 01742		13. Type of Report and Period Covered Final Report January 1978 - July 1980
16. Abstract This report documents the results of the Federal Aviation Administration (FAA)/ Environmental Protection Agency (EPA) air quality study which has been conducted to assess the impact of aircraft emissions of carbon monoxide (CO), hydrocarbons (HC), and oxides of nitrogen (NO _x) in the vicinity of airports. This assessment includes the results of recent modeling and monitoring efforts at Washington National (DCA), Los Angeles International (LAX), Dulles International (IAD), and Lakeland, Florida airports and an updated modeling of aircraft generated pollution at LAX, John F. Kennedy (JFK) and Chicago O'Hare (ORD) airports. The Airport Vicinity Air Pollution (AVAP) model which was designed for use at civil airports was used in this assessment. In addition the results of the application of the military version of the AVAP model the Air Quality Assessment Model (AQAM), are summarized.		14. Sponsoring Agency Code

Both the results of the pollution monitoring analyses in Volume I and the modeling studies in Volume II suggest that:

- o Maximum hourly average CO concentrations from aircraft are unlikely to exceed 5 parts per million (ppm) in areas of public exposure and are thus small in comparison to the National Ambient Air Quality Standard of 35 ppm.
- o Maximum hourly HC concentrations from aircraft can exceed 0.25 ppm over an area several times the size of the airport.
- o While annual average NO₂ concentrations from aircraft are estimated to contribute only 10 to 20 percent of the NAAQS limit level, these concentrations, when averaged over a one hour time period are estimated to produce concentrations as high as 0.5 ppm if one assumes that all engine produced NO is converted to NO₂ by the time these emissions reach places of public exposure. This value is at the upper end of the concentration range being considered for the short term NO₂ standard presently under review and can not be ignored. However a decision on the influence of aircraft emissions on a short term standard must await the release of this standard and the results of research under way to determine the rate at which engine produced NO converts to NO₂ in the ambient air.

This report, IMPACT OF AIRCRAFT EMISSIONS ON AIR QUALITY IN THE VICINITY OF AIRPORTS, is printed in two volumes with the following subtitles; VOLUME I: Recent Airport Measurement Programs, Data Analyses, and Sub-Model Development; and VOLUME II: An Updated Model Assessment of Aircraft Generated Air Pollution at LAX, JFK, and ORD.

17. Key Words Aircraft Emissions Dispersion Modeling Air Quality Impact of Aviation Airport Air Quality Monitoring		18. Distribution Statement This document is available to the public through the National Technical Information Service, Springfield, VA 22161	
19. Security Classif. (of this report) Unclassified	20. Security Classif. (of this page) Unclassified	21. No. of Pages 169	22. Price

PREFACE

This document has been prepared by the Energy and Environmental Systems Division of Argonne National Laboratory at the request of the Federal Aviation Administration. The report attempts to realistically simulate the air quality impact of aircraft in and around the airport property under adverse dispersion conditions. No attempt has been made to include the effect of non-aircraft sources.

A

TABLE OF CONTENTS

	<u>Page</u>
1 INTRODUCTION AND SUMMARY	1
1.1 INTRODUCTION.	1
1.2 OBJECTIVES.	4
1.3 APPROACH.	5
1.4 RESULTS	10
1.4.1 Carbon Monoxide.	10
1.4.2 Hydrocarbons	14
1.4.3 Oxides of Nitrogen	14
1.5 CONCLUSIONS AND RECOMMENDATIONS	16
2 HISTORICAL SURVEY OF AIRPORT AIR QUALITY STUDIES	23
2.1 HISTORICAL OVERVIEW	23
2.2 SUMMARY OF PREVIOUS AIRPORT MODELING AND MONITORING RESULTS	25
2.2.1 Carbon Monoxide Studies.	27
2.2.2 Hydrocarbon Studies.	29
2.2.3 Oxides of Nitrogen Studies	31
2.3 METEOROLOGICAL ASPECTS OF AIRPORT AIR POLLUTION WORST CASE ANALYSES.	35
3 THE WASHINGTON NATIONAL AIRPORT (DCA) STUDY.	43
3.1 INTRODUCTION.	43
3.2 THE DCA MONITORING PROGRAM.	43
3.3 HOURLY AVERAGE MONITORING DATA FOR CO	60
3.4 HOURLY AVERAGE MONITORING DATA FOR OXIDES OF NITROGEN	61
3.5 SUMMARY AND CONCLUSIONS BASED ON THE HOURLY AVERAGE CONCENTRATIONS.	83
3.6 ANALYSIS OF SINGLE EVENT DATA	83
3.6.1 Subjectively Analyzes Single-Event Data.	84
3.6.2 DCA Single Event Finding Program	85
3.6.3 DCA Research Model Results	87
4 ANALYSIS OF EXPERIMENTS AT DULLES INTERNATIONAL AIRPORT.	91
4.1 INTRODUCTION.	91
4.2 REGIONAL MEASUREMENTS	92
4.3 SOURCE FINDING APPLICATION AT DULLES.	92
4.3.1 Introduction	92
4.3.2 Model Development.	95
4.3.3 Model Application.	97
4.3.4 Model Results.	99
4.3.5 Conclusions.	99
4.4 THREE TOWER MEASUREMENTS OF CO.	101
4.5 PLUME RISE FROM JET AIRCRAFT DURING THE TAXI MODE	105
4.5.1 Introduction	105
4.5.2 Modeling Turbulent Jet Exhausts Without Plume Rise	106

TABLE OF CONTENTS (Cont'd)

	<u>Page</u>
4.5.3 Plume Rise Modeling	109
4.5.4 Event Modeling	110
4.5.5 The Ensemble Model	110
4.5.6 Results.	113
4.5.7 Conclusions.	118
4.6 RE-EXAMINATION OF DULLES SINGLE EVENTS (THC VS CO).	120
5 CARBON MONOXIDE MEASUREMENTS AT A HIGH ACTIVITY "FLY-IN" AT LAKELAND AIRPORT, FLORIDA.	123
5.1 INTRODUCTION.	123
5.2 APPROACH.	126
5.3 RESULTS	126
5.4 CONCLUSIONS	130
6 THE MEASUREMENT OF CO CONCENTRATIONS FROM QUEUING AIRCRAFT AT LOS ANGELES INTERNATIONAL AIRPORT.	135
6.1 INTRODUCTION.	135
6.2 APPROACH.	135
6.3 ANALYSIS.	137
6.4 MODELING CONSIDERATIONS	137
6.5 RESULTS	138
6.6 CONCLUSIONS	139
7 ACCURACY DEFINITION OF THE AIR QUALITY ASSESSMENT MODEL (AQAM) AT WILLIAMS AIR FORCE BASE.	147
7.1 OBJECTIVES.	147
7.2 APPROACH.	147
7.3 IMPACT OF AIRCRAFT ON LOCAL AIR QUALITY	148
7.4 PERFORMANCE OF THE MODEL.	151
7.5 DIFFICULTIES WITH THE THEORY VERSUS OBSERVATION COMPARISON.	153
7.6 CONCLUSIONS	155
8 REFERENCES	157

LIST OF TABLES

<u>No.</u>	<u>Title</u>	<u>Page</u>
1.1.	Summary of Recent Air Quality Experiments.	6
2.1a.	CO Measurement and Modeling Study Summary.	28
2.1b.	HC Measurement and Modeling Study Summary.	30
2.1c.	NO _x /NO ₂ Measurement and Modeling Study Summary	32
2.1d.	Reference Key for Measurement and Modeling Study Summary	33
2.2.	Frequency of Poor Atmospheric Dispersion Conditions at Five Major Airports.	37
2.3.	Annual Percentage Frequencies of Stable Stratification at LAX	39
2.4.	Annual Percentage Frequencies of Stable Stratification at DCA. All Hours	39
2.5.	Annual Percentage Frequencies of Stable Stratification at JFK. All Hours	40
2.6.	Annual Percentage Frequencies of Stable Stratification at ORD. All Hours	41
3.1a.	Air Quality Parameters Measured at Each Station.	45
3.1b.	List of Monitoring Equipment	46
3.2.	DCA Monitoring Experiment CO	52
3.3.	DCA Monitoring Experiment NO _x	64
3.4.	DCA Monitoring Experiment NO	65
3.5.	DCA Monitoring Experiment NO ₂	65
3.6.	Estimated Highest Hourly per Annum Concentrations for Oxides of Nitrogen (in ppm).	70
3.7.	Regressions of Hourly Average Concentrations Vs. Aircraft Departure Rate	81
3.8.	Annual NO ₂ Levels at Various Washington Area Locations	82
4.1.	Aircraft Engine Emission Parameters.	108
4.2.	Number of Events per Aircraft Type	114
4.3.	Ensemble Fit Parameters.	114
5.1.	Carbon Monoxide Concentrations During Different Operational Modes.	132
5.2.	Measured versus Theoretical Aircraft Plume Dispersion Rates.	133
7.1.	Williams AFB Aircraft Emissions Impact on Annual Average Hourly 6AM-6PM Concentrations.	150

LIST OF FIGURES

<u>No.</u>	<u>Title</u>	<u>Page</u>
1.1.	Analysis Procedure.	2
1.2.	Monitoring Locations at DCA. with the exception of site 2, positioned to monitor ambient background concentrations, the monitors were located to measure the impacts, as well as characterize the advection and dispersion, of pollution originating from the queuing mode under winds from the NNW thru NNE directions and from the takeoff mode under winds from the N thru E directions.	7
1.3.	NO _x Concentration Time Histories for Sites 1 and 3 for a Typical One Hour Period as Reconstructed from the High Sampling Rate DAS Tapes. Also shown are the computed background subtracted (dotted lines) and pulse integrated (shaded) time histories	8
1.4.	Cumulative Frequency Distributions of Hourly CO Concentrations at DCA Station 4. The three solid curves represent the total (1), background subtracted (2), and pulse integrated (3) CO signal components. The dashed lines are visual guides for estimating the range of expected worst-case, once per year concentrations. The estimated worst-case, aircraft related concentration of ~5 ppm suggests no violation of the 35 ppm NAAQS	12
1.5.	MODIFIED AVAP Simulation of "Worst Case" (E Stability, Westerly 2-Knot Wind, and an Equivalent Departure Rate of Approximately 30 B727 Aircraft, Each Queued for 8.2 Minutes) CO Conditions behind the Southern Runway Complex at LAX. Runways and Main Taxiway/Queueing Area shown as dotted lines. CO contour levels given in ppm and are found to be small relative to the 35 ppm NAAQS. Computation grid size = 0.05 mile.	13
1.6.	MODIFIED AVAP Simulation of "Worst Case" (E Stability, Westerly 2-Knot Wind, and Peak 8AM-9AM Departures and Queueing Emissions) HC Conditions at LAX. The area covered by the 0.25 ppm HC contour, corresponding to the 6AM-9AM Guideline limit for RHC, is found to be large compared to the size of the airport. Computation grid size = 1.0 mile	15
1.7.	Station 1 Average Pulse Integrated NO ₂ Concentration Versus Departure Rate at DCA. The slope of the regression line (solid line) times the average hourly departure rate of 10.1 aircraft impact of 5 ppb on the annual average NO ₂ nearby the runway. The annual average NAAQS for NO ₂ is 50 ppb.	17
1.8.	Cumulative Frequency Distributions of Hourly NO _x Concentrations at DCA Station 4. The three solid curves represent the total (1), background subtracted (2), and pulse integrated (3) NO _x signal components. The dashed lines are visual guides for estimating the high and low ranges of anticipated worst-case, once per year concentrations.	18

LIST OF FIGURES (Cont'd)

<u>No.</u>	<u>Title</u>	<u>Page</u>
1.9.	MODIFIED AVAP Simulation "Worst Case" (E Stability, Westerly 2-Knot Wind, and an Equivalent Departure Rate of Approximately 30 B727 Aircraft) NO _x Conditions behind a Typical Busy Runway Complex. Runways and Taxiways are shown as dotted lines. NO _x contour levels, given in ppm, suggest possible high NO ₂ concentrations but reactive plume calculation needed to confirm this. Computation grid size = 0.05 mile.	19
3.1.	Monitoring Site Locations at DCA. Sites were chosen to focus on the pollution clouds from the takeoff and queuing modes.	44
3.2a.	Synthesized Strip Chart from DAS Tapes for a Typical 2-hr Period of Northeast Winds Showing Noise and NO _x Signals.	47
3.2b.	Synthesized Strip Chart from DAS Tapes for a Typical 2-hr of the COP Episode Beginning 2100 February 22.	48
3.3.	Rapid Sampling Enables Confident Separation of Aircraft Produced and Background Signals.	49
3.4.	Synthesized Strip Charts of Hourly Average CO Concentrations, Wind Speed, and Wind Direction for the Period Jan. 24-Feb. 27, 1979. These averaged data are computed from 3-sec interval DAS data.. . . .	53
3.5.	Histogram of Hourly Average CO Concentrations at Station 6. Not Shown are Four Values Between 10 and 16.3 ppm.	54
3.6.	Cumulative Frequency Distributions of Hourly CO Concentrations at Stations 1, 4, and 6.	55
3.7.	Synthesized Strip Chart from DAS Tapes for the 8-hour Period Beginning 2100 February 22 and Including the Entire CO Episode.	56
3.8.	Cumulative Frequency Distributions of Hourly CO Concentrations at Station 1. The three curves are explained in the text.	58
3.9.	Cumulative Frequency Distributions of Hourly CO Concentrations at Station 4. The three curves are explained in the text.	59
3.10.	Cumulative Frequency Distributions of Hourly CO Concentrations at Station 6. The three curves are explained in the text.	60
3.11.	CO Concentrations Isopleths from Aircraft Operations on the Southern Runway Complex at LAX Under "Worst Case" Operations and Dispersion (i.e., E stability and a 2 knot wind from the West) Conditions. Computation Grid Size = 0.05 Miles.	62
3.12.	Cumulative Frequency Distributions of Hourly NO _x Concentrations at Stations 1, 3, 4 and 5. Dashed lines indicates instrument saturation.. . . .	66
3.13.	Cumulative Frequency Distributions of Hourly NO Concentrations at Stations 1 and 3. Dashed lines indicate instrument saturation.. . . .	67

LIST OF FIGURES (Cont'd)

<u>No.</u>	<u>Title</u>	<u>Page</u>
3.14.	Cumulative Frequency Distributions of Hourly NO ₂ (\equiv NO ₂ - NO) Concentrations at Stations 1 and 3	68
3.15.	Cumulative Frequency Distributions of Hourly Background Subtracted NO _x Concentrations at Stations 1, 3, 4 and 5	71
3.16.	Cumulative Frequency Distributions of Hourly Background Subtracted NO Concentrations at Stations 1 and 3	72
3.17.	Cumulative Frequency Distributions of Hourly Background Subtracted NO ₂ (\equiv NO ₂ - NO) Concentrations at Stations 1 and 3	73
3.18.	Cumulative Frequency Distributions of Hourly Integrated Pulse NO _x Concentrations at Stations 1, 3, 4 and 5	74
3.19.	Cumulative Frequency Distributions of Hourly Integrated Pulse NO Concentrations at Stations 1 and 3	75
3.20.	Cumulative Frequency Distributions of Hourly Integrated Pulse NO ₂ (\equiv NO _x - NO) Concentrations at Stations 1 and 3	76
3.21.	MODIFIED AVAP Simulation of "Worst Case" (E Stability, Westerly 2-Knot Wind and an Equivalent Departure Rate of approximately 30 B727 Aircraft) NO _x Conditions behind the Southern Runway Complex at LAX. Runways and Main Taxiway/Queueing Area shown as dotted lines. A departure rate of 30 aircraft/hour was assumed and should be compared to a peak DCA departure rate of about 25 aircraft/hour. NO _x contour levels, given in ppm suggest possibly high NO ₂ concentrations. Computation grid size = 0.05 mile	77
3.22.	The Mean Hourly Ratio of the Integrated Pulse Concentrations of NO and NO _x Versus Plume Transport Time	79
3.23.	Mean Hourly NO ₂ Concentration Versus Aircraft Departure Rate at DCA	80
3.24.	Observed versus Predicted Peak NO _x Concentrations at DCA.	89
4.1.	Regional Air Quality Monitoring Stations	93
4.2.	Background Stations.	94
4.3.	Computational Grid Superimposed on Map of Dulles International Airport.	98
4.4.	Source Finding Solution Contours for CO. Isopleths are proportional to the log ₁₀ of the CO emission density function found to give a best χ^2 fit to observed concentrations	100
4.5.	Peak CO Concentrations Vs. Sensor Intake Position.	102
4.6.	Concentration Measurement Parameters	104
4.7.	Coordinate System for Model.	107
4.8.	Frequency Distribution of Plume Rise Coefficient	115

LIST OF FIGURES (Cont'd)

<u>No.</u>	<u>Title</u>	<u>Page</u>
4.9.	Frequency Distribution of Power Law for Distance Dependence. . . .	117
4.10.	Scatter Plot Plus Projection Histograms for Observed Versus Calculated Peak CO at Ground Level Receptors ($z = 6$ ft.). The calculation uses equations 17-19 and the optimal parameters given in the text.	119
4.11.	Concentration Crossplot of CO vs THC from Taxiing Aircraft	121
5.1.	Aerial View of Lakeland Airport, Fla.	124
5.2.	Airport Operations During Easterly Winds - Lakeland Airport. . . .	125
5.3.	Airport Operations During Westerly Winds - Lakeland Airport. . . .	125
5.4.	Monitoring Sites - Lakeland Airport January 23-30, 1978.	125
5.5.	Monitoring Installation - Inside Automobile.	127
5.6.	Monitoring Installation - Outside Automobile	127
5.7.	Monitoring Installation - Non-mobile	127
5.8.	Trace of General Aviation Takeoff.	129
5.9.	Trace of B-25 Takeoff.	129
5.10.	Dispersion of Carbon Monoxide During Taxi and Takeoff - Lakeland Airport, Florida.	131
6.1.	Monitoring Site Locations.	140
6.2.	Monitoring Equipment	141
6.3.	Seven Airplane Queue	142
6.4.	Airplane Flow Diagram.	143
6.5.	Concentrations and Times in Queue.	144
6.6.	Reconciliation of Measured with Estimated Carbon Monoxide Concentrations During Aircraft Queuing at Los Angeles International Airport (LAX).	145
7.1.	Locations of the Five Ambient Air Quality Monitoring Trailers. . . .	149
7.2.	Cumulative Frequency Distribution for Observed and AQAM II Predicted CO at Station 1 -- 95% Confidence Bounds are Indicated.	152

1 INTRODUCTION AND SUMMARY

1.1 INTRODUCTION

The 1970 amendments to the Clean Air Act (U.S. Congress, 1970) directed the Environmental Protection Agency (EPA) to establish emission standards for aircraft and aircraft engines if such emissions are judged to cause or are likely to cause or contribute to air pollution which endangers the public health. The 1970 amendments also directed the EPA to conduct a study of the extent to which aircraft emissions affect air quality in Air Quality Control Regions (AQCRs) throughout the United States. Based upon information available in the early 1970's the EPA judged that aircraft and airports were then or were projected to be significant sources of emissions of carbon monoxide (CO), hydrocarbons (HC), nitrogen oxides (NO_x), and smoke in some of the AQCRs where the National Ambient Air Quality Standards (NAAQS) were being violated. Therefore, engine emission standards were promulgated on July 17, 1973 for Commercial and General Aviation aircraft. The basis for these emission standards was the air quality and technology assessments made during the early 1970's. Since that time major advancements have been made in the techniques for monitoring and modeling aircraft emissions and in the control of aircraft engine emissions, though this latter topic is beyond the scope of this report.

On March 24, 1978, a Notice of Proposed Rule Making (NPRM) was published in the Federal Register to announce the intention of the EPA to amend the 1973 engine emission regulation. Included in the NPRM was the establishment of an FAA/EPA air quality study to relate aircraft emissions to ambient air quality.

This report presents the results of this FAA/EPA air quality study to assess the impact of aircraft emissions of CO, HC, and NO_x at populated locations in the vicinity of airports. This assessment includes the results of the recent modeling and monitoring efforts at Washington National (DCA), Los Angeles International (LAX), Dulles International (IAD), and Lakeland Florida airports and a modeling update of aircraft generated pollution at Los Angeles International (LAX), John F. Kennedy (JFK), and Chicago O'Hare (ORD) airports, as pollution at these three airports was cited in the 1973 engine emission standards.

The study methodology is indicated in Figure 1.1. Measured air quality concentrations associated with the operation of commercial aircraft were both

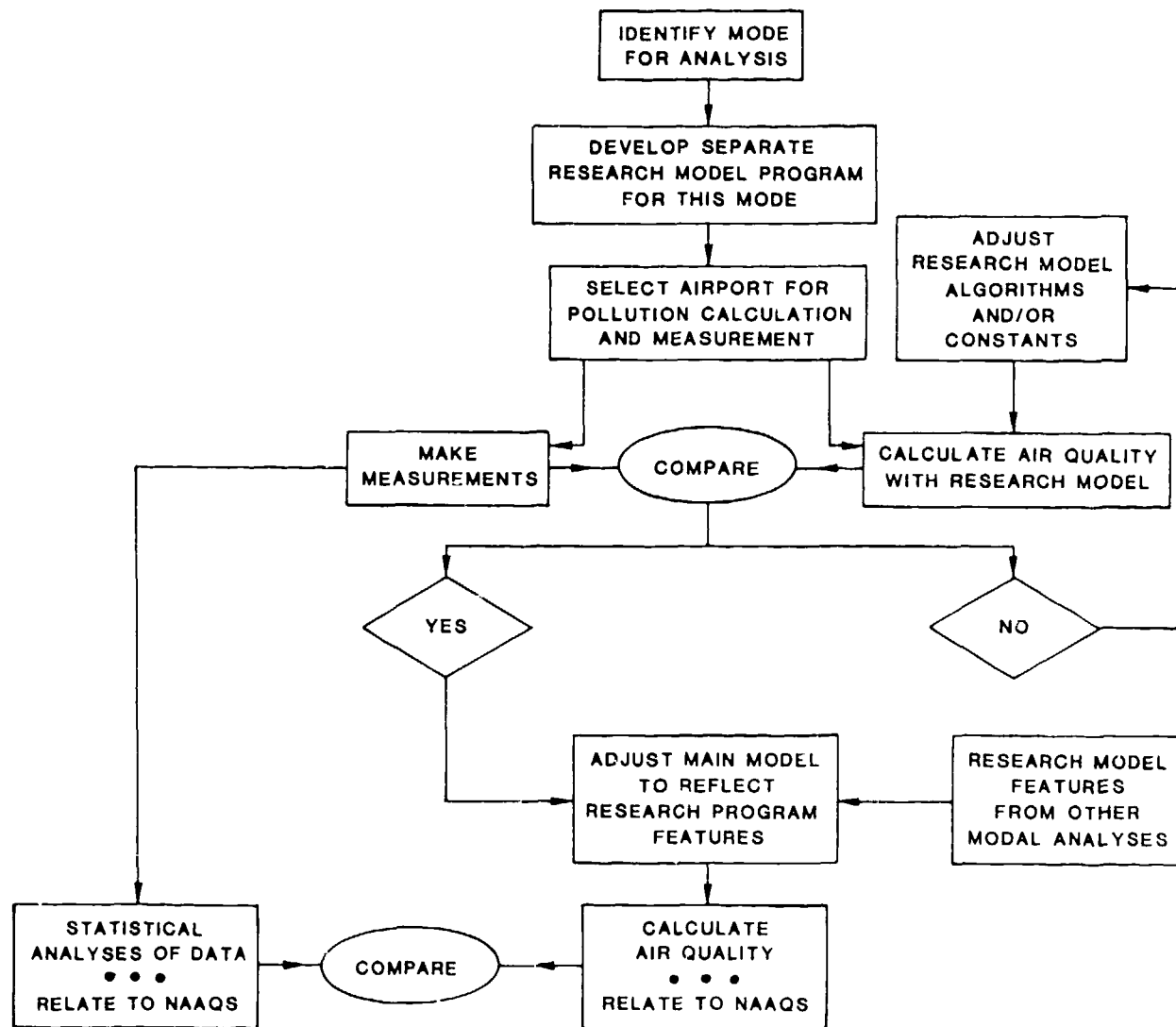


Fig. 1.1. Analysis Procedure

extrapolated to worst case conditions, as implied by the NAAQS, and also used to verify sub models. Features of these sub models were subsequently incorporated into a major airport model which was then used to reassess the impact of aircraft emissions on air quality at JFK, ORD, and LAX. In addition, the results of the modeling and monitoring of emissions from general aviation airports and the results of an airport model validation effort conducted at Williams Air Force Base are reported.

This report first presents a brief discussion of the history of air pollution measurements and the air quality models used in the EPA's most recent assessment of aircraft impacts as a basis for the NPRM. This discussion highlights the discrepancies between studies which have led to the present uncertainties about overall impacts of aircraft operations and the need for additional engine emission standards. Subsequent sections of the report discuss the recent monitoring and modeling studies which have been identified above, and the relationship of their results to these issues. It will be seen that one of the most difficult questions addressed, but not yet completely answered by these studies, is how significant the effect of enhanced initial dispersion of aircraft plumes is upon concentrations of pollutant reaching populated or public areas near an airport. Each of the recent studies sheds light on a facet of this problem, and leads to the development or refinements of more specific, sub-model components of the overall airport model via the methodology indicated in Figure 1.1. Review of the previous modeling efforts, as well as the results presented in this report, shows that the significance of these improvements is sometimes a matter of perspective. That is, if concentrations are predicted to be well below applicable standards by conservative screening models, identification of additional dilution factors is relatively unimportant. An underestimate of the source inventory, on the other hand, can lead to associated distrust of the capabilities of a pollutant dispersion model. Much of this volume and the supporting Airport Vicinity Air Pollution (AVAP) model calculations included in Volume II are, therefore, concerned with identifying worst case meteorological and aircraft operational conditions leading to the highest emission rates and concentrations of problem pollutants. In these cases, the accuracy and precision of modeling results supported by measurement data, can become a critical issue in defining the needs for additional standards.

Volume II contains the results of a detailed application of the updated AVAP model to LAX, JFK and ORD airports. The model incorporates the most recent submodels and sub-model parameters obtainable from the airport monitoring programs described herein, as well as the most recent updates to the theory of dispersion of atmospheric pollutants. The principal findings of Volume II have also been incorporated into this Summary.

1.2 OBJECTIVES

During the past several years a number of government agencies, including the EPA, FAA, and USAF have been engaged in a comprehensive program to assess the effects of aircraft emissions upon air quality. While the motivation to evaluate such impacts originated with the 1970 Amendments to the Clean Air Act, the March 24, 1978 Notice of Proposed Rule Making (NPRM), announcing the EPA's intention to modify the 1973 engine emission standards, provided a clear mandate to

- resolve the ambiguities of previous monitoring and modeling efforts,
- update airport dispersion modeling assessments to reflect recent modeling improvements, and
- measure pollutant levels near aircraft in a manner that would clearly determine aircraft emissions impact,

so that realistic engine emissions standards could be established on the basis of the best available information.

While the objective as stated above suggests a program of all-encompassing scope, it is useful at the outset to consider the limitations of this endeavor. The project concerns itself solely with the ground-level, air quality impacts of aircraft exhaust

- on or in the near vicinity of airports,
- in areas of possible public exposure, and
- relative to existing or potential National Ambient Air Quality Standards (NAAQS).

Thus, for example, this report is not concerned with stratospheric impacts, the hydrocarbon odor nuisance problem at airports, the combined effects of pollution from aircraft, access vehicles, and service vehicles, or the level

of pollution inside the passenger terminal, despite the fact that such considerations may have explicit or implicit effects on the determination of adequate aircraft emission standards.

1.3 APPROACH

The principal strategy was to assess the air quality impacts of aircraft exhaust through monitoring of aircraft pollution impacts within 0.5 km of the aircraft. This served the dual purpose of supplying actual measured impacts with which one could infer average and worst case⁺ pollutant concentrations and of providing a research grade data base with which one could investigate and parameterize the aircraft plume dispersion physics in order to improve the predictive accuracy of sub-models within an airport model, and hence, ultimately improve the predictive power of airport air quality assessment models. With one such improved model, AVAP, it was then possible to simulate worst case pollutant conditions at major U.S. airports: an objective that would have been unacceptably expensive to attain solely through ambient air monitoring programs.

The monitoring programs, that provided the basis for pursuit of the aircraft exhaust impact assessment objective through the above-described strategy, are summarized in Table 1.1. These experiments, described in this report and in other indicated documentation, share two important characteristics that set them apart from previous monitoring programs. First, they were designed to focus in on specific aircraft modes of operation. The orientation of receptors at Washington National (DCA), seen in Figure 1.2, provides an example of such a modal focus. Under winds from the NW-N directions, the pollution cloud from queueing aircraft is transported across the network of monitors while under winds from the NNE-SE directions, the plumes created by the high-thrust takeoff mode are sampled by the same monitors. Second, these experiments achieve a separation of aircraft pollution from other source related pollution via a multi-station receptor array either operating in a low-background environment, such as at Williams AFB, Arizona (Yamartino et al., 1980) or else sampling at a sufficiently high rate to

⁺"worst case" is generally taken here to indicate the highest hourly average concentration per annum or the meteorological and aircraft operations conditions leading to such concentrations.

Table 1.1. Summary of Recent Airport Air Quality Experiments

Airport	Source Categories Monitored	Duration or No. of Events	Pollutants Monitored (No. of Monitors)	Types of Aircraft	Relative Aircraft Activity	Pollutant Averaging Time	Results	Documentation
Dulles International	Airport Taxi Takeoff	1 year .150 events 50 events	CO(6), HC(2), NO _x (2) CO(15), HC(1) NO _x (3)	(Commercial)	Moderate N.A. N.A.	Hourly Cont. Cont.	Small Regional Impact Low CO + Plume Rise Model Prelim. Takeoff Model	T.R., FAA-AEQ-77-14 T.R., AMS-1 FAA-AEQ-77-14
Lake Land Florida	Taxi + Takeoff	1 week	CO(3)	General Aviation	Very High	Hourly + Cont.	Low CO Small dispersion rate	T.R. FAA-AEE-78-26 (pp 76-80)
Washington National	Queuing Takeoff	1 month 1 month	CO(4) NO _x (4), NO(2)	(B727) (B737) (DC9)	High	(Hourly + Cont.)	CO < 5 ppm Beyond 1000 ft. Signif. NO ₂ , Takeoff Plume Size Measured	T.R. T.R.
Los Angeles International	Queuing	1 week	CO(2)	(Commercial)	High	Cont.	Queue Model Low CO	T.R., APCA 80-3.5
Williams AFB	Airbase Taxi Takeoff	1 year	CO(5), THC(5) CH ₄ (5), NO(5) NO _x (5), SCAT(5)	(T37) (T38) (F5)	High	Hourly	AQAM Accuracy Determined	T.R., AFESC Report (in press) FAA-AEE-78-26 (pp 65-75) AMS-2

Symbols and Abbreviations

N.A. not applicable

T.R. this report

Cont. continuous or high sampling rate

AMS-1 Yamartino et al. AMS Fourth Symp. on

AMS-2 Yamartino and Lamich Turbulence, Diffusion, and

AQAM = Military Version of AVAP Air Pollution - Reno 1979

MONITORING LOCATIONS AT DCA FOCUSED ON QUEUEING AND TAKEOFF MODES

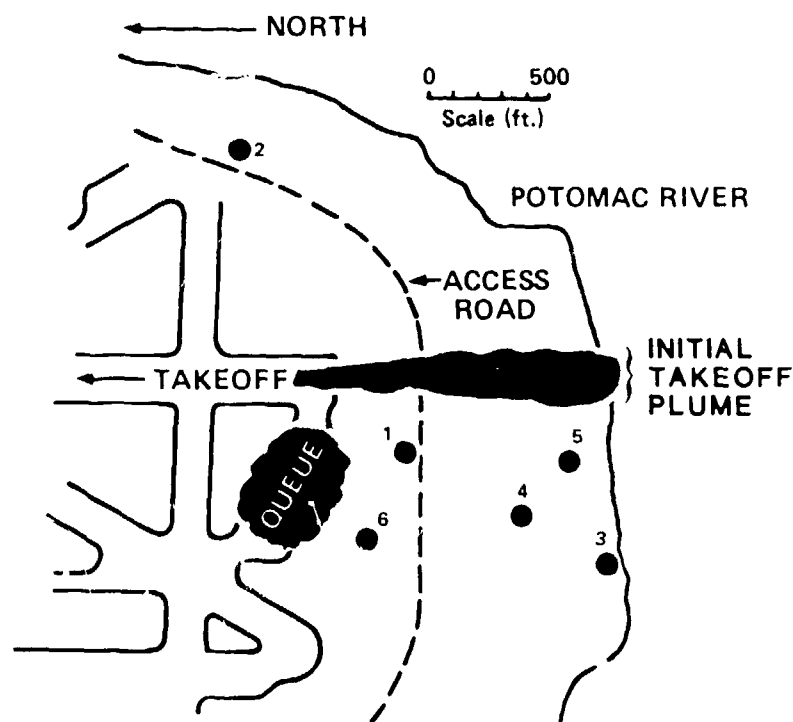


Fig. 1.2. Monitoring Locations at DCA. With the exception of site 2, positioned to monitor ambient background concentrations, the monitors were located to measure the impacts, as well as characterize the advection and dispersion, of pollution originating from the queuing mode under winds from the NNW thru NNE directions and from the takeoff mode under winds from the N thru E directions.

RAPID SAMPLING ENABLES CONFIDENT SEPARATION OF AIRCRAFT PRODUCED AND BACKGROUND SIGNALS

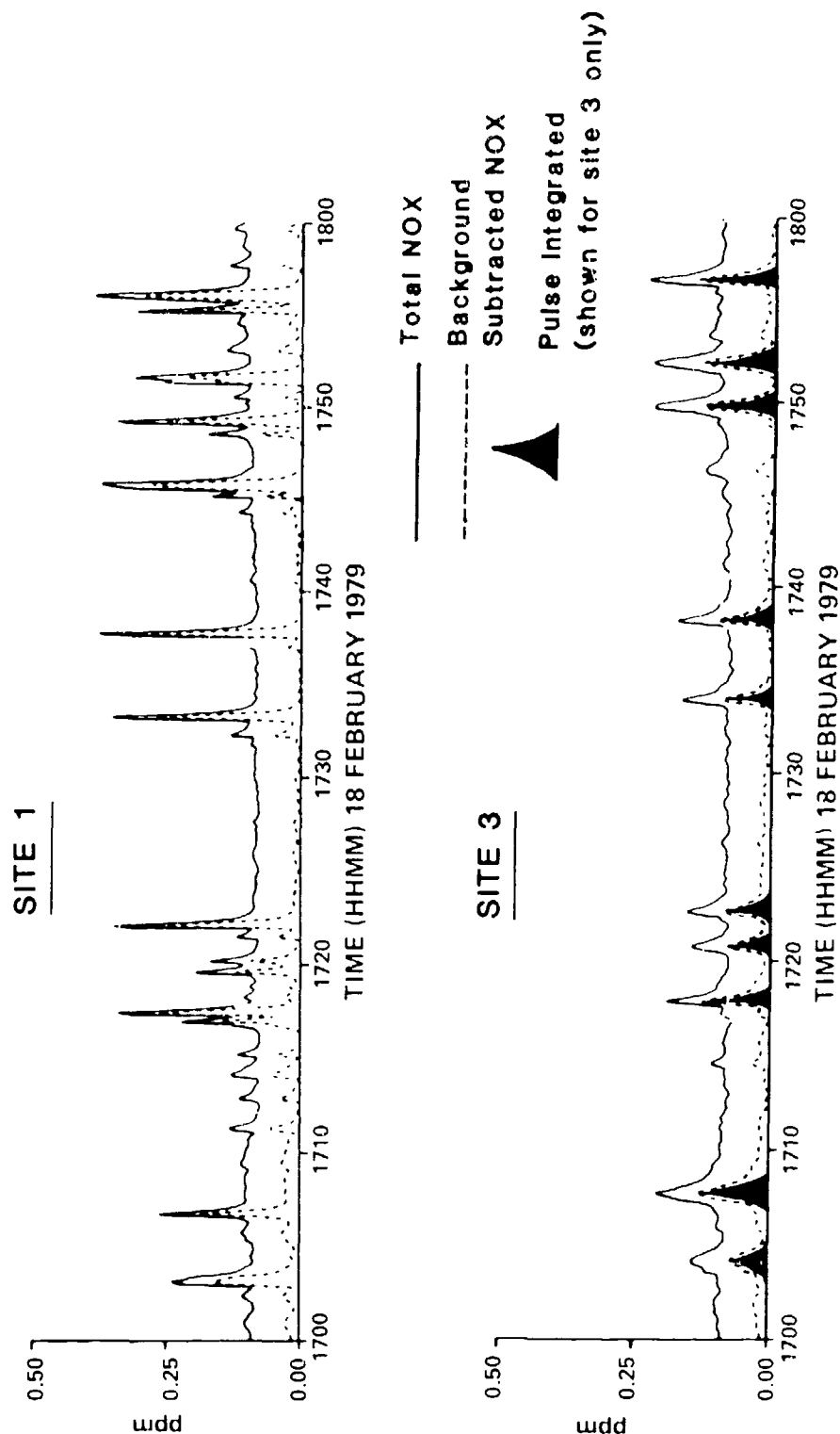


Fig. 1.3. NO_x Concentration Time Histories for Sites 1 and 3 for a Typical One Hour Period as Reconstructed from the High Sampling Rate DAS Tapes. Also shown are the computed background subtracted (dotted lines) and pulse integrated (shaded) time histories.

facilitate such a separation. The time history of NO_x pollution seen at two of the DCA monitors during a one hour period (Figure 1.3) illustrates the analysis possibilities created through this high sampling rate approach. Takeoff plume pollution, easily identified by the NO_x rise above background levels, are seen to disperse (i.e. reduce in peak concentration while spreading out in time) as they move from the nearby station 1 to the more distant station 3. The actual impact of these plumes may be estimated via a background subtraction (i.e. as seen by the dotted line) or through estimation of the summation of the areas under the major, aircraft related pulses (i.e. as indicated by the shaded areas) via a technique requiring a threshold concentration above background to be reached before inclusion of a particular pulse.*

In addition to the air monitoring programs considered above, improvements to the AVAP model and its predictive power resulted from a number of efforts, detailed in Volume II, that include:

- use of updated engine emission factors
- code modification to permit direct input of the hourly number of departures (previously computed on the basis of arrivals)
- use of airport specific times-in-mode for idle, taxi, and queueing that were observed during a three airport field study. These times often differed substantially from airport averaged, AP-42 LTO cycle times.

One of the more important findings of this AVAP modification and multi-airport analysis was that for worst case, "hot-spot" pollution assessments one need only consider the pollution from a single runway complex and the queueing area adjacent to it.⁺ These runway complexes are generally sufficiently well separated from one another that superposition of pollutants at the "hot-spot" from other complexes is negligible to first order. This observation should eliminate many needlessly repetitive analyses of similarly configured airports. It should further be noted that the USAF/USN sponsored, validation and accuracy evaluation program for the Air Quality Assessment Model (AQAM), provided accuracy measures for AQAM and its nearly identical civilian counterpart AVAP, that were previously only conjecture.

*These quantities will subsequently be referred to as "background subtracted" and "pulse integrated" concentrations.

⁺This characteristic subsequently referred to as "runway complex factorization."

1.4 RESULTS

Rather than to proceed from experiment to experiment, as is done in the text of the report, let us consider the various engine emitted pollutants and the information regarding those emissions' impacts as determined by these monitoring and modeling exercises.

1.4.1 Carbon Monoxide

Experimental and modeling efforts of the early 70's indicated that violations of the NAAQS one-hour CO standard of 35 ppm were indeed possible at airports. Measured and modeled peak hourly levels of 46 ppm and 24 ppm respectively at LAX (Platt et al., 1971), for example, suggested that aircraft emissions were a serious problem relative to the one-hour standard; however, a number of factors contributed to this misleading implication of aircraft including:

- aircraft source characteristics (i.e., initial plume volume and rise) were not understood and thus not modeled. Modeling of aircraft emissions neglecting initial dispersion can lead to arbitrarily high concentrations depending on source location.
- background concentrations were often not measured, making it difficult to isolate the aircraft or airport contributed concentrations from those of the surrounding region.
- building wake effects can greatly magnify the impact of the multitude of CO sources around the terminal. The modeling of such enhancing effects was (and still generally is because of the complexity) ignored.
- emissions from other sources, particularly service and access vehicles may dominate aircraft sources in the vicinity of the terminal where the highest concentrations were observed.
- peak observed concentrations were underpredicted by a factor of 2-3.

This latter consideration of 2-3-fold model underprediction, coupled with the other uncertainties, particularly the unknown and unmodeled characteristics of the aircraft plume, certainly invited the speculation that aircraft were responsible for the modeling deficit and thus were the principal source.

The CO monitoring experiment along the main taxiway at Dulles International (Smith et al, 1977) was the first to isolate the impact of aircraft emissions alone and indicated that the initial turbulent mixing caused by the

plume plus the subsequent plume rise and accompanying enhanced vertical dispersion lead to rather low CO concentrations near the aircraft (excepting, of course, directly behind the engines). While peak instantaneous CO levels reached 10 ppm at the first monitor, located only 65m from the taxiway centerline, the maximum impact of a single aircraft to the hourly average concentration remained below 0.06 ppm at this distance. Thus, even adjacent to a busy taxiway, it would be unlikely for hourly average CO concentrations to exceed several ppm.

Though substantially higher concentrations were anticipated downwind of a group of queueing aircraft, the recent 5-day experiment at Los Angeles (Section 6) failed to indicate peak hourly CO in excess of 3 ppm at a distance of 200-300 meters from the closest of the queueing aircraft.

Perhaps the most convincing evidence concerning peak hourly CO from taxiing and queueing aircraft comes from consideration of the cumulative frequency distributions (CFDs) of CO levels observed during the month-long DCA experiment. Keeping in mind the large error which is possible when estimating the worst case once per year on the basis of a one month data sample, Figure 1.4 indicates that, under the assumption of log-normality of the hourly CO frequency distribution, maximum hourly per annum CO levels of 10 ppm may be expected 300m downwind of the aircraft queue, with a probable maximum of ~5 ppm due to aircraft alone. Similar analyses applied to data from station 1, located only 100-150m from the queueing aircraft, suggests an aircraft attributable maximum hourly level of 10 ppm; however, it is unlikely that the general public would be sufficiently close to queueing aircraft to receive that CO dose.

Finally, we note that the AVAP model, adjusted to include the plume dynamical effects measured during the Dulles experiments, predicts "worst case" CO concentrations of 7 ppm 100-300 meters downwind of queueing aircraft at LAX. Figure 1.5 shows the isopleths resulting from the calculation, and one observes that levels of public exposure exceeding 6 ppm would be unlikely during this "worst case" scenario.

One notes that the combined effects of the phased daily cycles of aircraft operations and meteorological parameters related to dispersion, and wind direction variability make violation by aircraft exhaust plumes alone improbable. The single violation of the 8-hour standard of 9 ppm observed at DCA was accompanied by simultaneous violation over much of the Washington area.

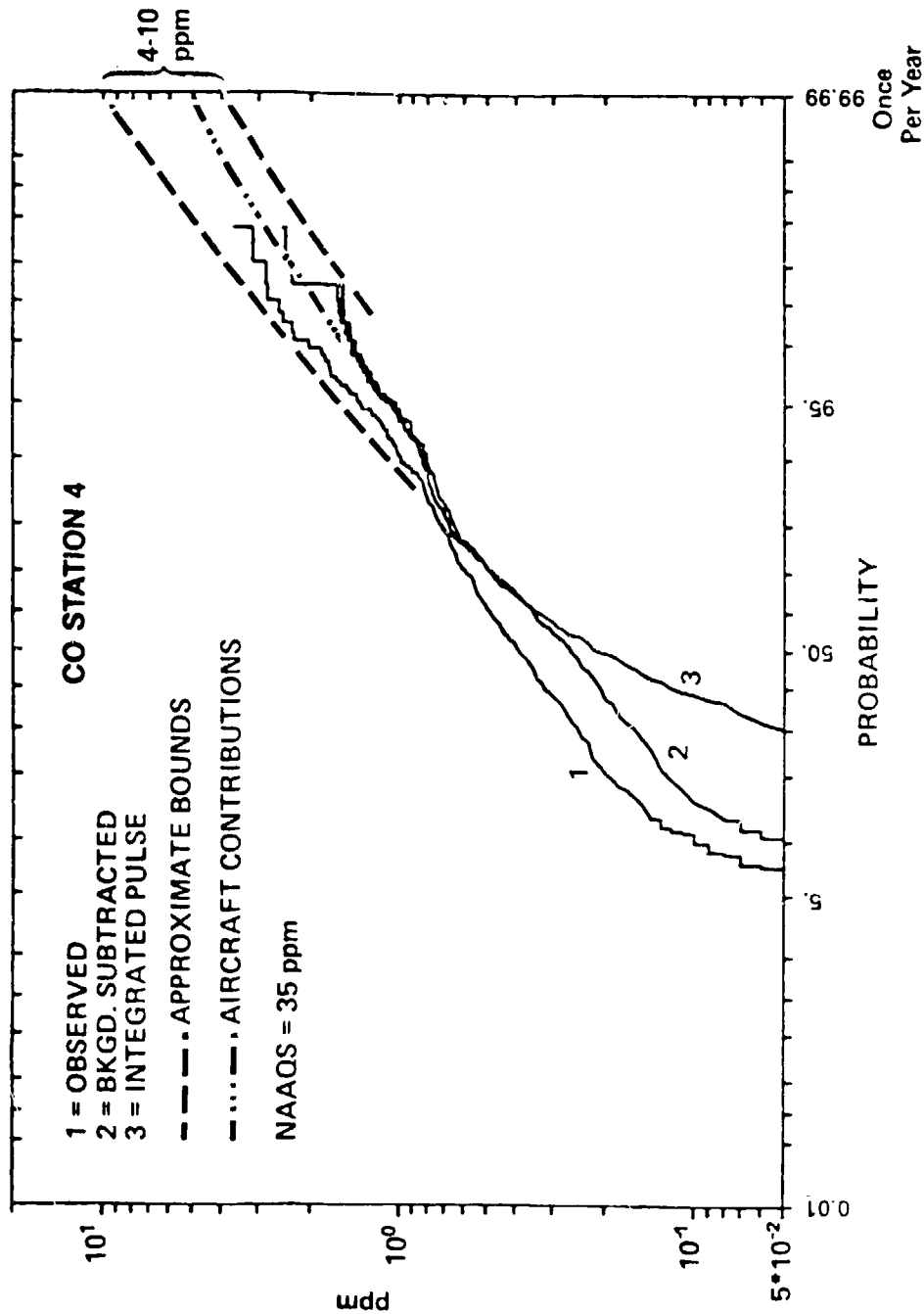


Fig. 1.4. Cumulative Frequency Distributions of Hourly CO Concentrations at DCA Station 4. The three solid curves represent the total (1), background subtracted (2), and pulse integrated (3) CO signal components. The dashed lines are visual guides for estimating the range of expected worst-case, once per year concentrations. The estimated worst-case, aircraft related concentration of 35 ppm suggests no violation of the 35 ppm NAAQS.

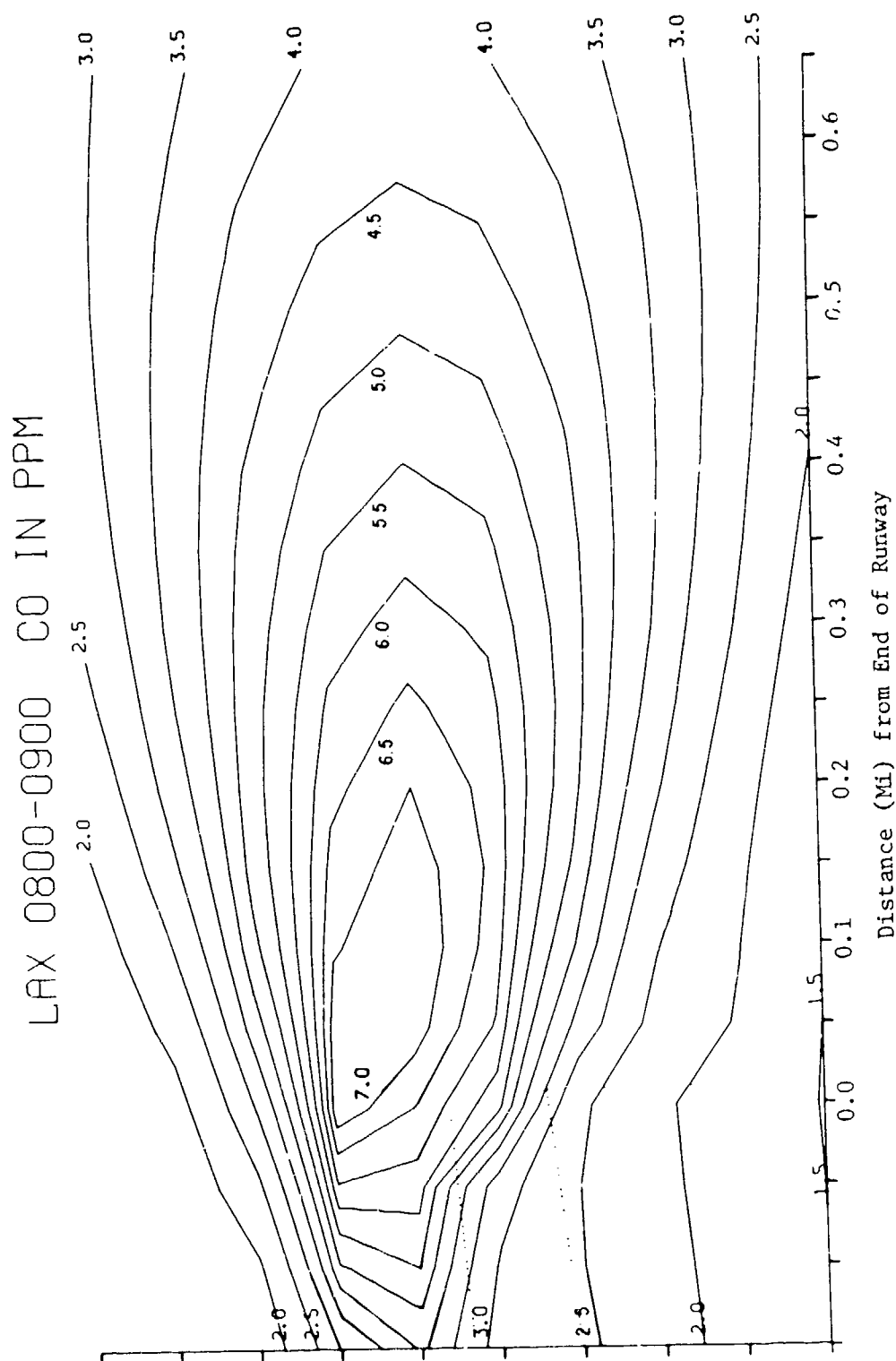


Fig. 1.5. MODIFIED AVAP Simulation of "Worst Case" (E Stability, Westerly 2-Knot Wind, and an Equivalent Departure Rate of Approximately 30 B727 Aircraft, Each Queued for 8.2 Minutes) CO Conditions behind the Southern Runway Complex at LAX. Runways and Main Taxiway/Queuing Area shown as dotted lines. CO contour levels given in ppm and are found to be small relative to the 35 ppm NAAQS. Computation grid size = 0.05 mile.

1.4.2 Hydrocarbons

Hydrocarbon emissions are of concern as the presence of reactive hydrocarbon species are conducive to the subsequent formation of ozone. Motivation for control of aircraft emitted HC results partly from estimates that aircraft account for 1-3% of the total HC emitted in an Air Quality Control Region (AQCR) on an annual basis; thus, while aircraft are not a dominant source, they represent a significant source for control as they are comparable with many other source categories.

Measurements at Dulles and AVAP modeling agree that total HC concentrations, expressed as ppm equivalent methane (CH_4), correspond well in space, time, and magnitude with CO levels associated with these commercial aircraft. This is not particularly surprising since hydrocarbons and CO are both emitted during the same, low power setting, aircraft operational modes. Figure 1.6 shows the peak hourly total HC (THC) contour resulting from a "worst case" modeling of LAX during the 8-9AM period. Though restrictive considerations of the reactive (RHC) component and the three-hour average would act to somewhat reduce the area of this contour, it is still anticipated that the 0.25 ppm contour covers an area several times the airport size.

1.4.3 Oxides of Nitrogen

The issue of oxides of nitrogen (NO_x) impacts created by aircraft is, as with CO, a localized "hot-spot" problem related to existing and possible additional NAAQS for nitrogen dioxide (NO_2), and has been addressed primarily through the DCA monitoring program. Unfortunately the issue is further complicated by the fact that

- present and possible future NAAQS standards pertain to NO_2 levels and not NO_x levels. ($\text{NO}_x \approx \text{NO} + \text{NO}_2$)
- there is presently only an annual average NAAQS of 0.05 ppm NO_2 though a peak hourly standard in the range 0.2-0.5 ppm is currently being reviewed by the EPA
- plume dispersion, while reducing the concentration of inert species, will entrain more ambient oxidant resulting in further conversion of engine emitted NO to NO_2 ; thus, NO_2 levels will peak at some distance downwind of the aircraft
- the peak NO_2 attributable to aircraft is a function of existing ambient levels of NO, NO_2 , O_3 , and sunlight.

LAX 0800-0900 THC IN PPM

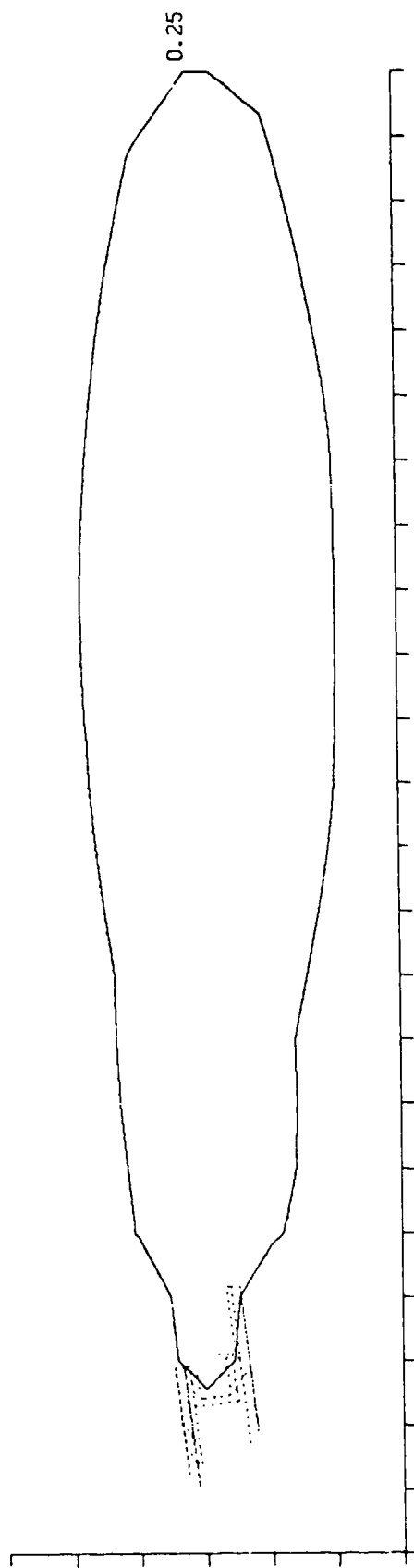


Fig. 1.6. MODIFIED AVAP Simulation of "Worst Case" (E Stability, Westerly 2-Knot Wind, and Peak 8AM-9AM Departures and Queueing Emissions) HC Conditions at LAX. The area covered by the 0.25 ppm HC contour, corresponding to the 6AM-9AM Guideline limit for RHC, is found to be large compared to the size of the airport. Computation grid size = 1.0 mile.

In order to determine the impact of aircraft emissions on annual average air quality for comparison with the annual NO_2 NAAQS, it was necessary to regress measured NO_2 concentration levels against airplane activity. Figure 1.7 shows this relationship for the pulse integrated NO_2 levels at Station 1. The statistical significance of the slope of the regression coupled with a regression "y" intercept consistent with zero enables one to confidently estimate the annual average aircraft impact. The projected annual average aircraft impact of 0.005 ppm (5 ppb) is small compared with the 0.05 ppm NAAQS.

This paucity of data results in greater uncertainties for estimation of maximum hourly average NO_x levels. Figure 1.8 indicates that, assuming log-normality of the hourly NO_x cumulative frequency distribution (CFD), maximum hourly per annum NO_x levels of 0.2 to 0.5 ppm due to aircraft operations alone may be expected several hundred meters downwind of the location where aircraft begin their takeoff roll. Depending on the oxidation rate of the aircraft emitted NO into NO_2 , NO_2 levels in excess of 0.2 ppm may materialize.

AVAP modeling of a typical busy commercial airport under worst case activity and dispersion conditions indicates (Figure 1.9) NO_x levels exceeding 0.5 ppm more than one-half mile from the end of the runway complex, but the key question is how these NO_x levels translate into NO_2 levels. The NO_2/NO_x ratio is a function of plume dispersion rate and transport time, sunlight intensity, and background levels of NO, NO_2 , and O_3 and a reactive plume calculation is required to obtain a more definitive prediction; however, using simple assumptions regarding the amount of NO_2 emitted directly by the aircraft, the rate of NO oxidation, and the ambient O_3 level, it is reasonable to expect several tenths of ppm of NO_2 at distances of possible public exposure. This is within the range of levels under consideration by the EPA as a possible short term NAAQS for NO_2 .

1.5 CONCLUSIONS AND RECOMMENDATIONS

Recent airport air quality monitoring studies at four airports suggest maximum hourly average CO concentrations of 5 ppm in areas of expected public exposure. These measurements and estimates based on extrapolation of measured results to probabilities corresponding to one hour per year suggest small likelihood of violating the 35 ppm NAAQS.

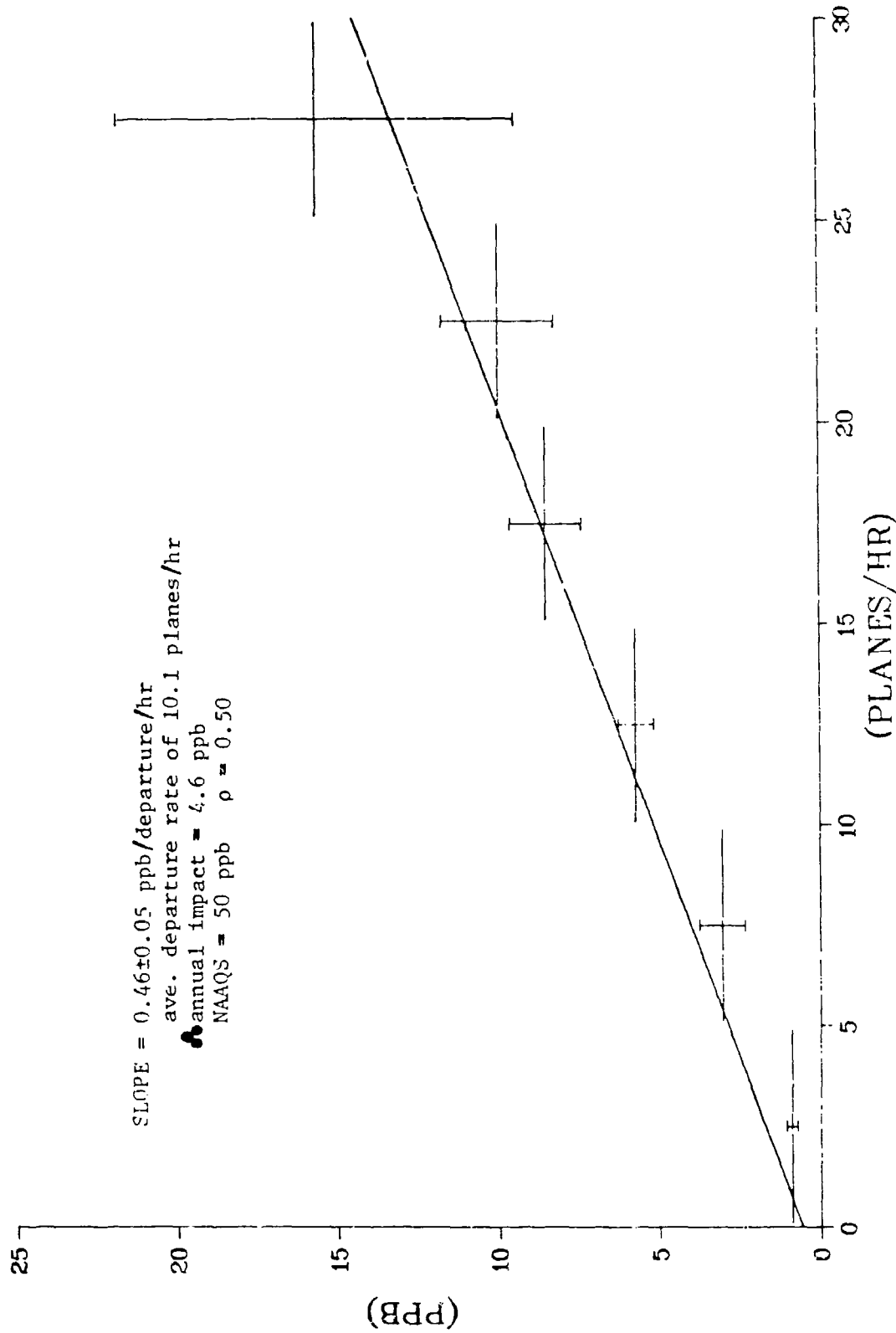


Fig. 1.7. Station 1 Average Pulse Integrated NO₂ Concentration Versus Departure Rate at DCA.
 The slope of the regression line (solid line) times the average hourly departure rate of 10.1 aircraft indicates an aircraft impact of 5 ppb on the annual average NO₂ nearby the runway. The annual average NAAQS for NO₂ is 50 ppb.

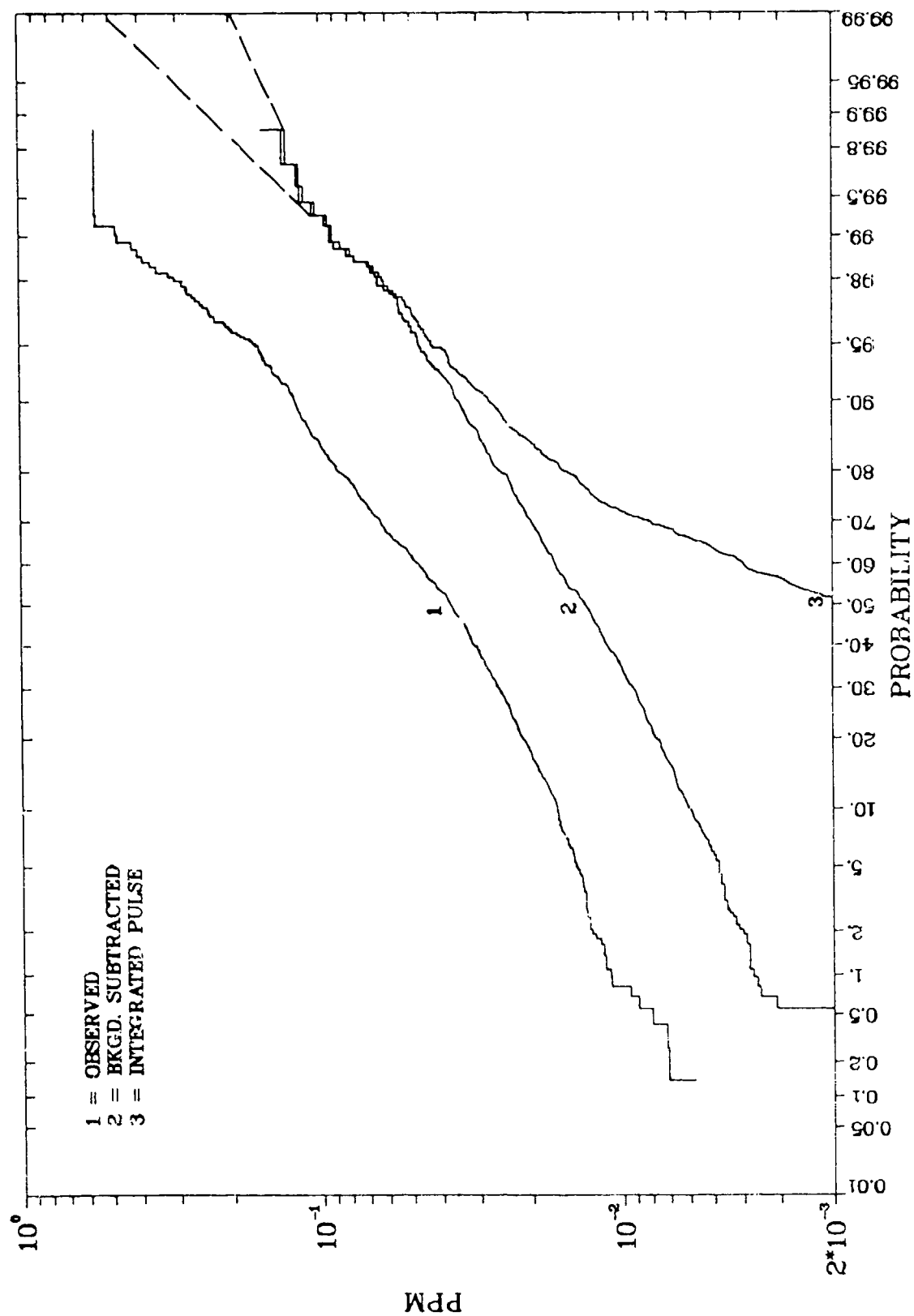


Fig. 1.8. Cumulative Frequency Distributions of Hourly NO_x Concentrations at DCA Station 4. The three solid curves represent the total (1), background subtracted (2), and pulse integrated (3) NO_x signal components. The dashed lines are visual guides for estimating the high and low ranges of anticipated worst-case, once per year concentrations.

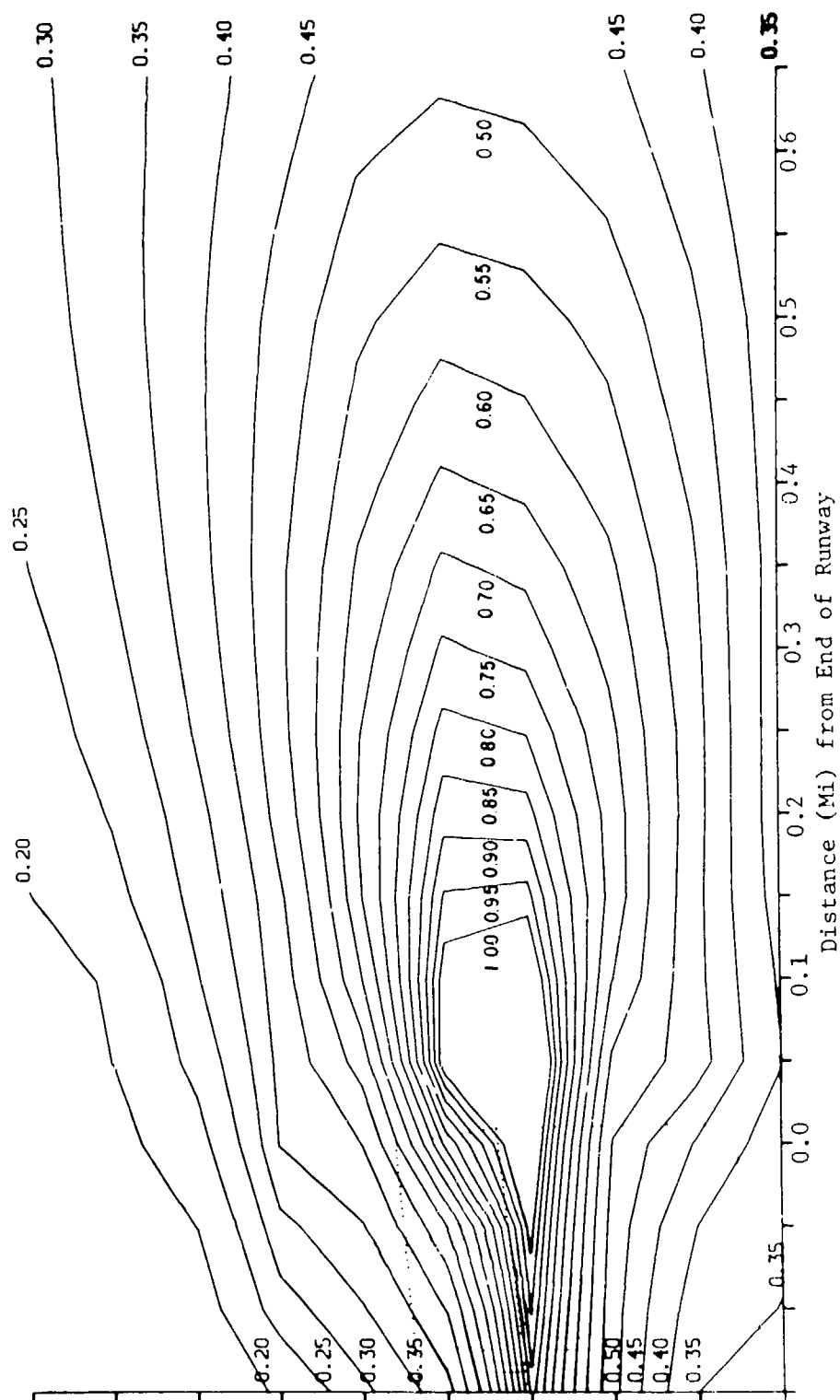


Fig. 1.9. MODIFIED AVAP Simulation of "Worst Case" (E Stability, Westerly 2-Knot Wind, and an Equivalent Departure Rate of Approximately 30 B727 Aircraft) NO_x Conditions behind a Typical Busy Runway Complex. Runways and Taxiways are shown as dotted lines. NO_x contour levels, given in ppm, suggest possible high NO_2 concentrations but reactive plume calculation needed to confirm this. Computation grid size = 0.05 mile.

Updated AVAP modeling studies of the major airports under assumed worst case meteorological and aircraft operations conditions also suggest maximum hourly CO concentrations of ~5 ppm at distances where public exposure might occur.

In light of anticipated CO reductions that will accompany and hydrocarbon control, the air quality benefits of a separate emission standard for CO are highly questionable.

The one potentially problematic area with respect to CO, and not dealt with in this report, is at and immediately around the terminal, where the combined effect of other CO sources and the effect of the building wake could conspire to cause violations; however, reduced engine running time in the terminal area (resulting primarily from a desire to save fuel) has greatly reduced the aircraft role in such an event.

Hydrocarbon emissions from aircraft engines contribute to the pervasive ozone air quality problem in many urban areas. While the overall contribution by aircraft is on the order of 1% to 3% of the total hydrocarbons, the need to control these emissions can be justified in that it will be necessary to control many other small and diversely located sources to achieve the ozone NAAQS in areas around most major airports. Further control impetus is generated by the desire to reduce hydrocarbon odors around airports.

Analyses of the oxides of nitrogen data from these airport studies suggest that aircraft impact on local, annual average NO₂ levels will be confined to 10-20% of the 0.05 ppm annual average NAAQS. However, the possibility of aircraft alone causing peak hourly NO₂ concentrations in excess of 0.2 ppm exists. Similarly, AVAP modeling suggests possible high NO₂ near the ends of runways. At the present time there is no short-term (e.g., hourly average) NO₂ standard; however, the EPA is reviewing the need to establish such a standard. The suggested range of such a standard is 0.2 ppm to 0.5 ppm hourly average. However, because the actual NO₂ level is strongly dependent upon a number of atmospheric parameters, incorporation of a reactive plume model with realistic background levels of NO, NO₂, and O₃ is needed before modeling can yield a more definitive prediction of peak hourly NO₂ concentrations.

Just as the issue of NO_2 impact assessment is more complicated than for CO or HC, so too is the issue of NO_x control. Plagued by poor control technology and high control costs, NO_x , which originates primarily from the high thrust takeoff mode, cannot be "managed" as effectively through minimization of engine idle time as can be CO and HC.

2 HISTORICAL SURVEY OF AIRPORT AIR QUALITY STUDIES

As consequences of the 1967 Air Quality Act (U.S. Congress, 1967) and the 1970 Clean Air Act Amendments (U.S. Congress, 1970) a number of studies have been conducted to determine the contributions of aircraft emissions to the air quality in the vicinity of airports. This chapter summarizes the history of these studies, their purposes, and the conclusions which have been previously drawn from them. Also pointed out is a number of study difficulties which have brought those study conclusions into question, and have led to additional studies aimed at resolving remaining questions. The final section of this chapter discusses the meteorological aspects of "worst case" air quality conditions.

2.1 HISTORICAL OVERVIEW

The contributions of aircraft as sources of air pollution were not seriously considered until the introduction of turbojet aircraft into air carrier service in the late 1950's. Even though the particulate emissions of those earlier engines were highly visible, the first two reviews of their potential contributions by the Los Angeles Air Pollution Control District (George and Burlin, 1960) and the Coordinating Research Council (1960) did not consider the total emissions significant enough to warrant further investigation.

It was not until a second study by the LAAPCD (Lemke et al, 1965) and the Report of the Secretary of HEW on the "Nature and Control of Aircraft Engine Exhaust Emissions" (U.S. DHEW, 1968) that the subject of control was brought into serious discussion as "feasible and desirable." Of principal concern were CO and organic particulates. These findings by the HEW led to further quantification of emissions inventories by Northern Research and Engineering Corporation (NREC) under contract to the Public Health Service of HEW and later to the U.S. EPA (e.g., Bastress et al, 1971). This was followed by the development of an air quality impact assessment technique by the Northern Research and Engineering Corporation (NREC) with assistance from Environmental Research & Technology, Inc. (ERT). The result was the first air quality model specifically designed for airports.

A major study of the potential impact of aircraft emissions upon air quality at six airports, including five of the busiest, was then launched by the EPA using the NREC methodology (Platt et al, 1971). It required compilation of emission inventories for Washington National (DCA), Chicago's O'Hare (ORD), New York's John F. Kennedy (JFK), and Los Angeles International (LAX), as well as for the new Tamiami, Florida and Van Nuys California airports. Since aircraft emissions data were lacking, the result was a good initial set of relative estimates but with uncertain overall accuracy. The dispersion model was relatively simple in its derivation, but the validity for its use with aircraft sources hadn't been fully tested.

At about this time (1971-72) air quality measurement data were being collected in the vicinity of LAX to provide a comparative data base in addition to a direct assessment of air quality in the airport vicinity (I 1971). The results of these LAAPCD measurements and the NREC modeling study served as the basis for the initial assessment by the EPA (EPA, 1972) of the air quality impact of aircraft engine emissions. Although the EPA used updated emissions data, the comparisons of model calculations with the few measurements available yielded several large discrepancies including some severe underpredictions. This led to a model verification study at DCA by Geomet. After several modifications the model was compared with a new set of monitoring data from DCA, but it still had a tendency to underpredict changes in concentrations as identified by Argonne National Laboratory staff (Wangen and Conley, 1975).

With FAA support Argonne developed the more complex Airport Vicinity Air Pollution (AVAP) model. AVAP, also a Gaussian dispersion and transport model, had several refinements for treating accelerating line sources as well as other types of point, area, and line sources. AVAP's emission inventory routine was also more sophisticated and tracked patterns of aircraft activities as a function of wind direction and functional mode (Rote et al, 1973). Simultaneous development of a military version, the Air Quality Assessment Model (AQAM), was undertaken by Argonne for the U.S. Air Force.

The comparison between AQAM (adopted for civilian application) and the Geomet model indicated that AQAM was relatively successful in describing the measurements made at DCA. An initial validation exercise for AVAP was performed at O'Hare Airport where especially detailed emissions data had been obtained.

Due to problems resulting from inadequate determination of off-airport sources of CO, the ORD validation effort (Rote et al, 1973) was more successful when NO_x measurements were compared with AVAP predictions. A subsequent effort to compare AVAP results with monitoring data from Hartsville International Airport in Atlanta was complicated by troubles with the measurement program (Cirillo, et al, 1975). Though absolute concentrations of CO, NO_x, and HC remained in doubt, the Atlanta study results have been useful in exploring the relative sensitivity of concentration patterns to various aircraft operational procedures.

2.2 SUMMARY OF PREVIOUS AIRPORT MODELING AND MONITORING RESULTS

There is continuing concern about impacts of aircraft related emissions upon air quality in public areas both inside and outside of airport boundaries. On a regional basis HC and NO_x emissions must be considered because of their role in photochemical oxidant formation, and, not surprisingly, many of the cities with oxidant standard attainment problems have large airports associated with them. An airport's contribution in these major urban areas usually constitutes 1-3% of the emissions burden from all sources of HC and NO_x.

An airport at a rural location may represent the largest single contributor on an annual basis to the inventories of CO, HC, and NO_x emissions in its area of air quality influence; but, it is local effects of these pollutants in comparison with shorter term standards which are currently of greatest concern.

The continuing questions about the adequacy of airport modeling methods can often be traced to one of the following:

1. There are several airport models which give widely varying results.
2. The modeling assumptions are not always clearly defined; and their applicability to specialized airport source geometries (e.g., jet engine exhausts in terminal areas) has been questioned.
3. The validation experiments for airport models are few, and those validations that do exist have not been particularly successful even for the relatively sophisticated models.
4. The scales of interest to the user may not coincide with those for which the mathematical model was developed. A user may often expect finer resolution of concentration patterns than is reasonable or better agreement between a few short-term measurements and predicted ensemble

average concentrations than is reasonable. Similarly, computations performed using an excessively crude grid may exaggerate the spatial extent of highly localized pollution problems.

5. Analysis of a "hot spot" problem may be attempted with a model that does not contain the right physical model to adequately simulate or describe it.

Many of these problems result as often from misunderstanding of model capabilities or user intents as from model design or documentation inadequacies.

Often the relevant question to ask is whether the problem of interest fits the assumptions and scale of resolution of the "standard" model to be selected. If not, a custom-designed model, or more often, a hybrid of several sub-models or complimentary models is called for. This new model may also require some validation via comparison with measurements, but at least it should be constructed to represent each of the physical processes by a sub-model that has been separately validated to be an adequate description of that process, consistent with the state of current knowledge.

There are relatively few major airports at which violations of air quality standards and guidelines have been measured and documented. Most of these have been described previously in the review of airport impacts prepared by the EPA (1972) and updated recently by Lorang (1978). There are also a larger number of airports at which violations have been predicted as a result of air quality modeling studies though supporting measurements are unavailable. Controversy often arises over relative contributions of emissions from sources related to aircraft, nonaircraft sources at airports, and those due to nonaircraft sources in the airport environs. A number of studies (Cirillo et al, 1975; Wang, 1975; Lorang, 1978) have clearly recognized the importance of environmental sources of CO, NO_x, and HC in that their dominance often interferes with the model validation or calibration goals of the study. As shown in the tables given in the subsections below, repeated assessments have given widely varying results at the same airports. The result has been that the federal EPA and several regulatory agencies continue to raise some of the same questions that were at issue before these modeling studies were undertaken.

In each of the study results reviewed in the following three subsections, the reliability of conclusions relating to the need for additional controls was thrown into some doubt because there was not convincing agreement between model predictions and measured concentrations. Although inventory quality or

measurement data quality can often be challenged, the lack of verification for the simpler sub-components of the model calculations has made it difficult to identify with any uncertainty the main reasons for poor overall comparisons.

As just recently pointed out by Turner (1979), it is only through the repeated verification of each of the sub-components of an air quality dispersion model, that the validity of the overall model results will be eventually demonstrated. The last section considers the question of the identification of the meteorological conditions that are associated with the highest ground level concentrations and that are presumably simulated by air quality models.

2.2.1 Carbon Monoxide Studies

The results of the principal investigations of CO concentrations at major airports are given in Table 2.1a. The results of these studies have been reported over the 1971 to 1979 period during which EPA development of aircraft engine control strategies has been continuing. The initial modeling estimates from the 1971 NREC study (Platt et al, 1971) for LAX, ORD, DCA and JFK airports are presented because they represent comparable modeling assumptions applied to a variety of airports. As can be seen in the table the majority of the remaining modeling studies utilized AQAM or AVAP. Careful examination of these results reveals that the majority of maximum measurements observed are within a factor of two of the predicted maximum for the same receptor areas. The model estimates of maxima are also generally higher even though the model may underpredict the majority of the cases which result in moderate concentrations. Interpretation of CO monitoring and modeling data is not complicated by significant chemical reactivity or measurement uncertainty. However, precise modeling of hot spot concentrations adjacent to obstructions requires modeling the flow around obstacles which is beyond the capability of present Gaussian-type airport models. Moreover, the locations where CO violations are often suspected have a large contribution of CO emissions by automobiles and access/service vehicles as well as aircraft.

When violations of the 8-hour standard are encountered, the aircraft may generally be identified as a major source only near the end of runways with heavy queuing activity during worst-case meteorological conditions. Since that is not an area in which the public is generally exposed, a modeled violation of ambient standards downwind of a queuing area probably does not

Table 2.1a. CO Measurement and Modeling Study Summary

Pollutant	Airport (Ref)**	Measurements* Max.	Method*	Max.	Modeling* Method	Comments
CO (ppm)	LAX (a)	46 8.3 (8hr)	NDIR	2.4-24	NREC	Model underpredicted max. hours by factor of >2; most meas. are near bldgs (46 outside, 141 inside). Fraction attributed to aircraft by model is about 50% for low values, and <25% for high values.
	ATL (b)		None	2.5-4.5	AVAP	Off-airport receptor. Decreases from 4.5 to 2.5 when towing aircraft.
	ORD (a,c)		None	9-41 7.7	NREC AVAP	Over std. at end of runways.
	JFK (a)		None	4-44 85-100	NREC	4 of 44 due to aircraft at end of runway. 85 to 100 due to aircraft operations at terminal.
	DCA (a)	15-78	NDIR	45-120	NREC	45 of 120 due to aircraft; model underpredicted most concentrations due to inventory omissions. Sequential pred. poor, through ave. is OK. Model better, but changes underpredicted due to high background not in model.
	(d)	22	NDIR	*** 60 9 (8 hr)	Geomet AQAM	
	DUL (e)	3.2-3.6 7.5 3.5 (8 hr)	NDIR Ecol. Ecol.	0.2-2.5	AVAP/ALSM	NDIR value is max. meas. at off-airport site AVAP near field predictions for aircraft only, 0.2 is AVAP value at site boundary.
	(f)	5.5 (bkg)	Ecol.	14	AQAM	Model calibrated for bkg. meas.; thus performance should be best.
	BOS (g)	2.0-5.9	Ecol.	2.3-7.1	AVAP/ERTAQ	Model OK for max. cases tested with refined model versions; 2-3.5 when wind from airport; 4-5.9 when wind from urban area.
	Williams AFB (h)	2.2-4.0	Beck. GC	4.5	AQAM	Max. hr. per year; good model pred. with 0.09 ppm ann. bkg. added to AQAM, max. near pkg. area; off-airport conc. very low. Underpred. worst case conc. by a factor of 1.7 at any one station.
	SEA (i)	4-12	Ecol.		None	4-7 worst case off-airport total with calm winds; 12 on airport.
	Van Muyt (j)		None	2-5.5	PAL	5.5 for 100m from main taxiway; less than 2 for all areas more than 270m from general aviation aircraft.

*Averaging time = 1 hr unless noted.

**See reference list. in Table 2.1d.

***Data not available.

*NDIR = Non-dispersive infrared detector; Ecol. = Ecolyzer electrochemical detector; Beck GC = Beckman 6800 gas chromatograph.

present a health hazard. Lorang's review (1978) claims that monitoring has shown that CO violations have occurred in terminal areas and that suggests that aircraft emissions were important contributors at both LAX and DCA. It may also be pointed out, however, that the CO levels due to the airport (as modeled in Atlanta) usually drops off very rapidly with distance. Therefore potential problems are localized within the airport property.

The recent measurement program at Boston's Logan Airport (Smith and Heinold, 1980) illustrated that measured concentrations were much below standards during periods of high airport activity in areas near the ends of runways with long queues of taxiing aircraft. The highest concentrations occurred instead, when winds from nearby urban centers coincided with a strong nocturnal inversion. These CO concentrations tend to be overpredicted by most present airport dispersion models. Therefore, it appears that proper modeling techniques must consider these situations as well as the microscale CO problem in terminal areas. The latter modeling must, however, account for building wake effects and local sources, such as vehicular traffic, if the true relative impacts of aircraft sources are to be realistically portrayed at the terminal.

2.2.2 Hydrocarbon Studies

The results summarized in Table 2.1b are for the same airports as those given in Table 2.1a, except that there were no studies of HC performed at the Seattle or the Van Nuys airports. It is immediately apparent that both nonmethane hydrocarbon (NMHC) and total hydrocarbon (THC) measurements as well as predictions are well above the $160 \mu\text{g}/\text{m}^3$ (6 AM-9 AM average) established as an EPA guideline for management of photochemical pollutants. Comparisons of the wide ranging concentrations among receptor points on and near airports reveals that aircraft do indeed contribute to the elevated values in the vicinity of airport boundaries. The maximum on-airport concentrations occur in idling and taxiing areas, and particularly in queues awaiting takeoff. The studies of pollutant control strategies at Atlanta (Cirillo, et al, 1975) and the recent Boston study (Smith and Heinold, 1980) both indicated that regulation of queuing and taxiing times may serve as effective measures for diminishing hydrocarbons and organic particulates (and the odors associated with these) with current aircraft engine designs.

Table 2.1b. HC Measurement and Modeling Study Summary

Pollutant	Airport (Ref)	Measurements* Max.	Method	Modeling* Max.	Method**	Comments
HC ($\mu\text{g}/\text{m}^3$) +	LAX (a)		***	560-1100(3hr) 1500	NREC EPA, 1972	Original inventory underprediction. 6-9AM conc. over guide for all of airport area, often aircraft emissions alone would not exceed guide.
	ATL (b)		None	1100-2700 450-1450	AVAP	1100 due to aircraft, 2700 due to all sources at off-site receptor; 450 due to aircraft, 1450 due to all sources at terminal and ramp.
	ORD (a) (c)	1900-4200	None THC	2-1200(3hr) 3650-1250	NREC AVAP	Conc. over guide for all of airport. Model validation test-poor correlation, but 70% estimated as due to aircraft.
	JFK		None	2200-8400(3hr)	NREC	Conc. over guide. pred 150% due to aircraft) for up to 5 km from terminal; no local validation meas. from terminal; no local validation of model.
	DCA (a) (d)	1600-1800	None THC	1400-1900 *** 450	NREC Geomet AVAP	Over guide near ends of runways and in ramp areas. Up to 160 pred. as due to aircraft. Model did not correlate well with meas. due to high background.
	DUL (e)	670-1630	THC	80-730	AVAP	1st THC value is net for on-airport location, 2nd THC value is max. total off-airport. Max. aircraft effect at end of runways.
	BOS (g)	600-2400	NMHC	970-1410(3hr)	AVAP+ERTAQ	NMHC (6-9AM) modeled (worst hour=1.5x 3 hr ave.); Model OK for maximum cases tested. AVAP for airport sources only.
	Williams AFB (h)	860-3170	NMHC	590-3050	AQAM	Max. hr. in yr. given; model did correlate well with meas. when 50 $\mu\text{g}/\text{m}^3$ ann. bkg. added to AQAM. Underpred. of 1 hr. worst case by up to a factor of 1.7 at one station.

*Averaging time = 1 hr unless noted.

**Modeling method generally predicts THC, except as noted.

***Data not available.

+Conversion to ppm usually based on molecular weight of methane.

A report on the air quality associated with Air Force bases (Daley and Naugle, 1978) and (Naugle et al, 1978) suggests that HC and NO_x emissions from aircraft at airports present the greatest potential harm according to the EPA's pollution standards index (PSI). Since present and projected jet engine designs are able to effectively decrease hydrocarbon (and CO) emissions by increasing combustion efficiency, control of HC and CO are expected to be less difficult than NO_x. Because of its rural location, the study at Williams AFB avoided the problem of high urban background pollution conditions for model-measurement comparisons. Using the AQAM model, THC's displayed the highest PSI levels at distances beyond the airport boundary. However, this PSI approach for HC analysis suffers from the problems inherent in using simple guideline HC levels as measures of O₃ production and oxidant health effects.

Unfortunately, most studies make no distinction between total and reactive hydrocarbons. Even when conservative assumptions are invoked, a distinction should be made between representing NO_x (NO, NO₂) and NO₂ and THC and NMHC. In an oxidizing atmosphere, NO is converted to NO₂, whereas CH₄ is nonreactive at ambient temperatures and ozone concentrations. To acknowledge the inconsistency but ignore it in the interpretation of monitoring and modeling studies [as in Lorang (1978)], leads to excessively pessimistic predictions about the role of airports in violations of the Air Quality Guideline.

2.2.3 Oxides of Nitrogen Studies

The results of NO_x and NO₂ measurements and NO_x model predictions are presented in Table 2.1c for the same airports (and studies) for which HC results were given in Table 2.1b. It should be noted that the values given in the NREC modeling study relate to an annual average standard. For most of the studies involving both measurements and modeling, hourly values are given in both instances. In addition, most measurement studies report both NO₂ and total NO_x, even though modeling generally assumes that NO_x is the more reliable parameter to predict. (This is especially true for long term average predictions).

Considering an annual standard of 0.05 ppm (100 µg/m³) for NO₂, the conservative assumption that NO₂ = NO_x concentrations leads to the conclusion that most of the airports modeled by NREC might have a problem meeting the

Table 2.1c. NO_x/NO₂ Measurement and Modeling Study Summary

Pollutant	Airport (Ref)	Measurements* Max.	Method	Modeling* Max.	Method**	Comments
NO ₂ /NO _x ($\mu\text{g}/\text{m}^3$)						
	LAX (a)		***	120-280 (Ann.)	NREC	Initial inventory may overpred. emission rate by 2.4 factor; annual ave. exceeds std at ends of runways.
	L (b)		***	92-167 (Ann.)	AVAP	1 out of 92 $\mu\text{g}/\text{m}^3$ off-airport annual ave. due to aircraft; 116 of 176 $\mu\text{g}/\text{m}^3$ on-airport is due to aircraft influence.
	ORD (c)	240-360	None	330 (Ann.)	NREC	Annual ave.; 23 of 330 due to aircraft AVAP validated best with hrly. NO ₂ data.
	(c)		NO _x	180-240	AVAP	180 pred. for hour that measures 240 downwind of runway (not public area); 330 pred hour spanning 10 min meas. of 300 to 360 at terminal.
	(c)	430-680	NO _x	300-360	AVAP	Gate F-6, model over or underpred. by factor of 1.5 or less.
	JFK (a)		None	7-11 (Ann.)	NREC	Ann. ave. at public terminal areas. Inventory adequate?
	DCA (a)	560-1240	NO _x	68-120 (Ann.)	NREC	Of modeled 68-120 ann. ave., 24-71 due to aircraft at runways; 17-22 due to aircraft at public areas.
	(d)	105	NO ₂	270	AVAP	Poor correlation of hourly conc. prediction.
	DUL (e)	50-150	NO ₂	25-75	AVAP	1st NO _x value is ret for an airport loc.; 2nd NO ₂ value is max. total of off-airport. AVAP model conc. (25) at site boundary, plus max. at end of runway (75).
	BOS (g)	200-660 180-340	NO _x NO ₂	500-400	AVAP/ERTAQ	1st value is max. for wind from airport 2nd value is max. for bkg. contrib. (Model OK for maximum cases tested.)
	Will. A. J. (h)	220-580 290-300	NO _x NO ₂	150-250	EQAM	Model generally showed good hour-by-hour agreement when 14 $\mu\text{g}/\text{m}^3$ ann. bkg. added to AQAM prediction (i.e., 65% within factor of 2). Worst ann. cases could be underpred. by factor of 3.

*Averaging time = 1 hr unless noted.

**Modeling methods all predicted total NO_x.

***Data not available.

Table 2.1d. Reference Key for Measurement and Modeling Study Summary

Symbol	Reference
a	Platt et al., 1971
b	Cirillo et al., 1975
c	Rote et al., 1973
d	Wangen and Conley, 1975
e	Smith et al., 1977
f	Shelar, 1978
g	Smith and Heinold, 1980
h	Yamartino et al., 1980
i	Greenberg, 1978
j	Schewe et al., 1978

annual standard; however, such an assumption may be grossly incorrect as aircraft emissions are predominantly NO.

Modeling of the nitrogen dioxide (NO₂) air quality impact resulting from airport operations has traditionally been based on the use of the standard Gaussian dispersion equation, assuming that 100% of all NO_x emissions are converted to NO₂ (e.g., EPA 1972, Cirillo et al, 1975). The 100% NO₂ conversion assumption is used because the Gaussian dispersion equation cannot accurately simulate the complex photochemical reactions that govern actual NO₂ concentrations. This assumption results in an overprediction of NO₂ concentrations; however, it is useful in identifying potential problem areas deserving of more detailed modeling and/or comprehensive monitoring efforts.

It has been pointed out by Jordan (1977a) that although this conservative convention for interpreting long-term averages may often be acceptable, more serious questions arise when the issue of a short-term (1 to 3 hr) NO₂ standard is considered. Jordan has examined both commercial airports (1977a) and general aviation aircraft (1977b) and presents evidence that the latter are not likely to contribute significantly to either long-term or short-term NO₂ concentrations. The magnitude of the maximum 1-hour NO₂ measurements at the airports listed in Table 2.1c, however, suggests that some commercial airports could have a problem in the near future if a stringent hourly standard is established. Of principal concern is the total NO₂ value at distances of 1 to 5 km from the runway areas associated with the maximum emission rates for NO. The rate of conversion of NO to NO₂ in these areas seems to be a

critical factor in determining the need for further action in controlling aircraft emissions of NO_x .

The actual conversion of aircraft NO_x emissions to NO_2 is a complex function of meteorology, atmospheric photochemistry, and ambient concentrations of NO_x , ozone, and hydrocarbons. NO_x emissions from aircraft mainly consist of nitric oxide (NO). For example, emission measurements from Pratt and Whitney JT3D, JT8D, and JT9D jet engines have shown a typical NO_2/NO_x emissions ratio of 4 to 8% by volume (Pratt and Whitney, 1972). This is reflected in ambient air monitoring measurements at airports, where the NO_2/NO_x ambient ratio was found to be lower on the airport grounds than in areas surrounding the airport (Lorang, 1978).

A qualitative assessment has been made of the influence of aircraft NO_x and hydrocarbon emissions on ozone formation downwind (Whitten and Hogo, 1976). The conclusion was that the mixing of aircraft jet exhaust with automobile exhaust can cause a more favorable hydrocarbon/ NO_x ratio for ozone formation than automobile exhaust alone. A simple semi-quantitative treatment of NO to NO_2 conversion at airports considered only one main chemical reaction (Jordan and Broderick, 1978, Jordan and Broderick, 1979); this treatment is valid only over short transport time scales where the presence of hydrocarbons can be neglected.

In order to quantitatively predict the NO_2 conversion of aircraft NO_x emissions and the effect of aircraft NO_x and hydrocarbon emissions on downwind ozone concentrations, a sophisticated photochemical air quality simulation model may be necessary. A number of photochemical models have been developed which can simulate chemistry, emissions, and atmospheric transport processes with detailed spatial and temporal resolution.* A methodology was developed to integrate an early photochemical model (NEXUS/P) with airport land use development (Norco et al., 1973); however, this photochemical model used a chemical kinetics mechanism that is now obsolete.

Only one study has been conducted that has used a detailed photochemical air quality simulation model to examine the effect of NO_x and hydrocarbon

*The discussion here is limited to photochemical models applicable in the urban troposphere. The impact of aircraft emissions aloft on the stratosphere ozone layer requires the use of very different photochemical modeling techniques (Oliver et al., 1977).

emissions from airport operations on air quality in the vicinity. This study (Duewer and Walton, 1978) was done in the San Francisco Bay area using the LIRAQ-2 grid-based photochemical model. The modeling showed that doubling airport emissions reduced ozone concentrations slightly at San Francisco Airport, but increased ozone downwind by approximately 0.003 ppm.

However, a grid-based photochemical model such as LIRAQ-2 is very expensive to run, both in terms of manpower and computer time, because concentrations must be calculated at a large number of grid cell points covering the entire urban region. A more useful modeling tool for studying the impact of airport emissions would be a trajectory-based photochemical model, such as the new ELSTAR model (Lloyd et al., 1979), which calculates concentrations along a specific path or trajectory of an air parcel. A trajectory-based photochemical model could economically study the effects of various airport emissions control strategies with a detailed consideration of both NO_2 and ozone formation in the vicinity of the airport.

2.3 METEOROLOGICAL ASPECTS OF AIRPORT AIR POLLUTION WORST CASE ANALYSIS

The ambient levels of air pollutants depend not only on the amount of pollutant emitted into the atmosphere but also upon the prevailing meteorological conditions. The dispersive capability of the atmosphere depends upon such meteorological parameters as the wind speed and the vertical temperature profile. Of course, the wind direction also plays an important role when considering any particular source-receptor pair. These parameters vary hourly, diurnally, and seasonally as both small- and large-scale weather patterns change.

The air quality effects of the prevailing meteorological conditions are not the same for all sources. Elevated sources have their greatest impact during unstable or neutral atmospheric conditions. High wind speeds, which may occur during periods of neutral stability will also reduce plume rise and bring plumes to the ground closer to the source than under lighter wind cases, thus diminishing the effect of greater initial dilution. Under stable atmospheric conditions or during a temperature inversion (ambient temperature increasing with height) the plume from an elevated point source may remain aloft and intact for many kilometers downwind. If the inversion layer exists above the elevation of the source, while the layer below is unstable, maximal concentrations may occur at short distances from the base of the source.

Conversely, the contribution of ground-level sources to ambient air pollutant levels is usually maximized under stable or inversion conditions provided wind direction is steady. At airports, it is the ground level emissions which predominantly impact nearby receptors. When stable conditions occur at the surface, the thermally turbulent surface mixing layer has effectively zero thickness and pollutants emitted at low levels are trapped near the surface. The dilution of pollutants by mechanically induced atmospheric turbulence is also inhibited. In these cases the concept of mixing depth is not useful since the vertical dimension of the plume usually remains smaller than the thickness of the stable layer. It should be noted, however, that light and directionally variable winds are also often associated with such stable atmospheric conditions. These wind conditions serve to spread the impact zone for any aggregate of low level sources. This spreading causes contributions from many spatially distributed sources to partially impact any particular receptor area over an hour's period, but also mitigates the impact of any single source. Thus, the wind direction meander acts like a spatial lowpass filter: reducing the highest observed concentration by distributing "hot spot" impacts to other nearby cross wind receptors.

A study of the meteorological factors involved in pollutant levels monitored around Los Angeles International Airport (Hallanger, 1974) showed that the potential for airport related air pollution at any given moment was greatest during stable atmospheric conditions accompanied by light and directionally variable winds.

To assess the frequency of high pollution potential a statistical compilation of the weather conditions observed at each of the five study airports was examined. Table 2.2 lists, by airport, the time periods of meteorological observations examined and the frequency of stable, low-moderate wind speed conditions having high pollution potential. Table 2.2 shows that low wind speed stable cases are indeed frequent at all of these airports; however, it should be mentioned that a large percentage of these cases are associated with low airport activity, nighttime conditions.

In order to assess the "worst-case" frequency for maximum concentrations at individual airports the orientation of "critical receptors" with respect to areas of high emissions density must be considered. A critical receptor is defined as an area which is accessible to the public for periods

Table 2.2. Frequency of Poor Atmospheric Dispersion Conditions^a at Five Major Airports

Airport	Time Period Examined	Frequency ^b
DCA	1968-1972	30.7
LAX	1955-1964	35.1
LGA (NY)	1965-1970	19.7
ORD	1960-1964	29.0
Dulles	1966-1970	37.0

^aDefined here as stable (E of F) stratification with a wind of 1-5 m/sec from any direction.

^bFrequencies are based on a five year annual average period.

exceeding an hour, and is relatively near an area of high emission density. This definition, in itself, requires some knowledge of the pollutant concentration patterns associated with each wind direction under a range of wind speeds and atmospheric stabilities. Critical receptors are most precisely defined by evaluating a series of dispersion model analyses which cover the range of potentially critical cases. Temporal variation of emission patterns must, of course, also be considered. Preliminary estimates may be made, however, based upon the knowledge of the receptor map, the emissions map, and wind frequency tables. The worst case frequencies identified here are based upon those considerations and model analyses carried out for LAX, JFK, and ORD airports as reported in Volume II of this report. The stability classification scheme used here is the well-known method of Turner, 1964. While this method may be less precise than one which uses actual onsite measurement of turbulence intensity, it is generally the only method available for prospective studies of impacts based on historical meteorological records.

For LAX airport there are two potentially critical receptors: (1) the terminal area and (2) the restaurant and golf course to the East of runway 24L. The worst case wind directions for the terminal as a receptor are N and E to ESE. For the restaurant and golf course receptors W to WNW winds are most important. North winds result in higher concentrations but are

less frequent than E or ESE winds. For LAX a previous study made available separate frequency distribution data for the 6 to 9 AM hour interval, which is the period of maximum aircraft takeoff activity coinciding with stable conditions.

Table 2.3 shows LAX wind frequencies for each of these critical receptor directions for the worst case 1-3 knot and 4-6 knot wind speed classes during stable (E and F) conditions. (For 1-3 knots, only F stability exists; for 4-6 knots, 60 to 70% of the cases are F stability; for 7-10 knots only E stability exists). Although many air quality studies indicate that the highest concentrations arising from a combination of ground level sources are associated with 1-3 knot winds and stable (F) turbulence levels; consideration of the buoyant plume rise of hot aircraft exhaust plumes leads to the conclusion that, for aircraft, wind speeds of 4-6 (or even 7-10) knots are necessary to bring the plume to the ground at receptors close to these sources (see Section 4.5). Frequencies of these stable cases for the 6 to 9 AM period are also given in Table 2.3.

The important wind directions for DCA airport are defined by the air quality monitoring experiments of 1972 and 1979. The N to ENE sectors are of principal interest. Critical airport receptors include the southern terminals and the parking areas SW to WSW of the ramp areas. SSE winds would also be important for aircraft emissions impacts at the public terminal areas. For that reason Table 2.4 lists frequencies of low wind speed stable conditions for each of these directions. The N and SSE directions each account for more than 100 hours per year of stable conditions with less than a 6 knot wind speed. However, in determining the frequency of worst-case occurrences it is important to consider the number of hours that these meteorological conditions coincide with periods of high airport/aircraft activity. At DCA there is virtually no activity between midnight and 7:00 AM (per observations, Feb. 1979 and CAG). Since stable conditions occur predominantly at night, there are likely to be fewer than 50 hours per year of "airport worst case" conditions at DCA.

For JFK a 280 degree direction has been assumed for the modeling in Volume II, where impacts of 2 knot stable winds upon the terminal building were evaluated. The important directions for off-airport receptors are more likely SE to S winds. Table 2.5 compares the frequencies for low speed

Table 2.3. Annual Percentage Frequencies^a of Stable Stratification at LAX

Wind Direction	All Hours			Hours 06-09		
	Wind 1-3	Speed 4-6	(Knots) 7-10	Wind 1-3	Speed 4-6	(Knots) 7-10
N	0.54	0.67	0.34	0.30	0.47	0.25
E	1.61	2.36	0.26	1.10	2.75	0.23
ESE	0.95	1.31	0.13	0.85	1.10	0.10
W	1.03	2.30	1.75	0.17	0.27	0.06
WNW	0.48	0.81	0.28	0.19	0.16	0.06

Table 2.4. Annual Percentage Frequencies^a of Stable Stratification at DCA. All Hours

Wind Direction	Wind Speed (Knots)		
	1-3	4-6	7-10
N	0.34	0.96	0.41
NNE	0.15	0.50	0.30
NE	0.24	0.68	0.31
ENE	0.10	0.45	0.12
SSE	0.50	1.30	0.12

^aNote that 0.02% is approximately two hours per year. Any calculated concentration exceeding a federal ambient air quality standard and associated with a greater frequency could result in a violation.

Table 2.5. Annual Percentage Frequencies^a of Stable Stratification at JFK. All Hours

Wind Direction	Wind Speed (Knots)		
	1-3	4-6	7-10
ESE	0.07	0.13	0.05
SE	0.06	0.25	0.09
SSE	0.06	0.25	0.09
S	0.02	0.11	0.08
W	0.11	1.44	0.76

stable flow in these three sectors with the much higher frequency occurring for W winds.

For ORD the worst case directions considered in Volume II are NNE and SE. These directions were also selected to evaluate impacts upon the terminal area. However, the communities to the North of the airport may also be defined as important off-airport receptors. Thus the high frequency of low speed stable winds from the S are also shown in Table 2.6 for comparison with the NE and SE frequencies.

Further consideration of the results of the DCA and Dulles model validation experiments has shown that any final determination of the critical wind speed for a worst case condition at a particular airport is highly sensitive to the specific geometric relationship of critical receptors to areas of high emission density. It is therefore expected that some model sensitivity analyses will be necessary before conclusions about a single critical wind speed and stability can be extended to any other airport. However, on the basis of the frequency tables presented here, it can be concluded that stable conditions accompanied by a wide range of wind speeds and directions occur at all of the listed airports.

On the basis of the monitoring experience at Dulles International and Washington National Airports, the definition of worst case conditions for on-airport monitoring stations located within 500 m of taxiways and runways was a somewhat different problem from that outlined above. For detection of impact of CO pollutant emissions from individual taxiing aircraft at Dulles,

Table 2.6. Annual Percentage Frequencies^a of Stable Stratification at ORD. All Hours

Wind Direction	Wind Speed (Knots)		
	1-3	4-6	7-10
NE	0.14	0.58	0.25
SE	0.32	0.75	0.08
SSE	0.35	0.82	0.16
S	0.79	2.28	0.62
SSW	0.60	1.25	0.55
SW	0.55	1.30	0.00

^aNote that 0.02% is approximately two hours per year. Any calculated concentration exceeding a federal ambient air quality standard and associated with a greater frequency could result in a violation.

the critical wind speed was about 10 mph (Smith, et al., 1977). This speed was sufficient to delay plume rise until after the exhaust plume was advected past the monitoring sites. In addition, the higher wind speeds reduced total final plume rise and therefore increased relative ground level concentrations. However, at DCA the highest NO_x and CO total concentrations were measured during episodes of light and directionally variable winds accompanied by moderately stable temperature stratification, though it should be noted that high concentrations were simultaneously observed throughout the D.C. area, thus obscuring the role of aircraft emissions.

Thus, one arrives at a somewhat complex and uncertain characterization of the meteorological conditions leading to worst case, ground-level concentrations at airports. Considerations include:

- the predominant ground-level nature of the sources suggests that F stability and very low wind speeds (e.g., 2 mph) leads to the highest concentrations;
- the plume rise dynamics associated with the buoyancy of the aircraft exhaust suggests that peak ground-level concentrations will occur at higher wind speeds (e.g., 7-10 mph);
- the strong dynamic peaking of aircraft operations at most airports biases worst case overall conditions toward less stable atmospheric conditions;

- d) the proximity of large bodies of water or urban areas adjacent to many airports influences the range of possible stabilities and is generally not considered in worst case air quality assessments; and
- e) the large, engine generated turbulence causes engine emitted pollutants to undergo an initial mixing that is somewhat stability class independent.

These considerations together with modeling approximations and limitations discussed in Volume II suggest that the compromise choice of E stability and a wind speed of ~ 2 mph might best characterize worst case conditions.

3 THE WASHINGTON NATIONAL AIRPORT (DCA) STUDY

3.1 INTRODUCTION

A major constituent of the United States program to determine the impact of aircraft emissions on airport air quality consists of the recently completed measurement of pollutants at Washington National Airport (DCA). The air quality monitoring program at DCA, sponsored by the EPA and FAA, was designed to measure NO, NO_x, and CO within 0.5 km of queueing and takeoff operations to permit an unambiguous assessment of the aircraft contribution to nearby pollutant levels.

In this section the DCA monitoring program is briefly described, followed by statistical analyses of the CO and oxides of nitrogen (i.e., NO, NO₂, and NO_x = NO + NO₂) concentration data. Two methods, background subtraction and pulse integration, are described and applied to the data to estimate the aircraft portion of observed pollutant levels. These hourly data, together with extrapolations of the cumulative frequency distributions of these data, are then compared to relevant National Ambient Air Quality Standards (NAAQS). In addition, regression analysis is employed to estimate the impact of aircraft operations on annual average NO₂ levels adjacent to the runway.

Further analyses of the NO_x data include consideration of the NO/NO_x ratio as a function of plume travel time and a comparison of the predictions of four dispersion models with measured NO_x levels. In addition, individual NO_x takeoff plumes passing across the array of receptors are analyzed to extract initial takeoff-mode plume dimensions for subsequent input to air quality dispersion models. Finally the results of an AVAP model simulation, using these latest plume dimensions, is presented to indicate the quantitative agreement between model predictions and monitoring data in suggesting the potentially serious impact of aircraft relative to a possible NO₂ hourly standard in the 0.2-0.5 ppm range.

3.2 THE DCA MONITORING PROGRAM

Aerometric data was recorded from rapid response pollutant monitors (TECO and Bendix chemiluminescent monitors for NO/NO_x and Bendix NDIR and Ecolyzer electrochemical monitors for CO) at the six sites shown in Fig. 3.1

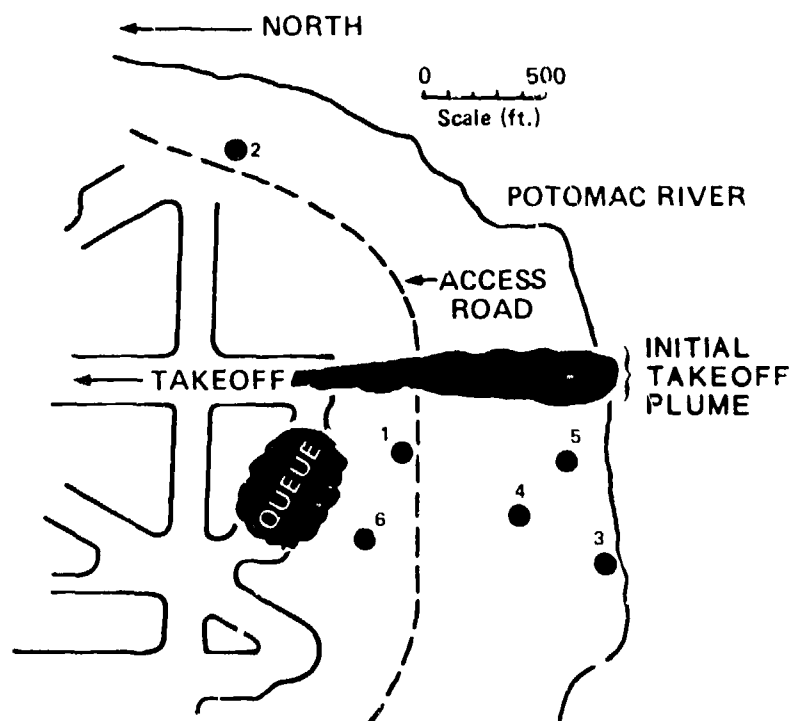


Fig. 3.1. Monitoring Site Locations at DCA. Sites were chosen to focus on the pollution clouds from the takeoff and queueing modes.

during the period January 15-February 27, 1979. With the exception of station 2, which was sited specifically to obtain background pollutant levels under northerly to easterly wind conditions, Table 3.1 indicates the air quality parameters measured at each station. In addition, airport meteorological data were supplemented by measurement of wind speed and direction, wind azimuth and elevation angles, temperature, vertical temperature gradient, and dew point temperature at a site ≈ 20 m north of station 5. During the latter half of the program a decibel meter nearby station 4 measured aircraft engine noise and provided a convenient time reference for takeoff and landing operations.

Pollutant concentrations, noise level, and meteorological parameters were recorded on three independent systems: individual strip chart recorders for each instrument, a set of multi-pen strip chart recorders synchronized by an external time reference, and on magnetic tape via a 15-channel data acquisition system (DAS). While hourly average concentrations, as extracted from the strip charts, have been previously analyzed and compared to PAL predictions

Table 3.1a. Air Quality Parameters Measured at Each Station

Parameter	Station				
	1	3	4	5	6
NO _x	X	X	X	X	-
NO	X	X	-	-	-
CO	X	X	X	-	X
CO Ecolyzer	-	-	X	-	X

X: measured

-: not measured

(EPA, 1980), this report utilizes the data provided via the DAS; thus a brief description of its operational characteristics and subsequent data analysis assumptions are essential.

The DAS, operating basically as a recording voltmeter, interrogates each of its 15 inputs once every 3 sec, converts these analog voltage signals to digital form (0-255), and then writes these numbers onto magnetic tape. Assumptions concerning the conversion from engineering units (e.g., ppm) to voltage and subsequently back to engineering units are based on manufacturer specifications and EPA calibrations. In addition, an independent EPA audit (Arey et al, 1979) confirmed that all of the CO and NO/NO_x instruments exhibited satisfactory or excellent response to the audit concentrations. Hence, the air quality data in this report should be considered accurate to the $\approx 10\%$ level.

Some of the program objectives can be visualized with the aid of Figs. 3.2a and 3.2b which show sample sets of "strip charts" produced using the DAS acquired magnetic tapes. Numerous comparisons between these synthesized strip charts of pollutant and noise level and actual strip charts of pollutant levels and log sheets of aircraft operations permitted confident matching of NO and NO_x pollutant pulses with specific aircraft operations. Figure 3.3 illustrates the analysis possibilities created through this high sampling rate approach. Takeoff plumes, easily identified by the NO_x rise above background levels and the presence of a noise pulse accompanying takeoff, are seen to disperse (i.e. reduce in peak concentration while spreading out in time) as they move from the nearby station 1 to the more distant station 3. The actual impact of these plumes may be estimated via a background subtraction (i.e. as

Table 3.1b. List of Monitoring Equipment

Site No.	Shelter No.	Shelter Dimensions	Parameter Measured	Equipment Instrument Manufacturer	Voltage Output
1	Self Propelled EPA #313	27'x8'x 14'*	NO, NO _x	Thermo Electron Company (TECO) Bendix	10V 10V 1V
			Single pen strip chart recorders (SCR) for each parameter.		
2	Self Propelled EPA #376	27'x8'x30'*	CO	Bendix	10V
Background			O ₃	Dasibi	
			HC	Bendix	1V
			NO _x	Bendix	1V
			Wind Direc- tion & Velocity	Climatronics	
			Single pen strip chart recorders (SCR) for each parameter which is also input into data processing computer.		
3	Trailer EPA #577	8'x14'x14'*	CO	Bendix	10V
			NO _x NO	TECO	1V
			Wind Direc- tion & Velocity	Climet	10V
			Wind Direc- tion & Velocity (2 Dimen- sions)	MRI Vector Vane	
			Temperature and Temperature Gradient	Climet	
			Single pen SCR for each paramter.		
4	Self Propelled EPA #315	Same as Site 1	NO _x	Bendix	1V
			CO	Bendix	10V
					1V
			Single pen SCR for each parameter.		
			4 multi pen SCR coordinated to common time reference to simultaneously record concentrations at Sites 1, 3, 4, 5, 6. Data logger computer to record 15 chan- nels of data from Sites 1, 3, 4, 5, 6.		
5	Trailer EPA #575	Same as Site 3	NO _x	Bendix	1V
			Single pen SCR for each parameter		
6	Trailer EPA #576	Same as Site 3	CO	Bendix	10V
			CO	Energetic Sciences Co. (2), mobile	
			HC	Beckman 400	
			Single pen SCR for each parameter		

*Includes Air Intake Probe.

**Includes 22 foot high wind set.

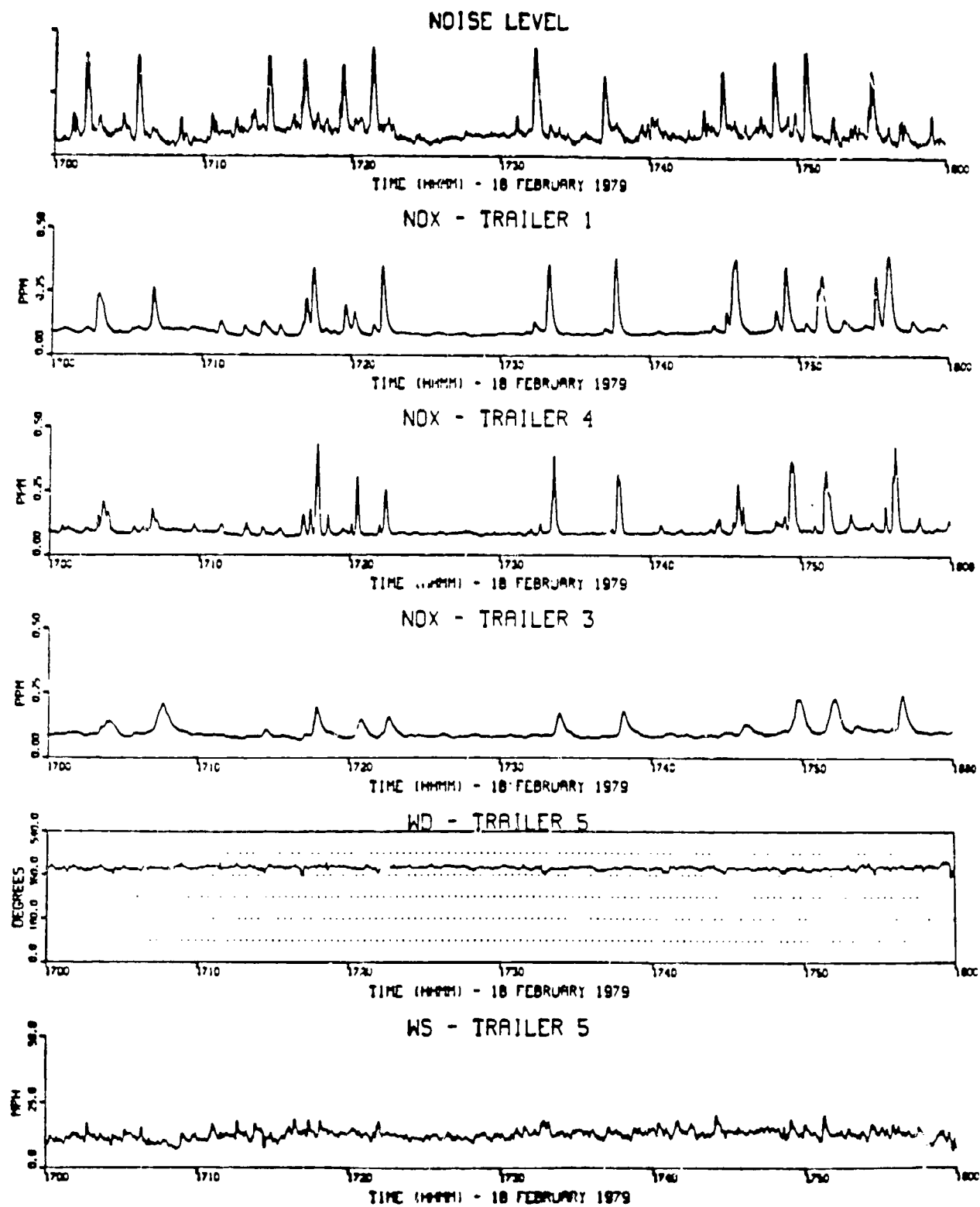


Fig. 3.2a. Synthesized Strip Chart from DAS Tapes for a Typical 2-hr Period of Northeast Winds Showing Noise and NO_x Signals

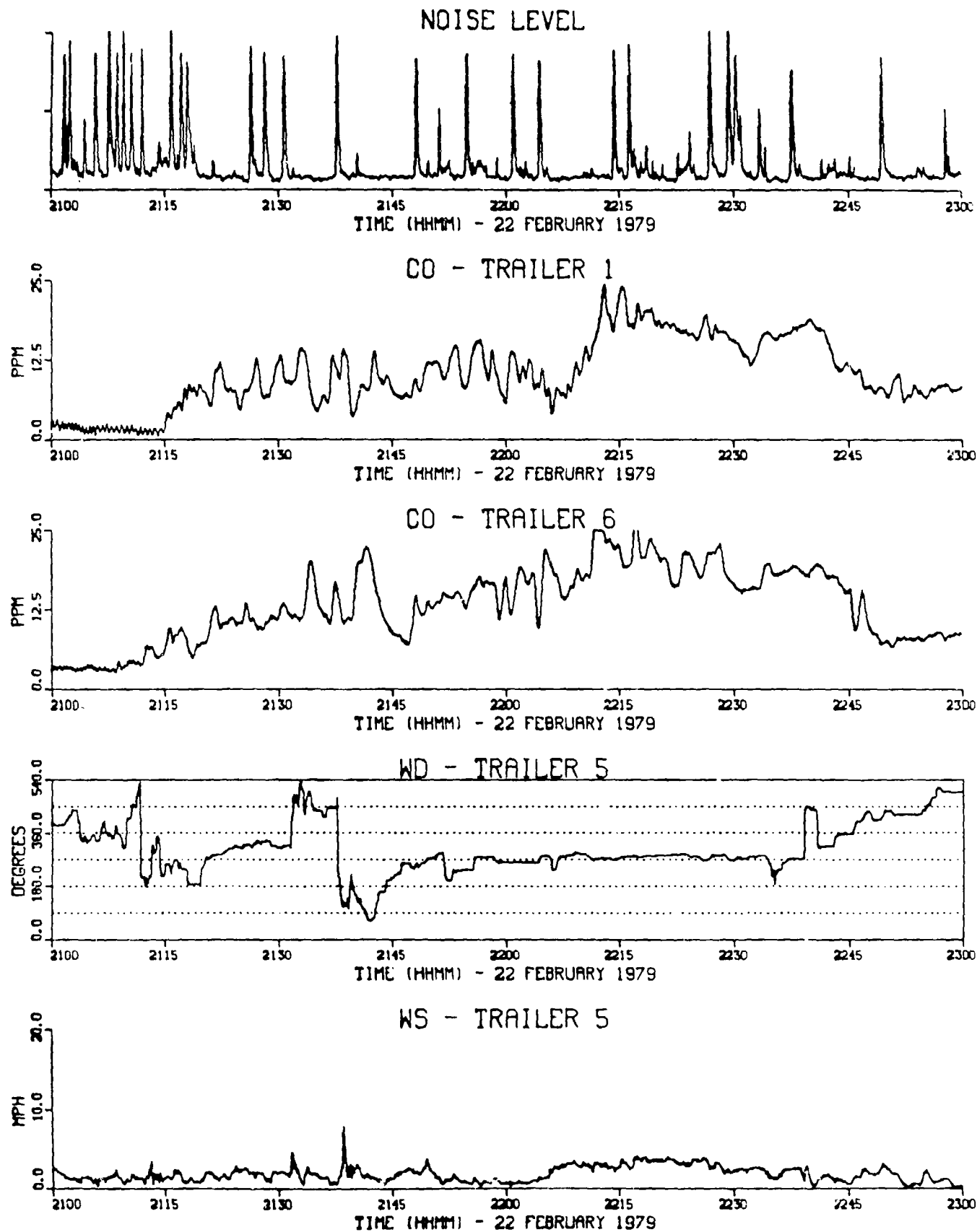


Fig. 3.2b. Synthesized Strip Chart from DAS Tapes for a Typical 2-hr of the CO Episode Beginning 2100 February 22.

RAPID SAMPLING ENABLES CONFIDENT SEPARATION OF AIRCRAFT PRODUCED AND BACKGROUND SIGNALS

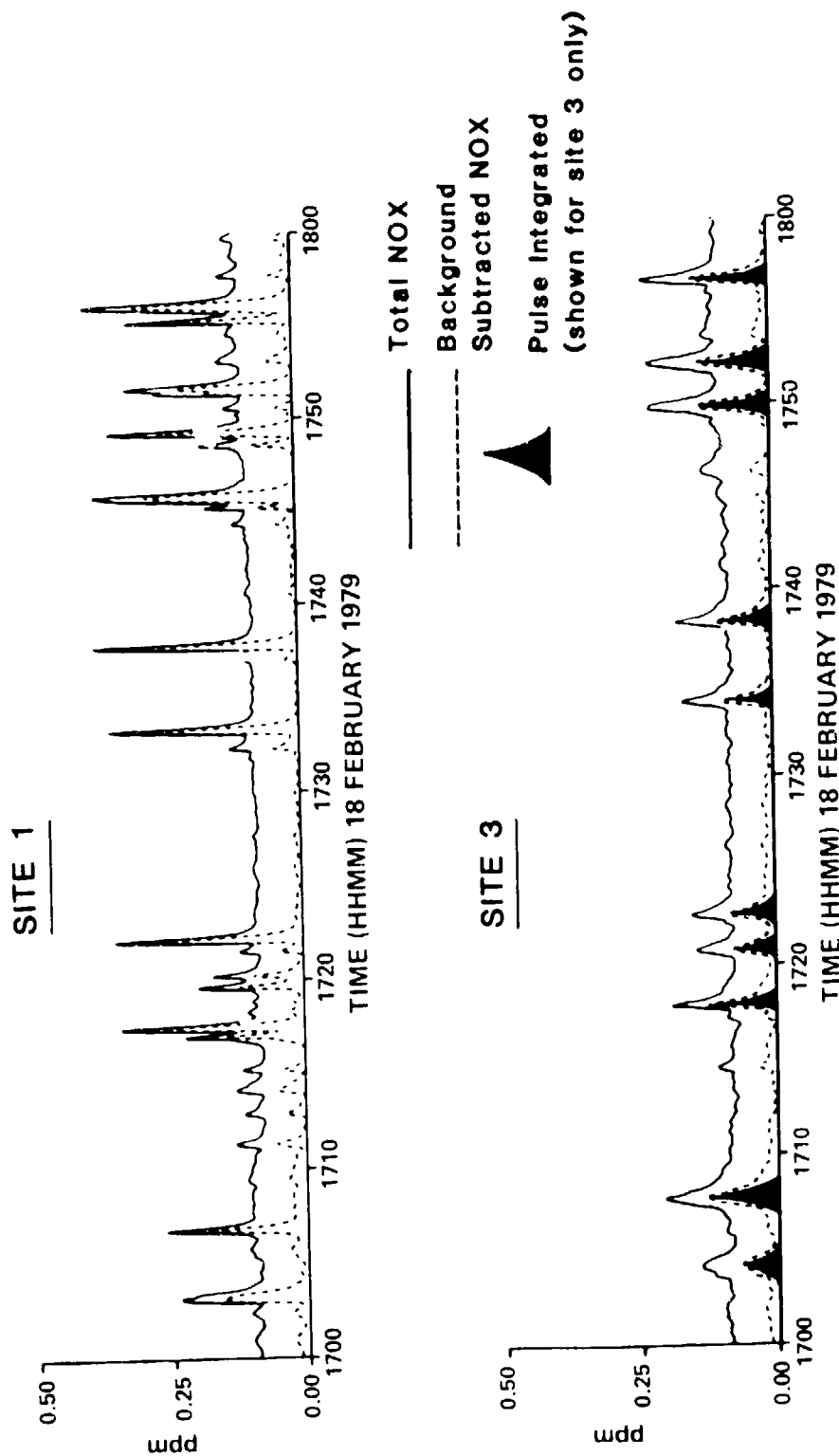


Fig. 3.3. Rapid Sampling Enables Confident Separation of Aircraft Produced and Background Signals

seen by the dotted line) or through estimation of the area under the major, aircraft related pulses (i.e. as indicated by the hatched area) via a technique requiring a threshold concentration above background to be reached before integration and thus inclusion of a particular pulse.* Analysis of these individual, aircraft generated NO/NO_x signals, with the aid of an integrated Gaussian-puff type model that simulates the high thrust, high NO_x-emitting takeoff roll and parameterizes the NO_x plume behavior in terms of initial plume dimensions and subsequent plume transport and dilution rates is reported in Section 3.6. These new plume parameterizations permit more realistic prediction of peak, short-term, NO_x levels near runways. Analysis of the CO signals, which are more difficult to associate with single aircraft operations due to the complexity of aircraft queueing, will now be discussed.

3.3 HOURLY AVERAGE MONITORING DATA FOR CO

While a number of agencies and groups concerned with the air quality impact of major airports have undertaken monitoring programs as well as theoretical studies based on the use of atmospheric dispersion algorithms, a recent review of these efforts by Lorang (1978) suggests that the issue is particularly confusing with respect to carbon monoxide. Ambient measurements conducted at Los Angeles International by Thayer et. al. (1974) and Washington National Airports by Platt et. al. (1971) were ambiguous as to their attribution of measured levels to either aircraft or non-aircraft sources. Similarly, initial modeling predictions using the NREC model [Platt et. al. (1971)] indicated the likelihood of violations of both the 1-hr ($40 \mu\text{g}/\text{m}^3$: 35 ppm) and 8-hr ($10 \mu\text{g}/\text{m}^3$: 9 ppm) standards for CO, while a more recent modeling exercise [Yamartino and Rote, (1978)] for LAX suggests "worst case" hourly CO concentrations, attributable to aircraft alone, of less than 5 ppm beyond 1000 ft from the aircraft queueing area and 2 ppm or less at the passenger terminals. Given the uncertainties generated by these monitoring and modeling experiences, the EPA and FAA chose to monitor CO near an aircraft queueing area at DCA.

*These techniques will subsequently be referred to as "background subtracted" and "pulse integrated" concentrations.

In order to facilitate comparison with air quality standards, hourly average concentrations were computed from the high repetition rate data (i.e., 1200, 3-sec scans = 1 hr). Figure 3.4 shows synthesized "strip charts" for hourly averaged CO concentrations for the entire monitoring period. In addition, a statistical summary of the hourly average CO concentrations is given in Table 3.2 for the 708 hours of nearly continuous DAS operation. Reductions in sample size result from a combination of equipment calibrations and failures and/or deliberate changes in the allocation of the 15 DAS channels among the 20 channels of incoming data. DAS logging of station 3 CO was suspended after 10 days by just such a DAS channel prioritization and because station 3 levels were not markedly different in magnitude or time dependence from those at station 4.

Figure 3.5 shows a histogram of hourly CO concentrations observed at station 6. This nearly lognormally-shaped distribution peaks near 1 ppm, which is not surprising for a receptor surrounded by a large metropolitan area. The more interesting higher concentration values and interstation comparisons are more conveniently presented in the cumulative frequency distributions of Fig. 3.6. One observes that concentrations at monitors 1 and 6, located within 500 ft of the aircraft, are less than 3 ppm 90% of the time. Concentrations at station 4, located 1000 ft from the queueing aircraft and at a distance comparable to that where the closest public exposure might occur, are not observed to exceed 3.2 ppm.

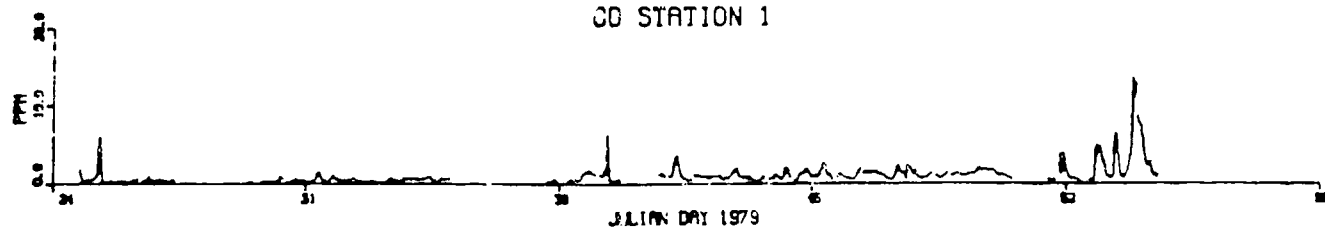
It should be pointed out that all station 1 and 6 concentrations in excess of 10 ppm correspond to a single episode that persisted from 2100 hrs February 22 through 0500 hrs February 23, under near calm, stable conditions. CO levels, wind speed and direction, and noise level (indicating departures) for this period are shown in Figure 3.7. Though the 1-hr standard was never approached, the 8-hr standard was exceeded by 38%. More careful analysis of this rather unique period suggests that airport snowplows, operating intensively in the vicinity of station 1 and 6, may have been significant contributors to these maximum observed CO values. In addition, the generally westerly nature of the wind would not have been conducive to transporting pollutants from the queueing area. However, because of the very low wind speeds 2 mph and the highly variable wind direction ($\sigma_\theta \approx 60^\circ$), significant contribution of aircraft cannot be precluded. Further, linear extrapolation (appropriate here assuming

Table 3.2. DCA Monitoring Experiment CO

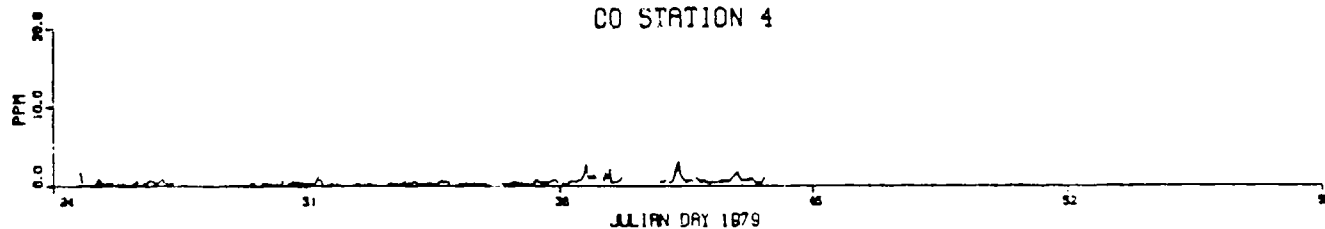
	Station 1	Station 4	Station 3	Station 6	EcoLyzer 6
Mean (ppm)	0.98	0.46	0.36	1.30	1.68
Standard Deviation (ppm)	1.32	0.41	0.34	1.46	1.57
Minimum (ppm)	0.13	0.13	0.13	0.13	0.29
Maximum (ppm)	13.43	3.14	2.37	16.34	17.81
Number of Hours	562	386	168	679	708
Geometric Mean (ppm)	0.62	0.33	0.26	0.39	1.36
Geometric Standard Deviation (ppm)	2.58	2.55	2.11	2.22	1.81
Number of Values < Threshold*	89	130	74	29	0

*Values < instrument threshold (0.25 ppm) included as 1/2 threshold.

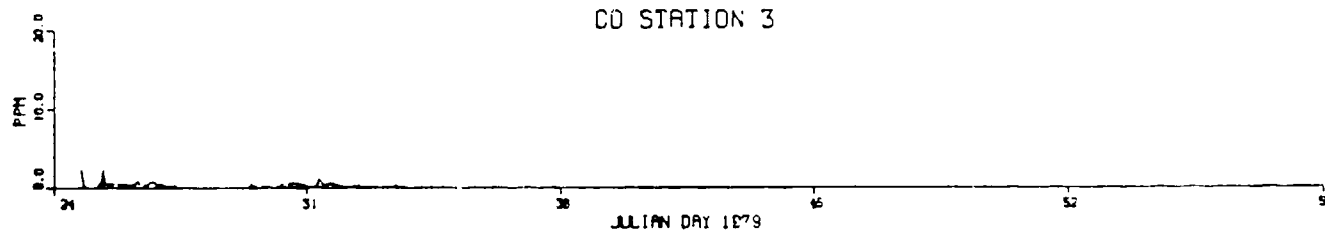
CO STATION 1



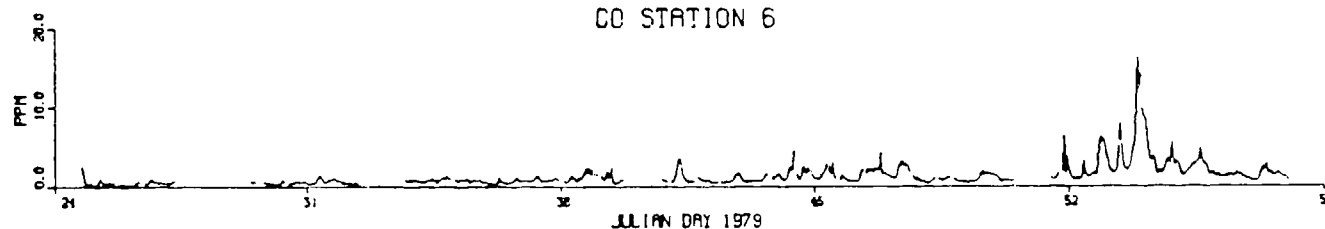
CO STATION 4



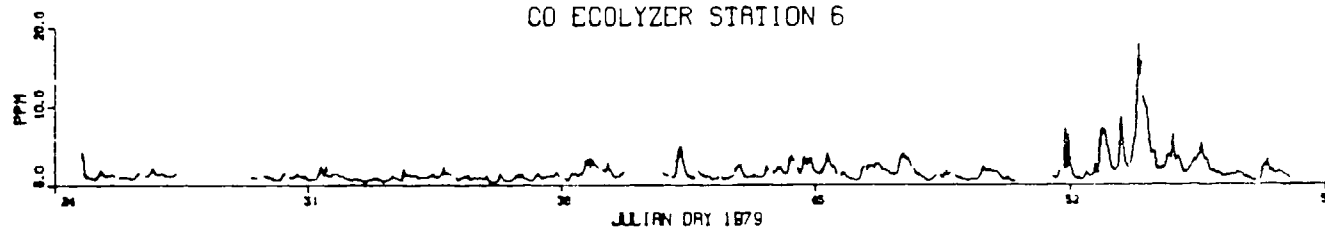
CO STATION 3



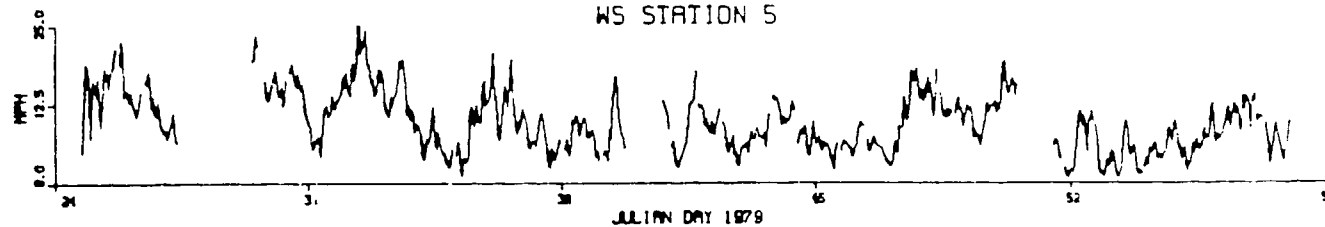
CO STATION 6



CO ECOLYZER STATION 6



WS STATION 5



WD STATION 5

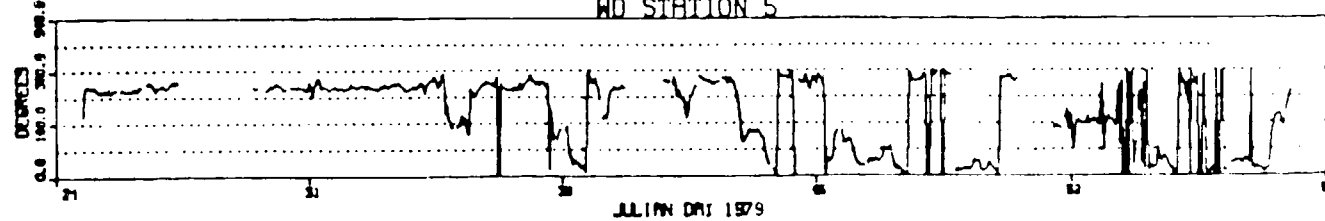


Fig. 3.4. Synthesized Strip Charts of Hourly Average CO Concentrations, Wind Speed, and Wind Direction for the Period Jan. 24-Feb. 27, 1979. These averaged data are computed from 3-sec interval DAS data.

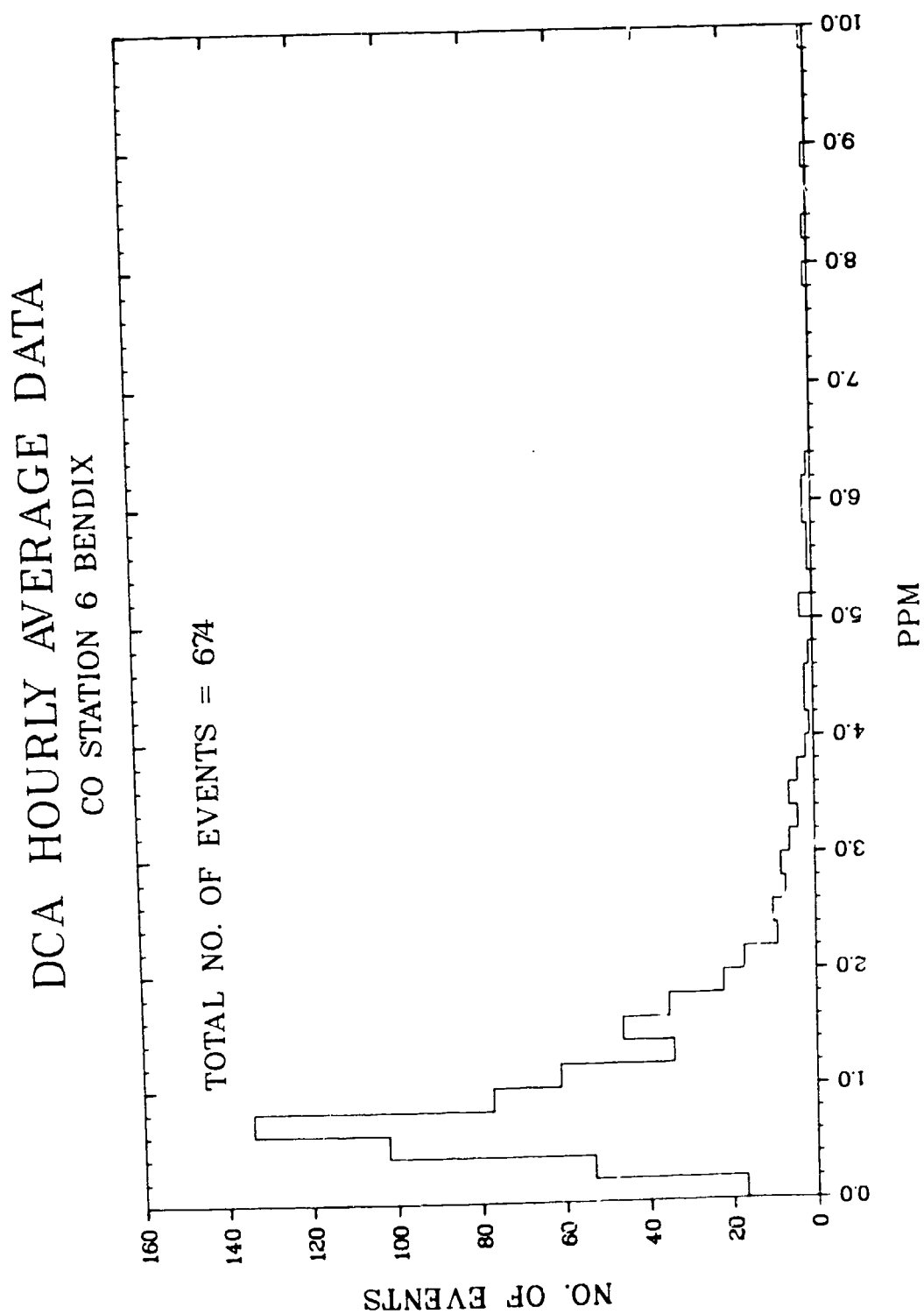


Fig. 3.5. Histogram of Hourly Average CO Concentrations at Station 6.
Not Shown are Four Values Between 10 and 16.3 ppm.

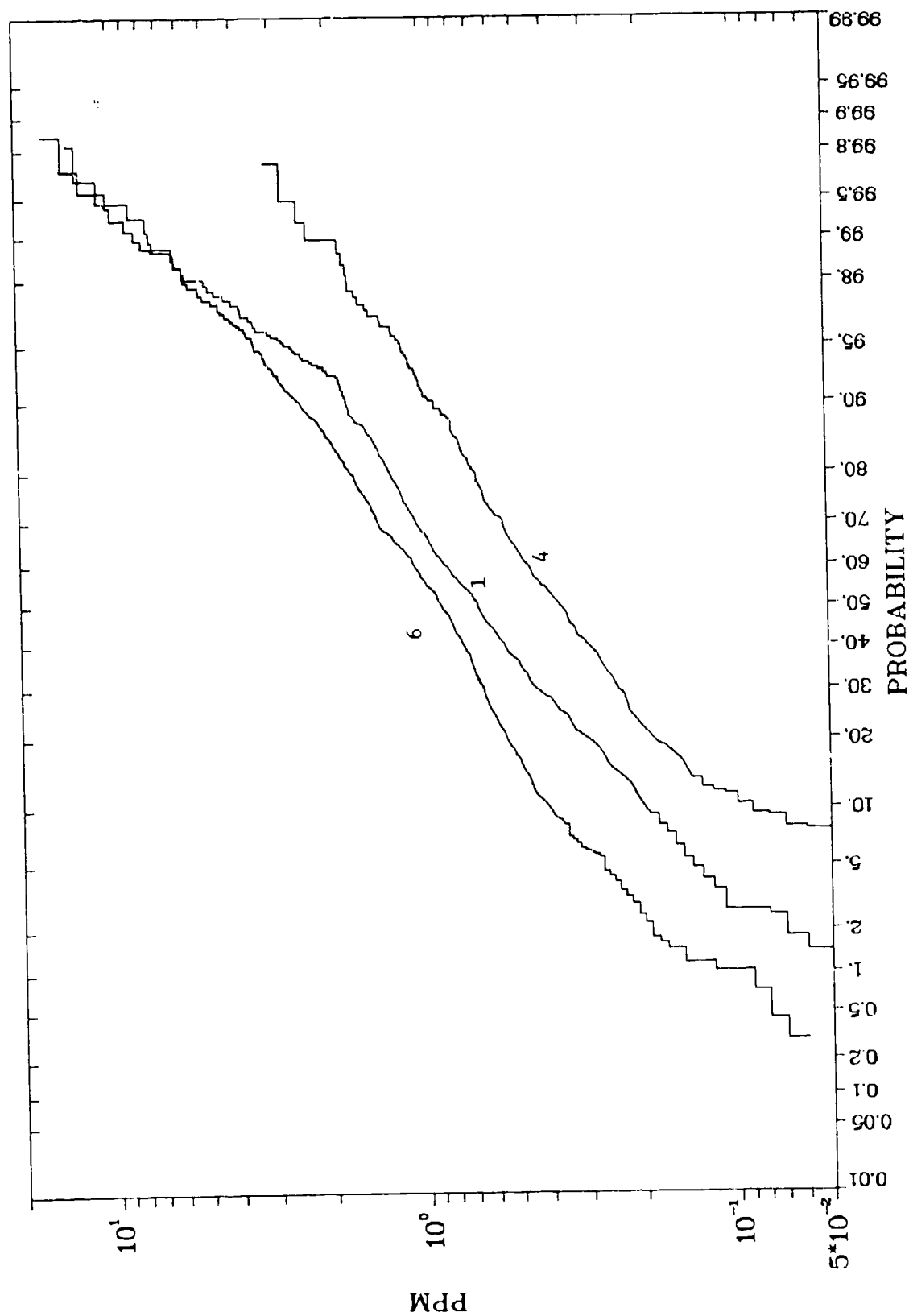


Fig. 3.6. Cumulative Frequency Distributions of Hourly CO Concentrations at Stations 1, 4, and 6.

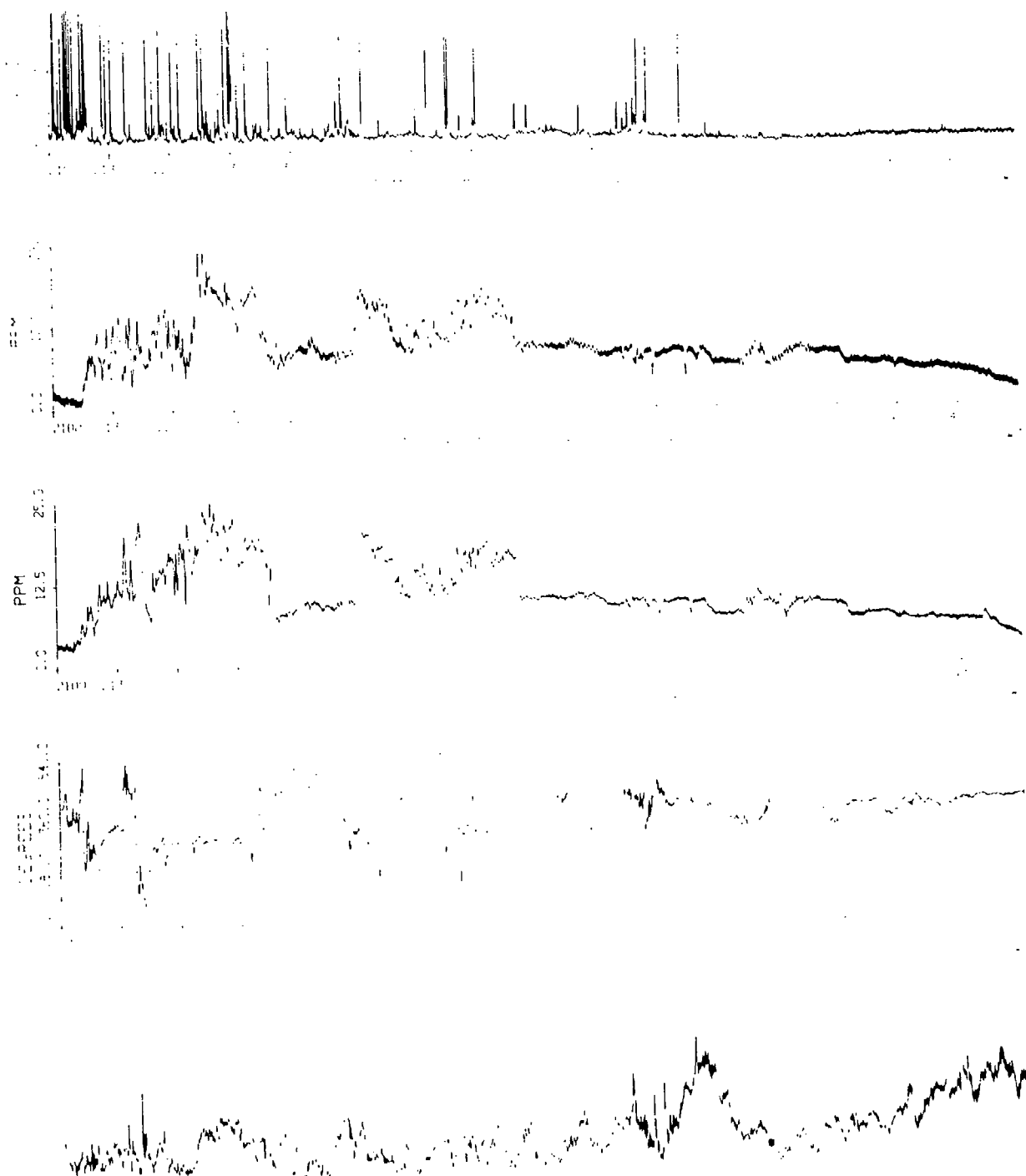


Fig. 3.7. Synthesized Strip Chart from DAS Tapes for the 8-hour Period Beginning 2100 February 22 and Including the Entire CO Episode

lognormal concentration distributions) of the cumulative frequency distribution upward from below 10 ppm suggests that these greater-than-10 ppm values could occur. However, there is some question whether the observation of high concentrations at locations in such close proximity to the aircraft is relevant to the question of NAAQS violations. Lastly, we note that similarly high CO values were observed during this period by the local pollution control agency monitors throughout the entire Washington area.

Extrapolation of the curves in Fig. 3.6 out to the 99.99% probability level (i.e., 1 hr in 10,000 or approximately once per year), while informative, should be viewed with caution, as not only is such extrapolation based on only 1/12 of a year's data, but all these data come from a single contiguous set of hours rather than from a random selection of hours throughout the year.

Figures 3.8-3.10 represent an attempt at setting bounds on the aircraft contribution to the three curves in Fig. 3.6. In each of these figures the uppermost curve represents the distribution of total hourly average CO concentrations (same as Fig. 3.6), and thus represents the maximum possible impact of aircraft. The next lower lying curves (labeled 2) represent the "background" subtracted concentrations, where, in lieu of station 2 observations, "background" is defined as the average of the 12 minimum concentrations observed during the consecutive 5-min periods making up the hour. Coincidence of curves 1 and 2 at the lower concentrations arises when actual background is below instrument threshold and thus yields a "zero background" upon subtraction. The lowest lying curves (labeled 3) represent the average concentrations contributed by pollution pulses rising at least 0.35 ppm* above a 15-min average "background" and subsequently corrected upward by the factor $1/\text{erf} [\sqrt{\ln (C_p/C_T)}]$, where C_p is the peak pulse concentration above background, to compensate for this 0.35 ppm "barrier" C_T . Curve 3 thus isolates the contribution of nearby transient pollution sources. The fixed size of the "barrier" accounts for convergence of curves 2 and 3 at high concentrations. Thus, the actual aircraft (or more properly, local source) contribution to observed concentrations probably lies somewhere within the band defined by curves 1 and 3.

*This threshold barrier and the 0.035 ppm barrier for the NO_x analysis were chosen by searching for the plateau region which is observed when the pulse integrated concentration is plotted as a function of threshold barrier level.

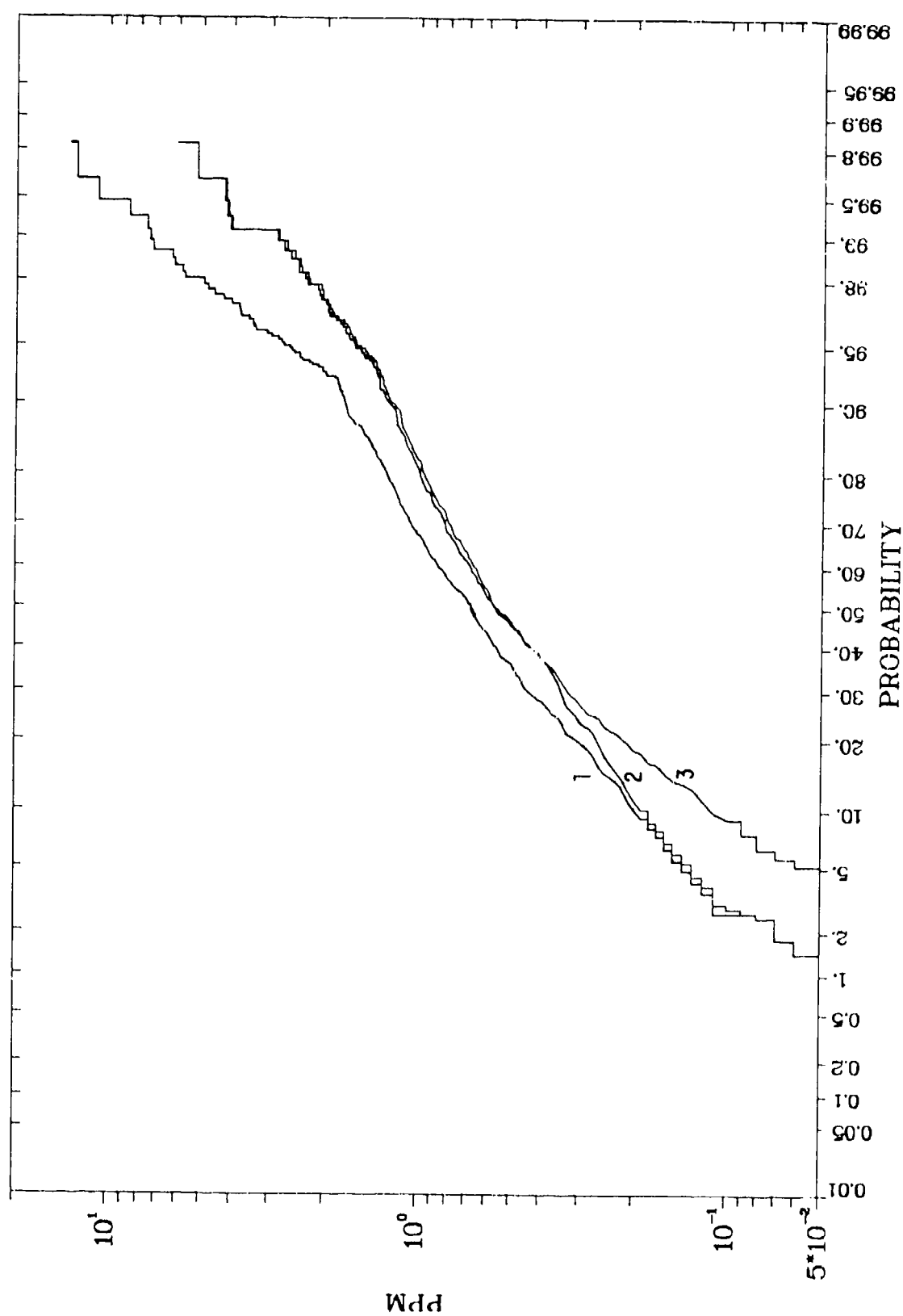


Fig. 3.8. Cumulative Frequency Distributions of Hourly CO Concentrations at Station 1. The three curves are explained in the text.

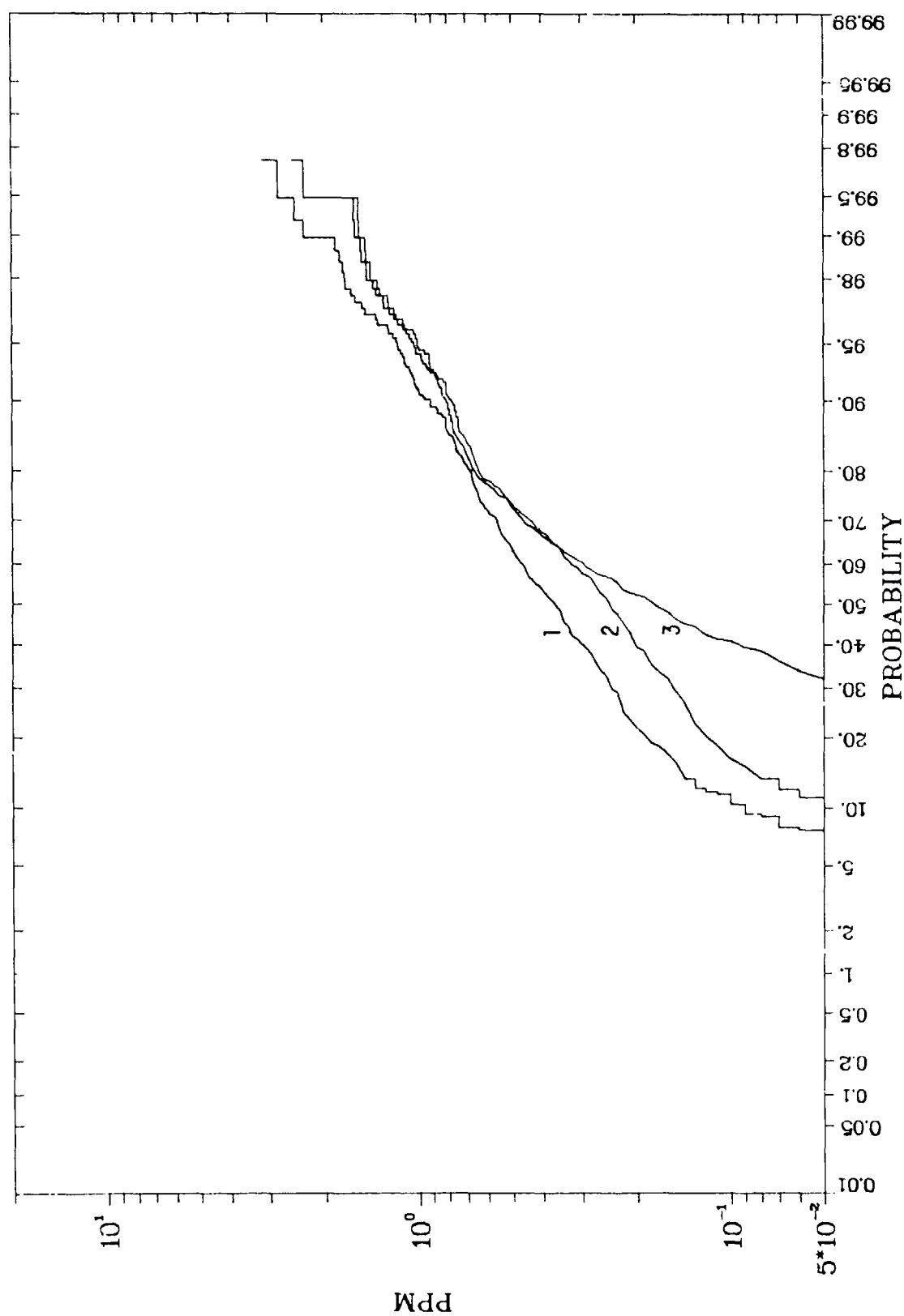


Fig. 3.9. Cumulative Frequency Distributions of Hourly CO Concentrations at Station 4. The three curves are explained in the text.

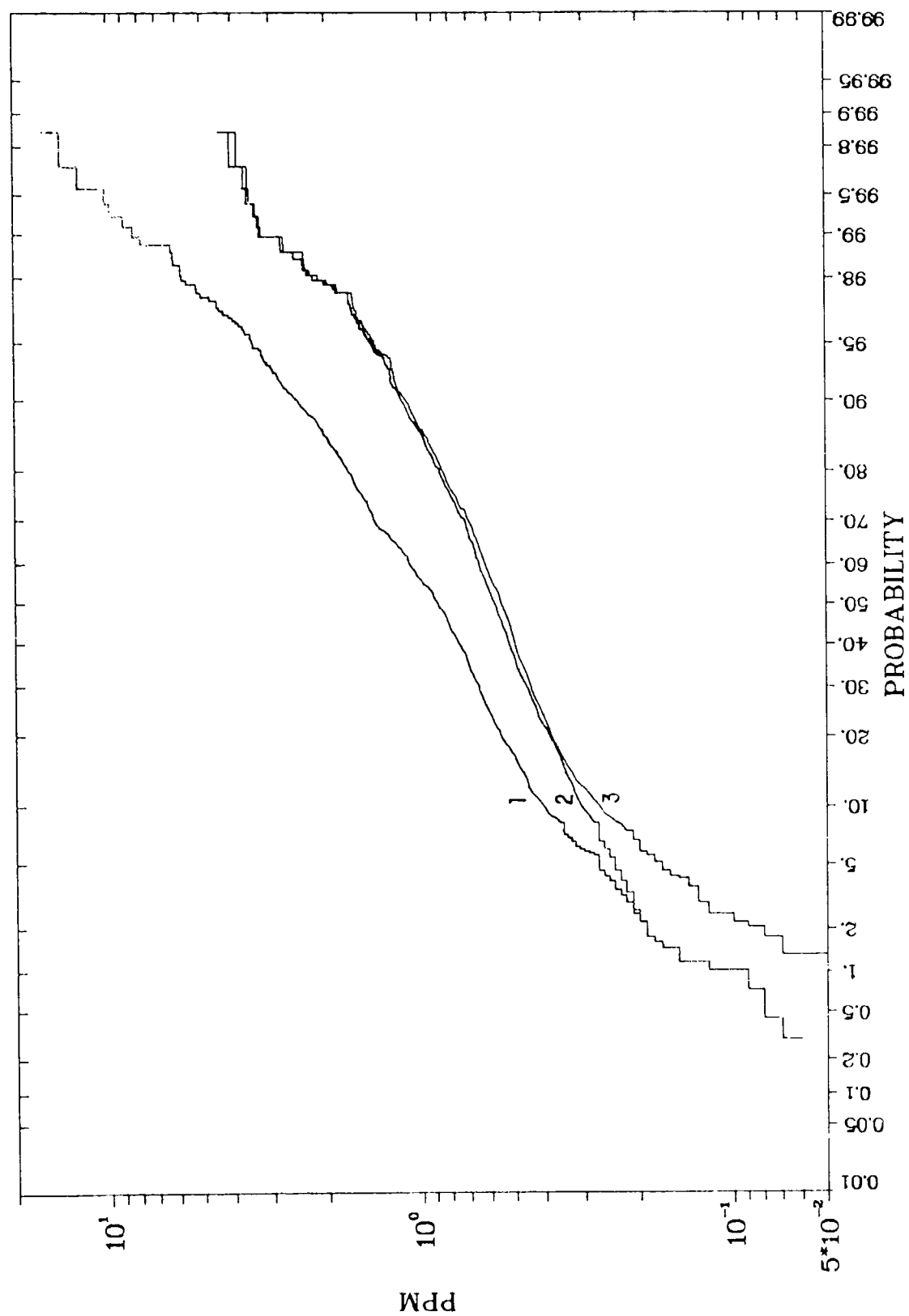


Fig. 3.10. Cumulative Frequency Distributions of Hourly CO Concentrations at Station 6. The three curves are explained in the text.

Keeping in mind previous cautions about extrapolation of these curves, one notes that at station 4, located ≈ 1000 ft from the queueing area, a maximum hourly CO concentration of ≈ 5 ppm may be expected about once per year. This result is consistent with "worst case" predictions for LAX, seen in Fig. 3.11, where a fleet mix and queueing emissions comparable to DCA are assumed. Further extrapolations or generalizations from the DCA results to other airports should be tempered by the following considerations:

- DCA is closed between 10:00 p.m. and 6:00 a.m. These nighttime hours are associated with stable atmospheric conditions and thus potentially poor pollutant dispersion conditions.
- Runway 36 at DCA is shared between arrivals and departures. Though not an unusual situation, airports having dedicated departure runways should, for the same departure rate, have shorter queueing times and correspondingly reduced CO emissions and concentrations.
- Nearly all operations at DCA are by medium range jets (e.g., 727, 737, DC9) primarily using the JT8D-17 engine. This engine has a relatively low CO emission rate at idle (≈ 40 lbs/hr)⁸ compared to some other engines (e.g., 88 lbs/hr for the CF6-50C and ≈ 140 lbs/hr for the JT9D-7 and RB-211-22B).⁸

3.4 HOURLY AVERAGE MONITORING DATA FOR OXIDES OF NITROGEN

The issue of oxides of nitrogen (NO_x) impacts created by aircraft is, as with CO, a localized "hot-spot" problem related to existing and potential NAAQS. Unfortunately the issue is further complicated by the fact that

- present and possible future NAAQS standards pertain to NO_2 levels and not NO_x levels. ($\text{NO}_x \approx \text{NO} + \text{NO}_2$)
- there is presently only an annual average NAAQS of 0.05 ppm NO_2 through a one hour average standard in the range 0.2-0.5 ppm is presently being considered by the EPA
- plume dispersion, while reducing the concentration of inert species, will entrain more ambient oxidant resulting in further conversion of engine emitted NO to NO_2 ; thus, NO_2 levels will peak at some distance downwind of the aircraft
- the peak NO_2 attributable to aircraft is a function of existing ambient levels of NO, NO_2 , O_3 , and sunlight.

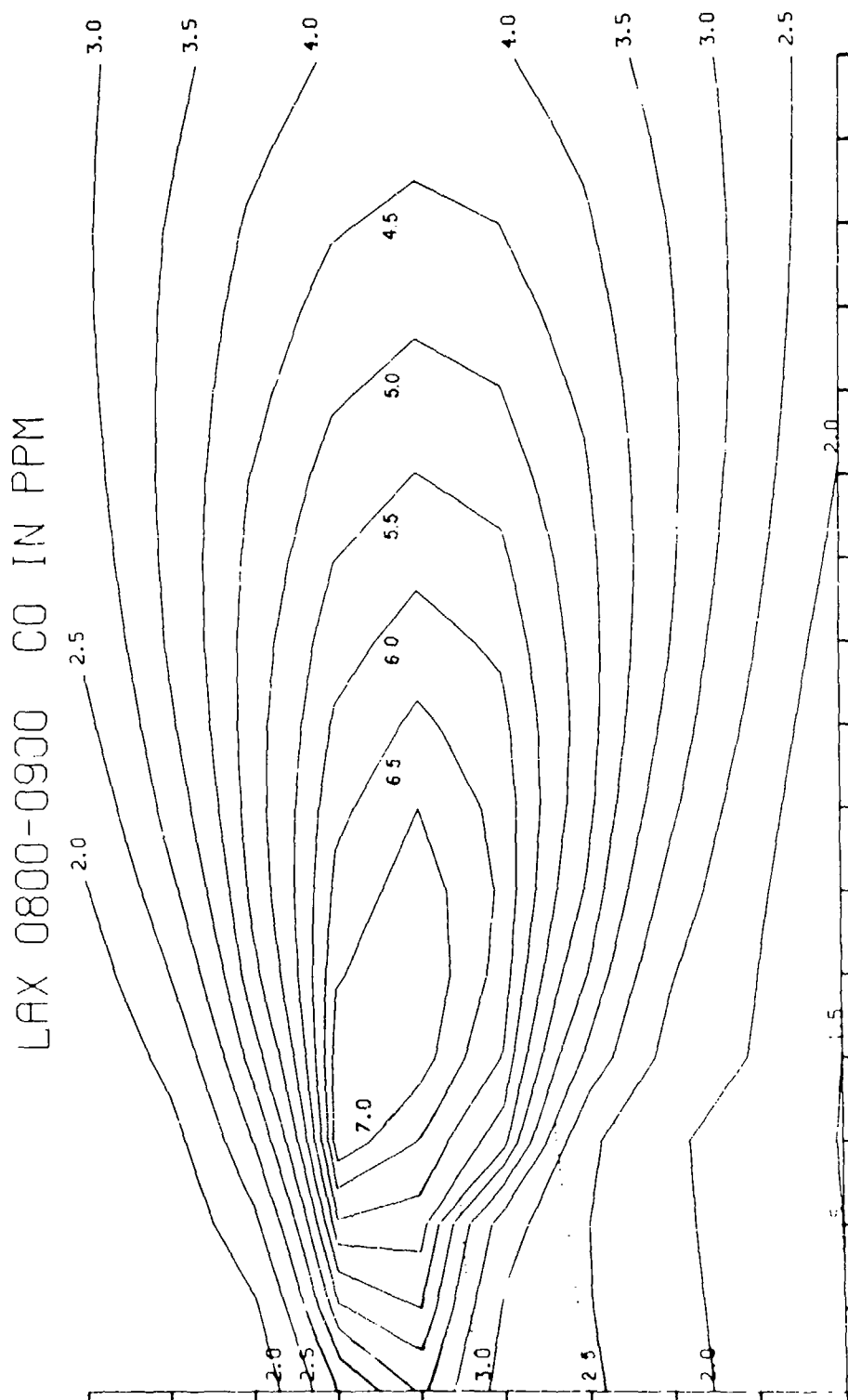


Fig. 3.11. CO Concentration Isopleths from Aircraft Operations on the Southern Runway Complex at LAX Under "Worst Case" Operations and Dispersion (i.e., E stability and a 2 knot wind from the West) Conditions. Computation Grid Size = 0.05 Miles.

The potential for violation of possible NO_2 peak hourly standards at airports has recently been reviewed by Jordan and Broderick (1978). Finding that both worst case modeling predictions and previous monitoring results were in the same 0.25-0.5 ppm range as the potential NO_2 standards, was one of the principal motivating factors for the DCA experiment. Rather than simply accumulating more NO/NO_x data, the placement of monitors and data recording rate at DCA were chosen so as to enable separation of the aircraft contribution (i.e. in the form of short pulses associated with takeoff/landing) from continuous source and background contributions. Such a resolution of aircraft from non-aircraft sources was considered vital to the assessment of the aircraft impact on the NO_2 standard since previous monitoring [Lorang, (1978)] identified NO_2 levels of 0.3 ppm without such a separation while AVAP modeling, unable to separately predict NO_2 levels, indicates that under worst case conditions, aircraft contribute NO_x concentrations of the order of 1 ppm.

Statistical summaries of the hourly average concentrations, as computed from the high sampling rate data, are given in Tables 3.3-3.5 for NO_x , NO , and NO_2 ($= \text{NO}_x - \text{NO}$) respectively. The fact that the highest observed values of NO and NO_x saturate the recording equipment and are outside the calibrated range of the NO/NO_x instruments is indeed unfortunate and casts some doubt upon the validity of the NO_2 data computed by subtraction of the NO from the NO_x concentrations.

Figures 3.12-3.14 show the cumulative frequency distributions of concentrations for NO_x , NO , and NO_2 respectively. Aside from slightly lower NO and NO_x values at station 1, one notes a striking similarity between the distributions from the different stations. Examination of these plots indicates that 95% of the time concentrations of NO_x , NO , and NO_2 are less than 0.2 ppm, 0.1, and 0.07 ppm respectively.

Interestingly, the hours corresponding to saturations of the recorders for NO and NO_x are the same hours of the CO episode. The fact that NO and NO_x from station 1 were not recorded during this episode period (due to the severing of the signal lines by a snowplow) accounts for the lowered distribution in these highest percentile ranges. Further, the fact that this pollution episode affected stations 3 and 5, in addition to 1 and 6, tends to further confirm that the episode covered a wider area than could be inferred from the CO data.

Table 3.3. DCA Monitoring Experiment NO_x

	Station 1	Station 4	Station 3	Station 5
Mean (ppb)	54.79	62.16	58.63	63.29
Standard Deviation (ppb)	50.54	74.81	69.62	74.64
Minimum (ppb)	2.50	5.80	7.00	6.40
Maximum (ppb)	433.00	559.20 ^s	551.90 ^s	534.20 ^s
Number of Hours	683	708	683	704
Geometric Mean (ppb)	38.80	42.58	41.24	43.31
Geometric Standard Deviation	2.35	2.23	2.15	2.24
Number of Values < Threshold*	7	0	0	0

*Values < instrument threshold (5 ppb) included as 1/2 threshold

^sindicates instrument saturation

Table 3.4. DCA Monitoring Experiment NO

	Station 1	Station 3
Mean (ppb)	25.06	29.26
Standard Deviation (ppb)	38.92	62.70
Minimum (ppb)	2.50	2.50
Maximum (ppb)	360.50	549.20 ^s
Number of Hours	683	683
Geometric Mean (ppb)	10.85	11.32
Geometric Standard Deviation	3.66	3.62
Number of Values < Threshold*	227	196

*Values < instrument threshold (5 ppb) included as 1/2 threshold

^sindicates instrument saturation

Table 3.5. DCA Monitoring Experiment NO₂

	Station 1	Station 3
Mean (ppb)	30.22	29.38
Standard Deviation (ppb)	17.39	15.04
Minimum (ppb)	2.5	2.7
Maximum (ppb)	91.90	86.70
Number of Hours	679	683
Geometric Mean (ppb)	24.84	25.49
Geometric Standard Deviation	1.97	1.74
Number of Values < Threshold*	-	-

*Values < instrument threshold (5 ppb) included as 1/2 threshold

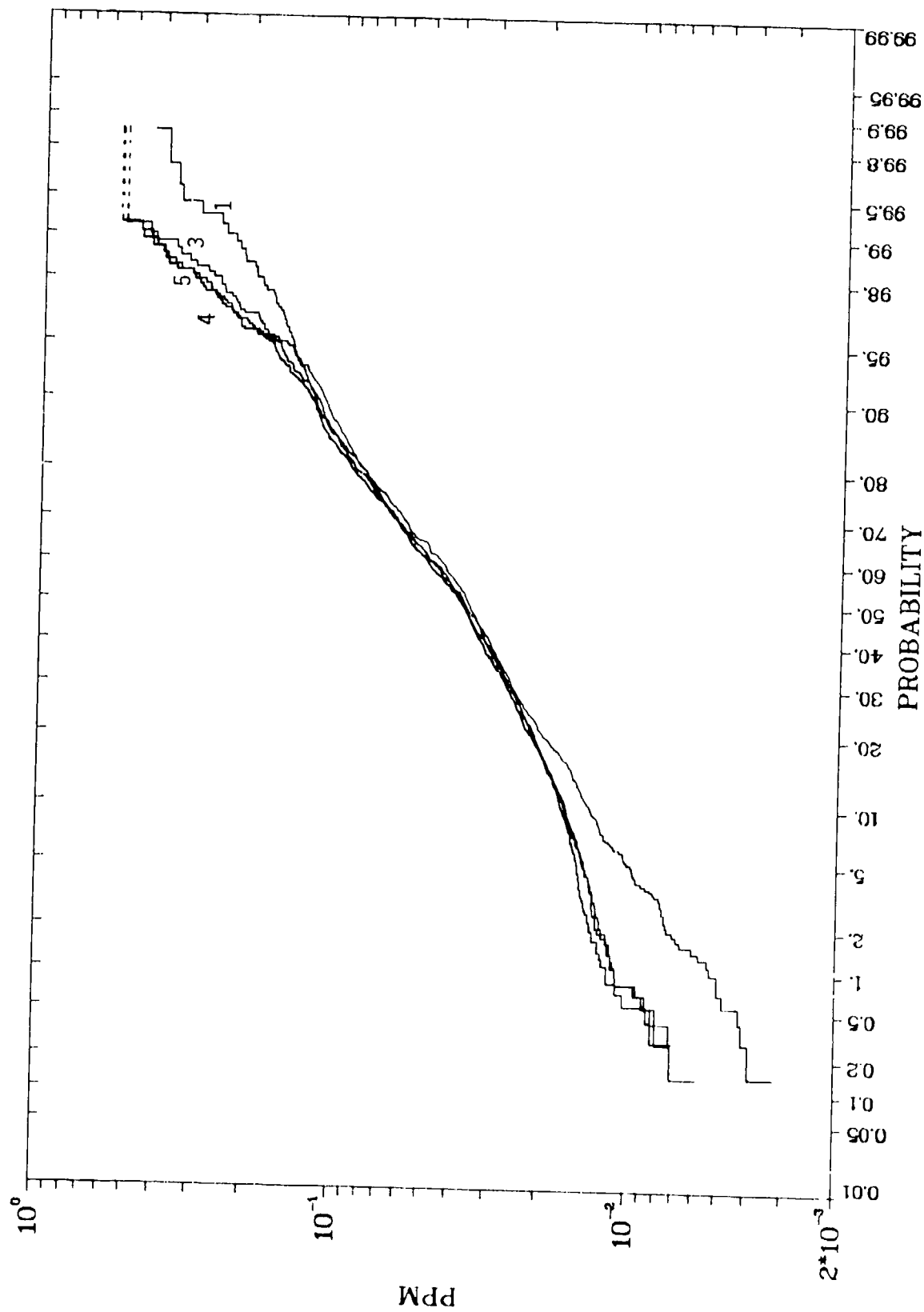


Fig. 3.12. Cumulative Frequency Distributions of Hourly NO_x Concentrations at Stations 1, 3, 4, and 5. Dashed lines indicate instrument saturation.

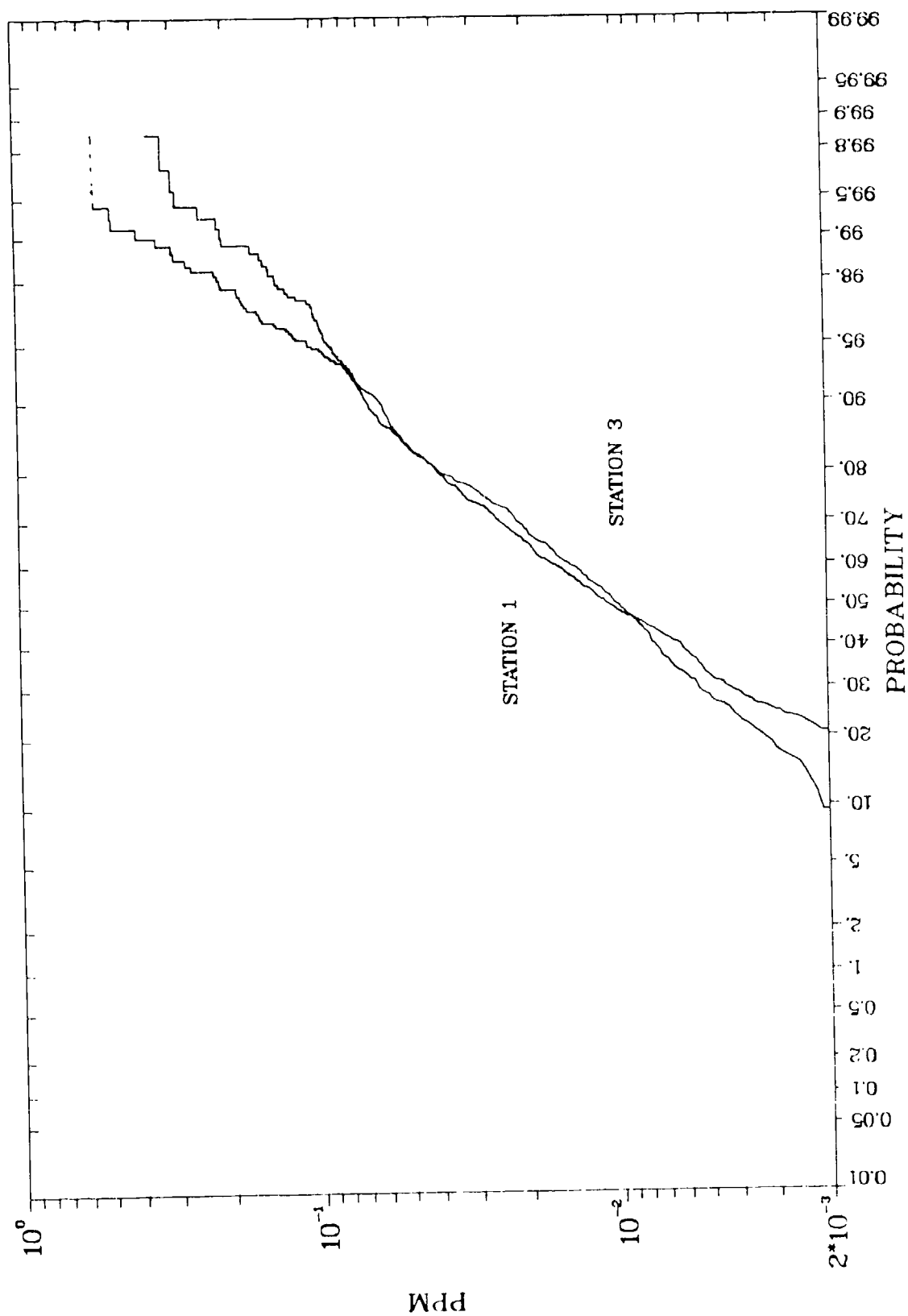


Fig. 3.13. Cumulative Frequency Distributions of Hourly NO Concentrations at Stations 1 and 3.
Dashed lines indicate instrument saturation.

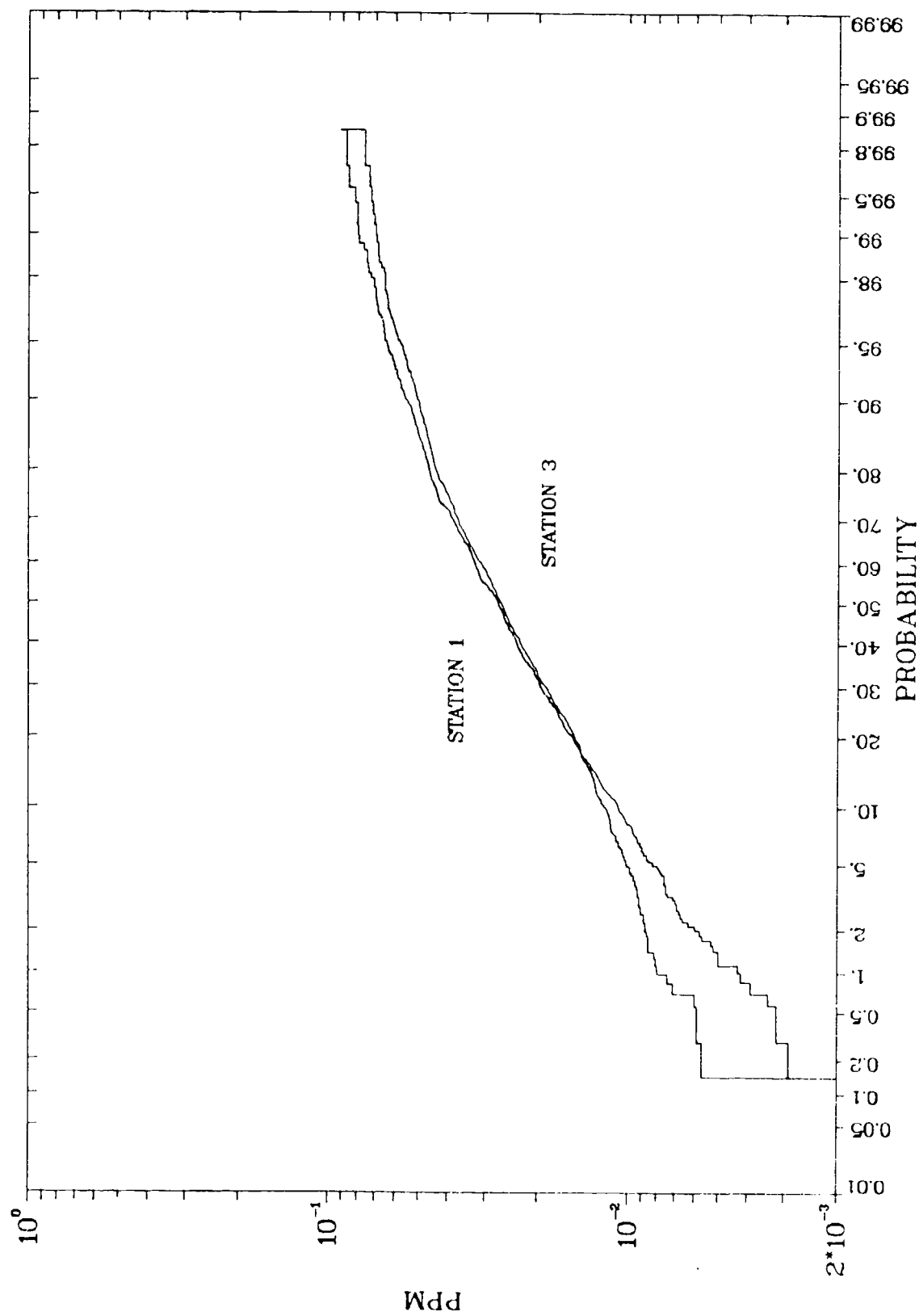


Fig. 3.14. Cumulative Frequency Distributions of Hourly NO_2 ($\equiv \text{NO}_2 - \text{NO}$) Concentrations at Stations 1 and 3.

In an analogous manner to the method used for the CO analysis, Figures 7.15-7.20 represent an attempt to estimate the aircraft contributions to the distributions given by Figs. 3.12-3.14. Figures 3.15-3.17 represent the "background" subtracted concentrations, where, in lieu of continuous station 2 observations, "background" is defined as the average of the 12 minimum concentrations observed during each 5-min period making up the hour. Figures 7.18-7.20 represent the average concentrations contributed by pollution pulses rising at least 0.035 ppm above a 15-min average "background" and subsequently corrected upward to compensate for this 0.035 ppm "barrier." These curves thus isolate only the nearby transient sources of pollution.

As with CO, extrapolation of the curves in Figs. 3.12-3.20 out to the 99.99% probability level (i.e., 1 hr in 10,000 or approximately once per year), as is presented in Table 3.6, should be viewed with some caution as such an extrapolation is based on only 1/12 of a year's data and all these data come from a single contiguous set of hours rather than from a random selection of hours throughout the year. That the sensitivity of such an extrapolation to extreme measured values is very high is evidenced by the fact that elimination of the one severe episode period lowers the estimated "worst case" values of NO and NO_x from ~4 ppm to ~1 ppm.

Though observed values of background subtracted and integrated pulse concentrations do not exceed 0.2 ppm for NO or NO_x and 0.05 ppm for NO₂, the extrapolations to 99.99% probability, present in Table 3.6, while highly speculative in nature, generate some cause for concern as NO₂ concentrations of order 0.3 ppm would be very close to potential hourly average NO₂ standards being investigated by the EPA.

As with CO, these NO_x results are consistent with current "worst case" model predictions for LAX, where a fleet mix and takeoff emissions comparable to, though perhaps as much as 25% higher than, DCA are assumed. AVAP modeling of LAX under worst case activity and dispersion conditions indicates (Figure 3.21) NO_x levels exceeding 0.5 ppm more than one half mile from the end of the southern* runway complex but the key question is how these NO_x levels translate into NO₂ levels. The NO₂/NO_x ratio is a function of plume dispersion rate and

*even more widespread high NO_x values are associated with the jumbo jet departures on the northern runway complex

Table 3.6. Estimated Highest Hourly per Annum* Concentrations for Oxides of Nitrogen (in ppm)

	NO _x	NO	NO ₂
Total Concentration	1.0-4.0	0.8-4.0	0.1-0.3
Background Subtracted	0.2-0.4	0.1-0.3	0.05 ³ -0.1 ¹
Pulse Integrated	0.2-0.5	0.2-0.3	0.1 ³ -0.3 ¹

*Based on visual linear extrapolation of cumulative frequency distributions to 99.99% probability. Care has been taken to avoid underestimates caused by NO/NO_x saturation at 0.5 ppm. A range is given where linear extrapolation is not unambiguous.

¹Station 1

³Station 3

transport time, sunlight intensity, and background levels of NO, NO₂, and O₃ and a reactive plume calculation is required to obtain a more definitive prediction; however, using simple assumptions regarding the amount of NO₂ emitted directly by the aircraft, the rate of NO oxidation, and the ambient O₃ level, it is reasonable to expect several tenths of ppm of NO₂ at distances of possible public exposure. Further extrapolations or generalizations to other airports should be tempered by the following considerations:

- DCA is closed between 10:00 p.m. and 6:00 a.m. These nighttime hours are associated with stable atmospheric conditions and thus potentially poor pollutant dispersion conditions.
- Nearly all operations at DCA are by medium range jets (e.g., 727, 737, DC9) primarily using the JT8D-17 engine. This engine has a relatively low NO_x emission rate at takeoff (~200 lbs/hr)⁸ compared to some other engines (e.g., 670 lbs/hr for the CF6-50C and ~475-500 lbs/hr for the JT9D-7 and RB-211-22B).⁸
- This experiment was conducted during winter months. A similar experiment during summer months could be accompanied by higher oxidant levels with resulting higher NO₂ levels.

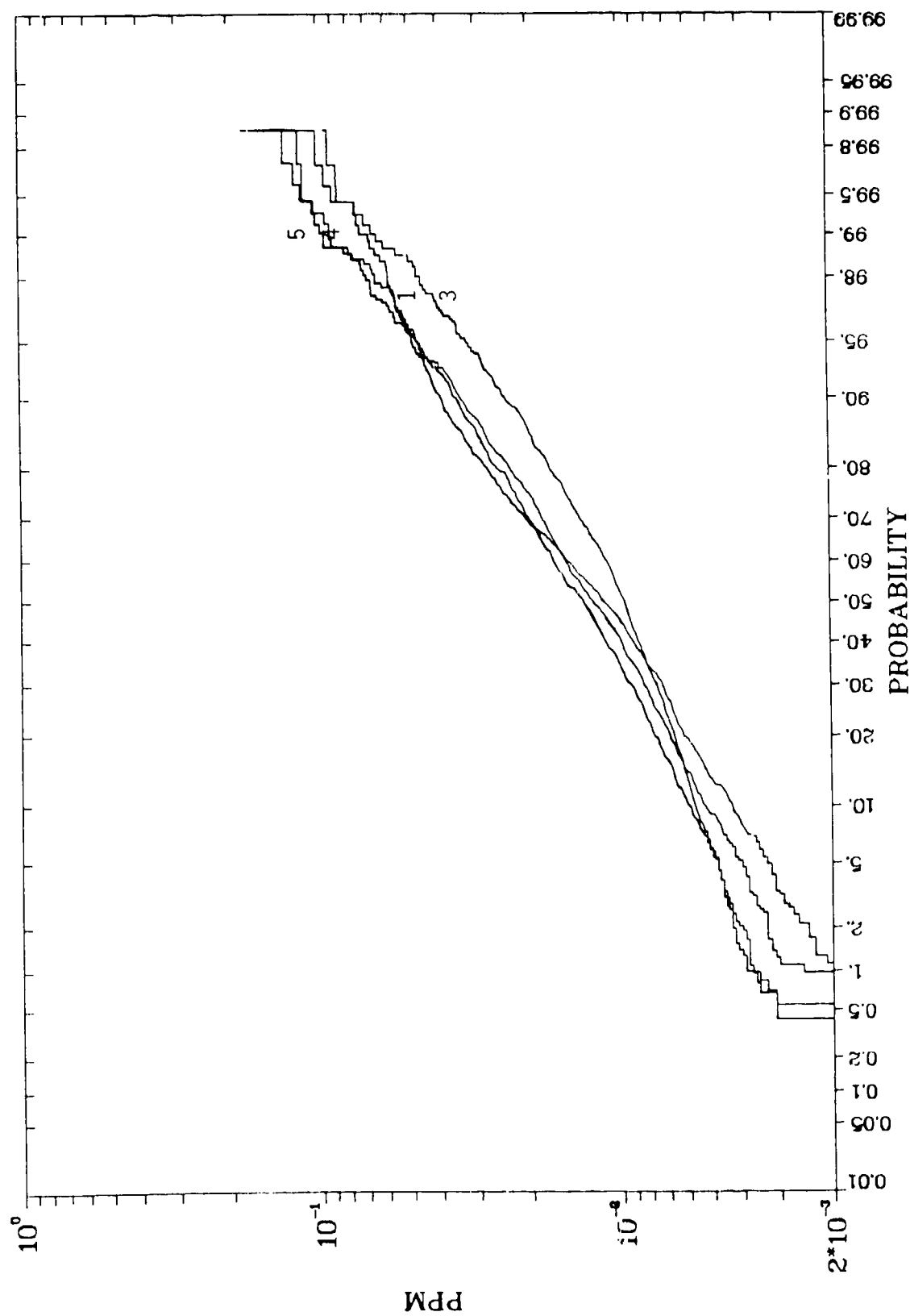


Fig. 3.15. Cumulative Frequency Distributions of Hourly Background Subtracted NO_x Concentrations at Stations 1, 3, 4, and 5

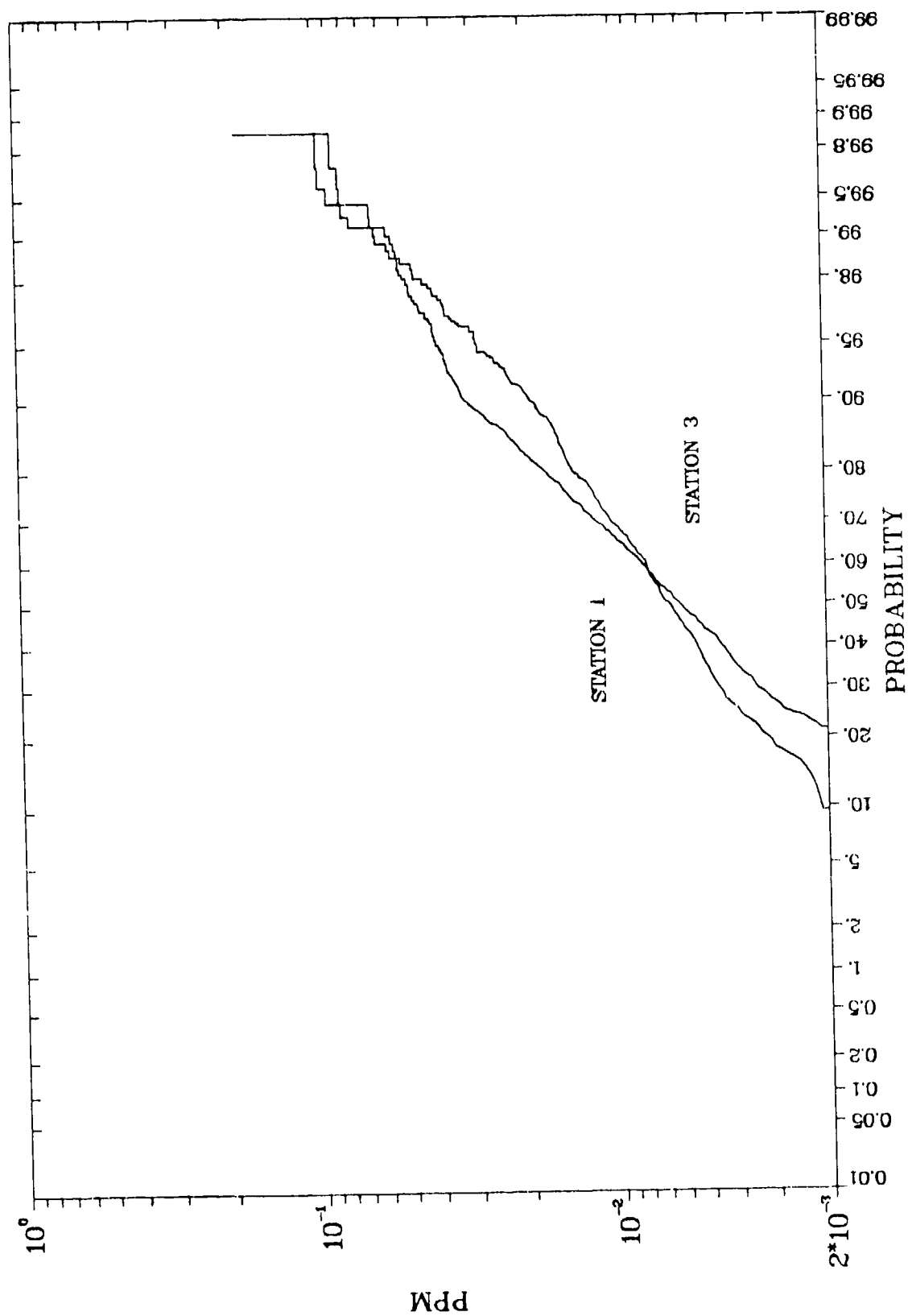


Fig. 3.15. Cumulative Frequency Distributions of Hourly Background Subtracted NO Concentrations at Stations 1, and 3.

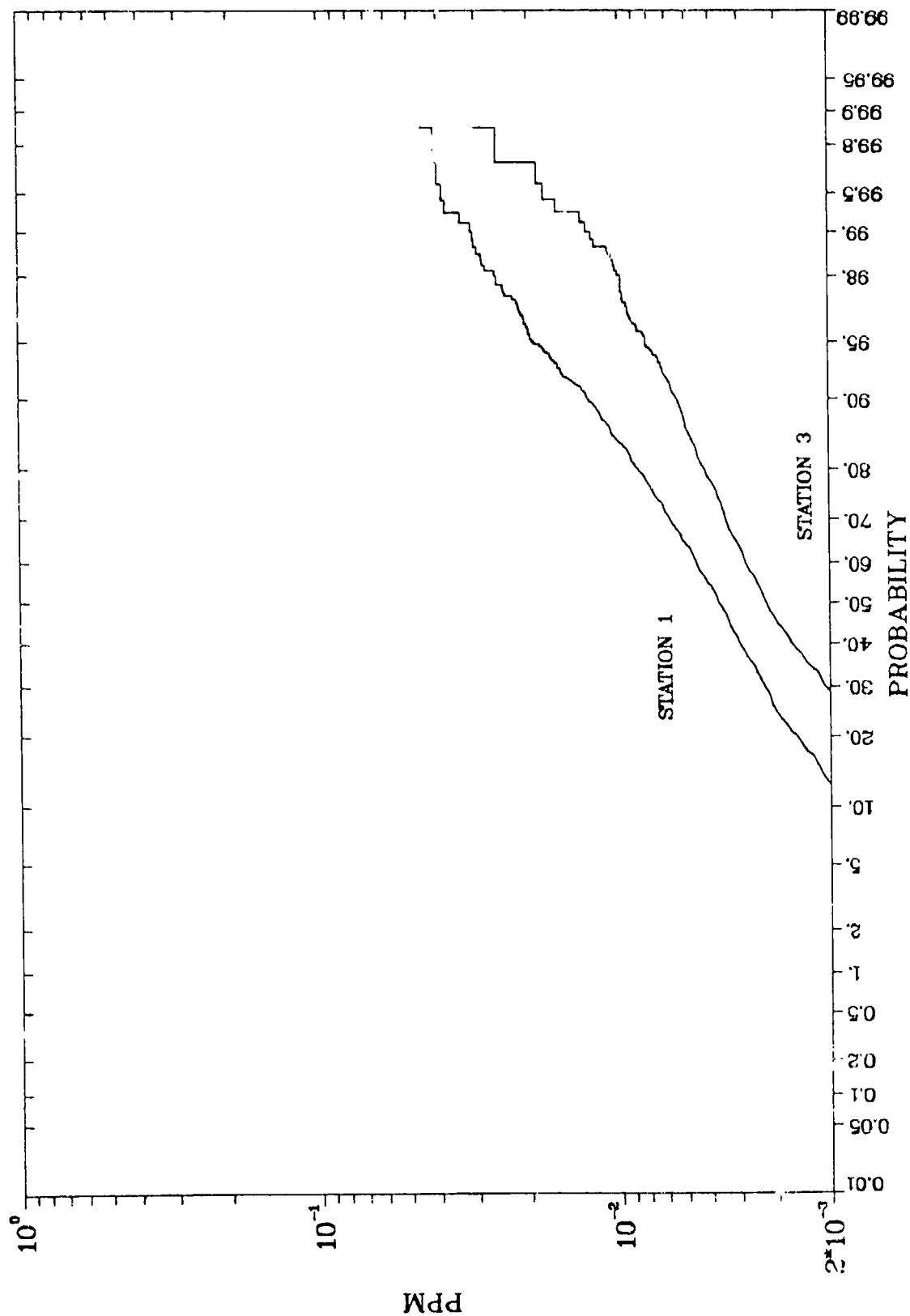


Fig. 3.17. Cumulative Frequency Distributions of Hourly Background Subtracted NO_2 ($\equiv \text{NO}_2 - \text{NO}$) Concentrations at Stations 1 and 3.

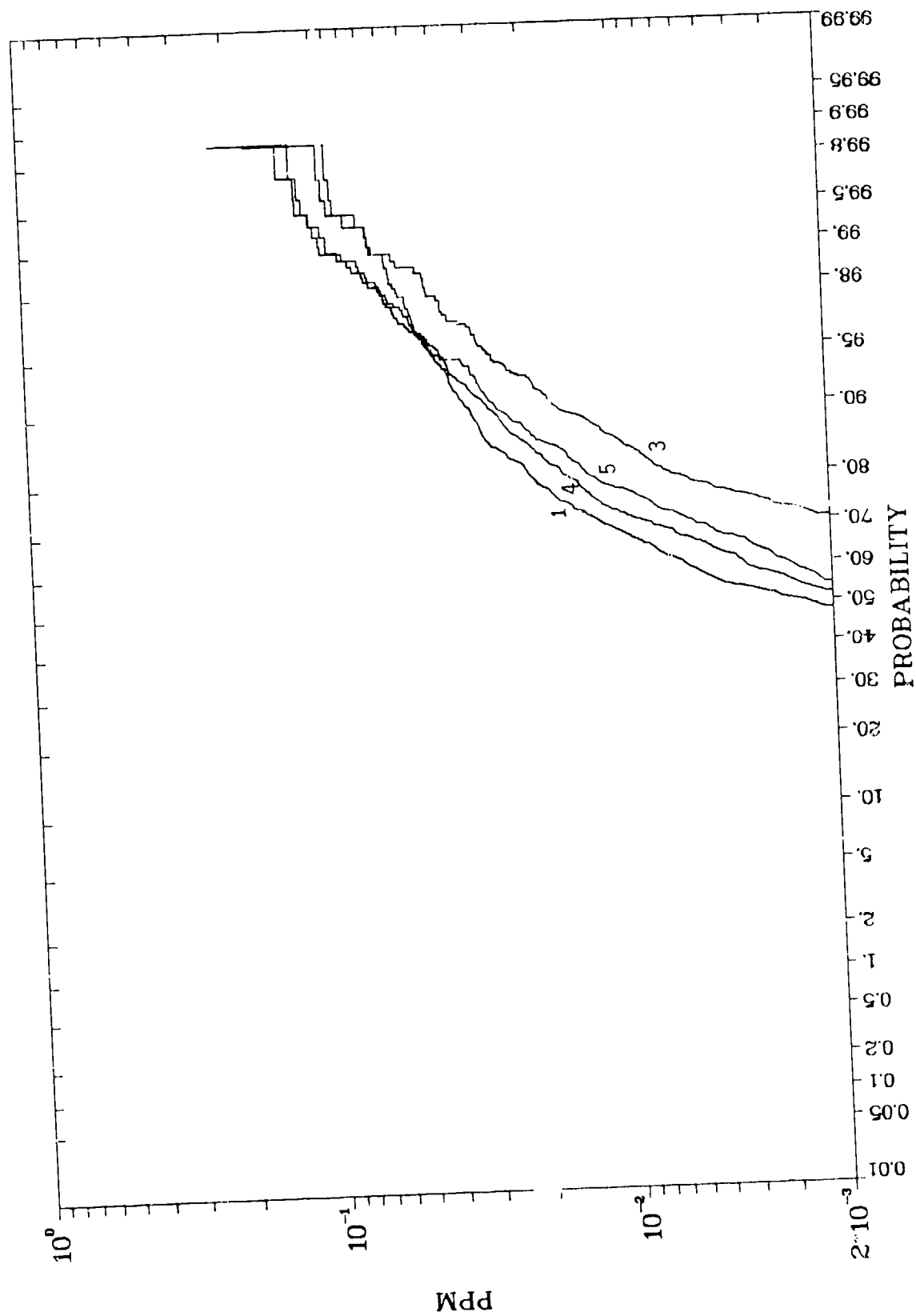


Fig. 3.18. Cumulative Frequency Distributions of Hourly Integrated Pulse NO_x Concentrations at Stations 1, 3, 4, and 5.

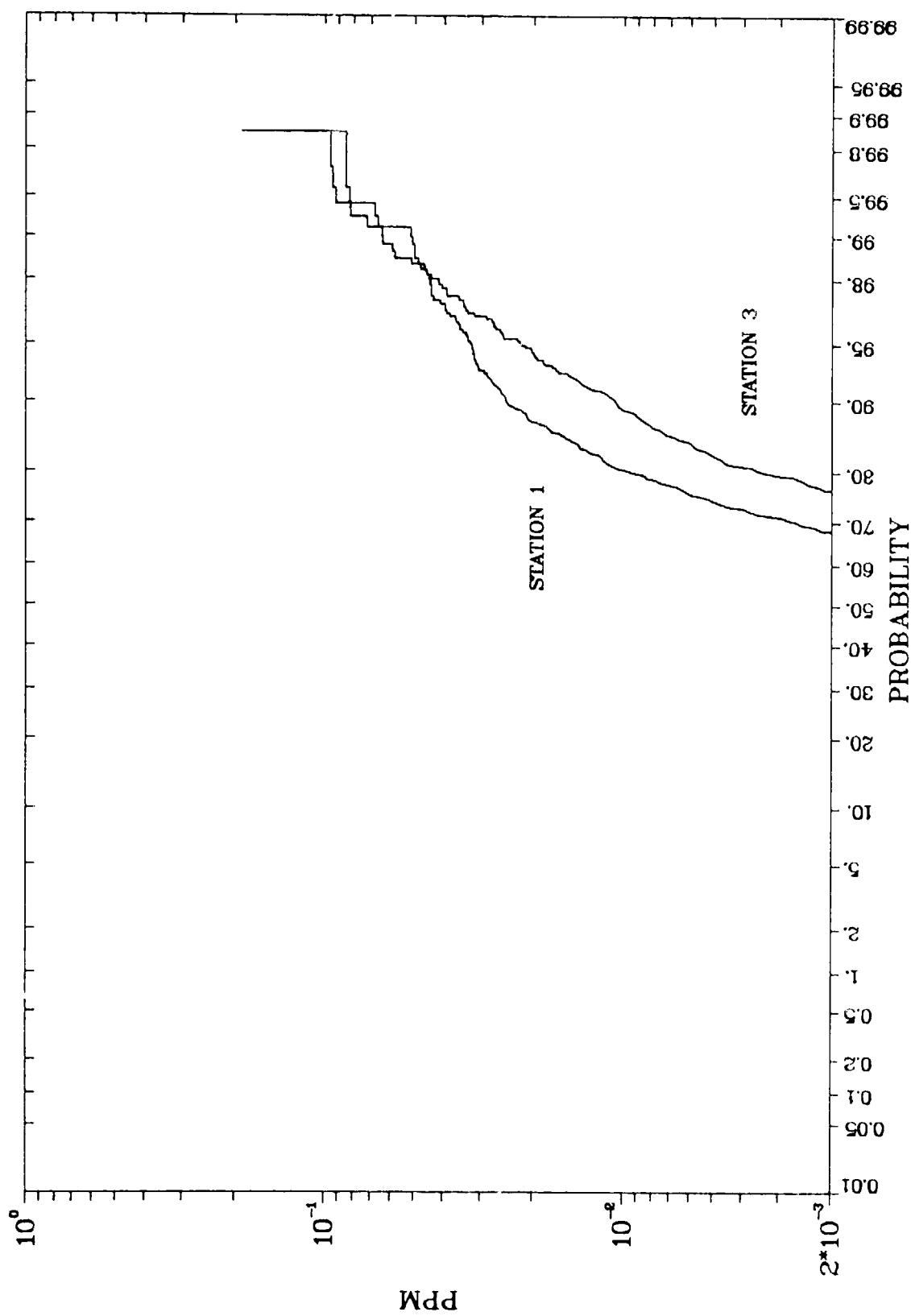


Fig. 3.19. Cumulative Frequency Distributions of Hourly Integrated Pulse NO Concentrations at Stations 1, and 3.

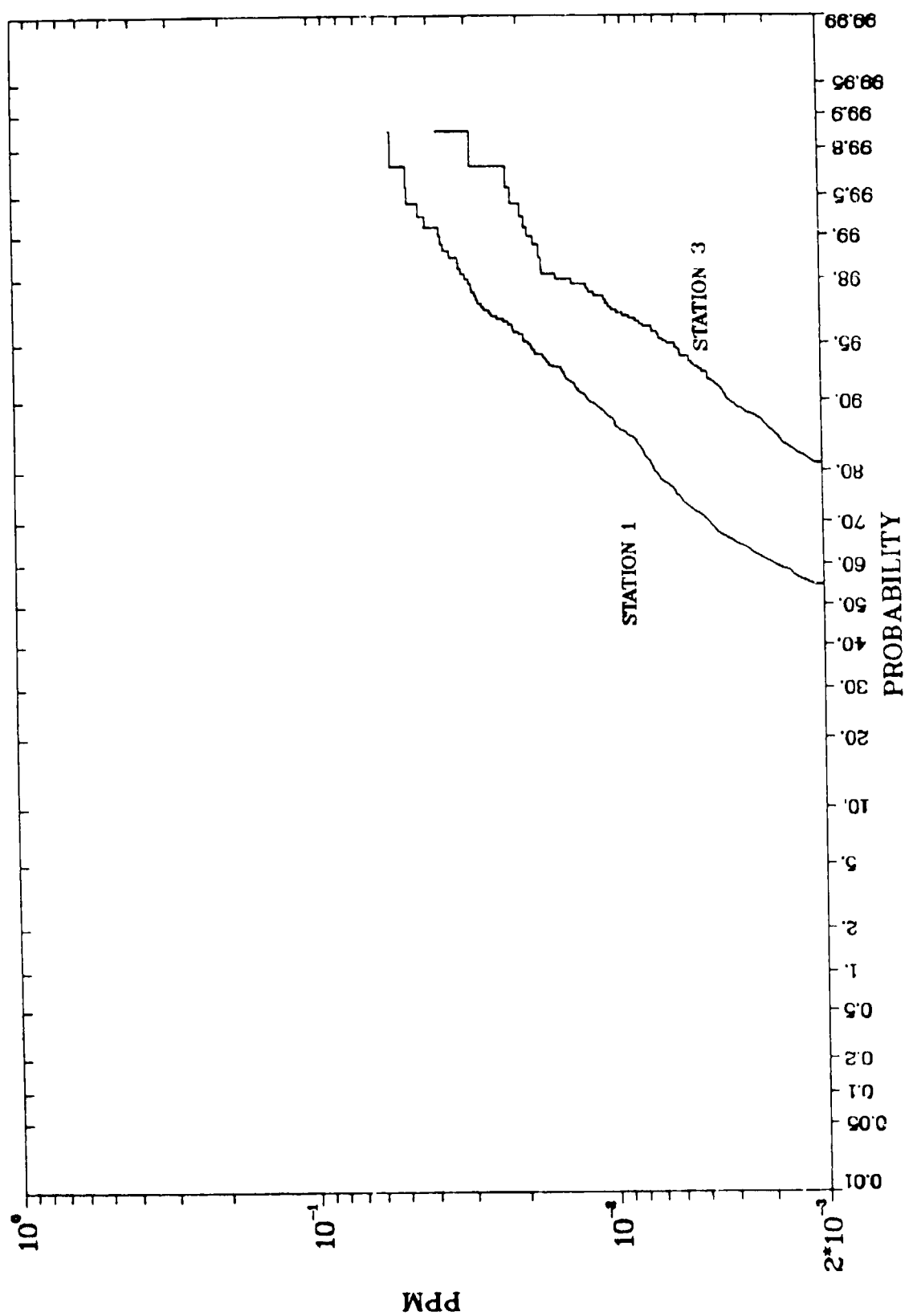


Fig. 3.20. Cumulative Frequency Distributions of Hourly Integrated Pulse NO_2 ($\equiv \text{NO}_x - \text{NO}$) Concentrations at Stations 1 and 3.

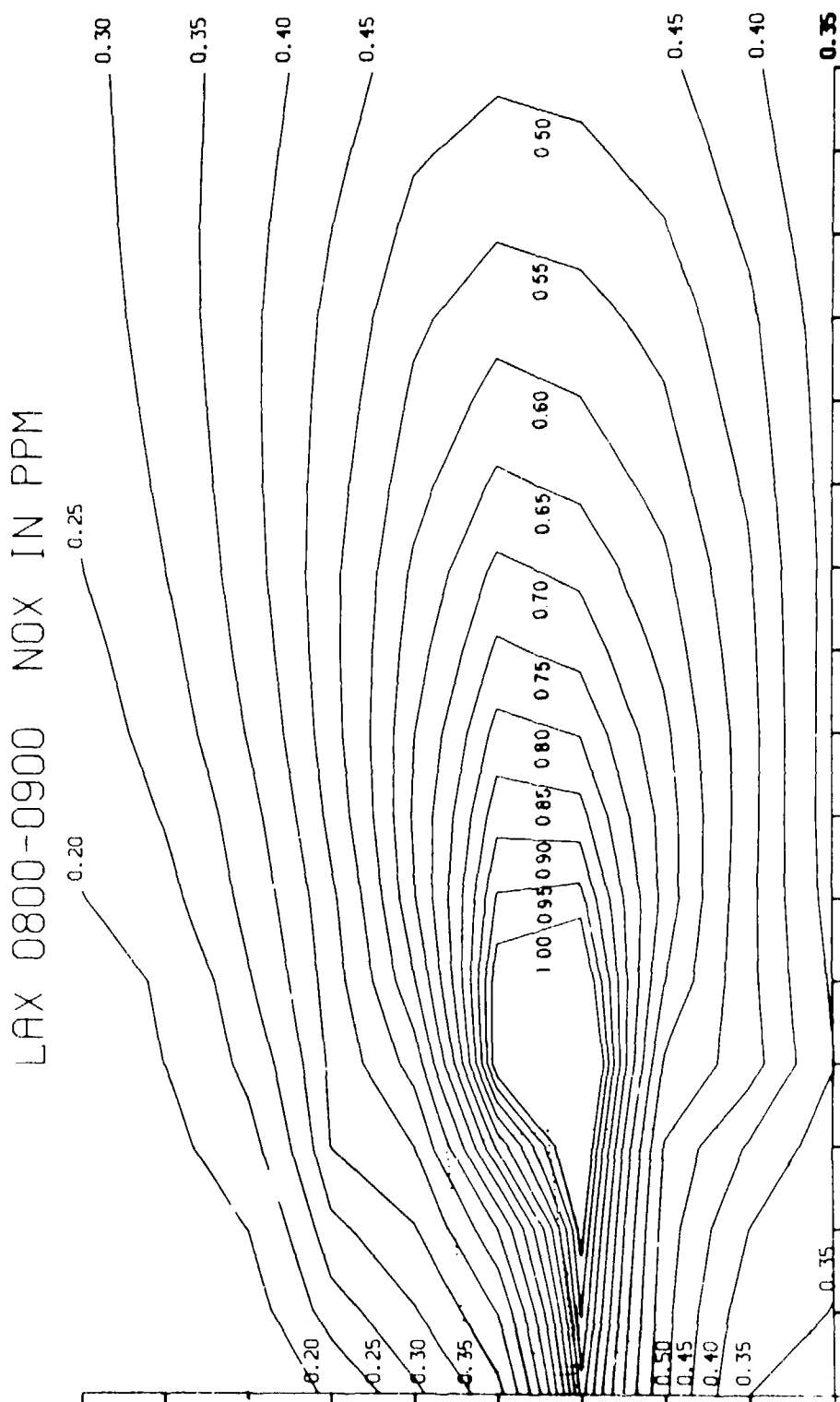


Fig. 3.21. MODIFIED AVAP Simulation of "Worst Case" (E Stability, Westerly 2-Knot Wind and an Equivalent Departure Rate of approximately 30 B727 Aircraft) NO_x Conditions behind the Southern Runway Complex at LAX. Runways and Main Taxiway/Queueing Area shown as dotted lines. A departure rate of 30 aircraft/hour was assumed and should be compared to a peak DCA departure rate of about 25 aircraft/hour. NO_x contour levels, given in ppm suggest possibly high NO₂ concentrations. Computation grid size = 0.05 mile.

In order to relate observed NO_2 and NO_x levels with modeled NO_x concentrations it is essential to note the difference in behavior of the $[\text{NO}]/[\text{NO}_x]$ ratios for ambient air and for aircraft plumes, before such plumes have completely mixed with the ambient air. During periods of good ventilation (sufficient mixing depth and moderate windspeed), the value of $[\text{NO}]/[\text{NO}_x]$ is generally near 0.4 during the morning decreasing to 0.10 or less during the afternoon, remaining low throughout the night. This temporal decrease in the ratio is due to photochemical processes during daylight hours. It has been observed that at takeoff thrust more than 95% of the NO_x emitted by jet aircraft engines is in the form of NO. The concentrations above background for aircraft induced peaks measured at the sites generally have a $[\text{NO}]/[\text{NO}_x]$ ratio exceeding 0.8, indicating that some transformation of NO to NO_2 is taking place in the near field under the winter conditions observed.

The actual NO to NO_2 plume oxidation rate is a complex function of plume dispersion rate and transport time, sunlight intensity, and background levels of NO, NO_2 , and O_3 , and a reactive plume calculation is required to predict the $[\text{NO}]/[\text{NO}_x]$ ratio. Clear evidence for this oxidation process, on the short transport time scales of the DCA experiment, is seen in Figure 3.22. Plotted is the ratio of the hourly integrated-pulse concentrations of NO to NO_x as a function of estimated plume travel time from the departing aircraft to the receptor. The linear regression line is indicated for comparison purposes only and has no theoretical basis.

During periods of light, variable winds, the hourly NO_x concentrations surpassed 0.1 ppm on more than ten (10) separate occasions. For such periods hourly background accounts for greater than 70% of the mean total NO_x implying that most of the important sources are nonlocal. The $[\text{NO}]/[\text{NO}_x]$ ratio of this background component generally is between 0.5 and 0.8. Several of these high concentration episodes are coincident with low airport activity and/or non-airport wind directions.

Considering now the issue of aircraft impact on the annual NO_2 standard of 0.05 ppm, one notes that the regression of observed pollutant levels against departure rate should provide some insight. Figure 3.23 shows the distributions and regression lines for the hourly total, background subtracted, and pulse integrated NO_2 concentrations at stations 1 and 3 versus aircraft departure rate. The regression parameters are then summarized in Table 3.7 along with

STATIONS 1 AND 3 INTEGRATED PULSE

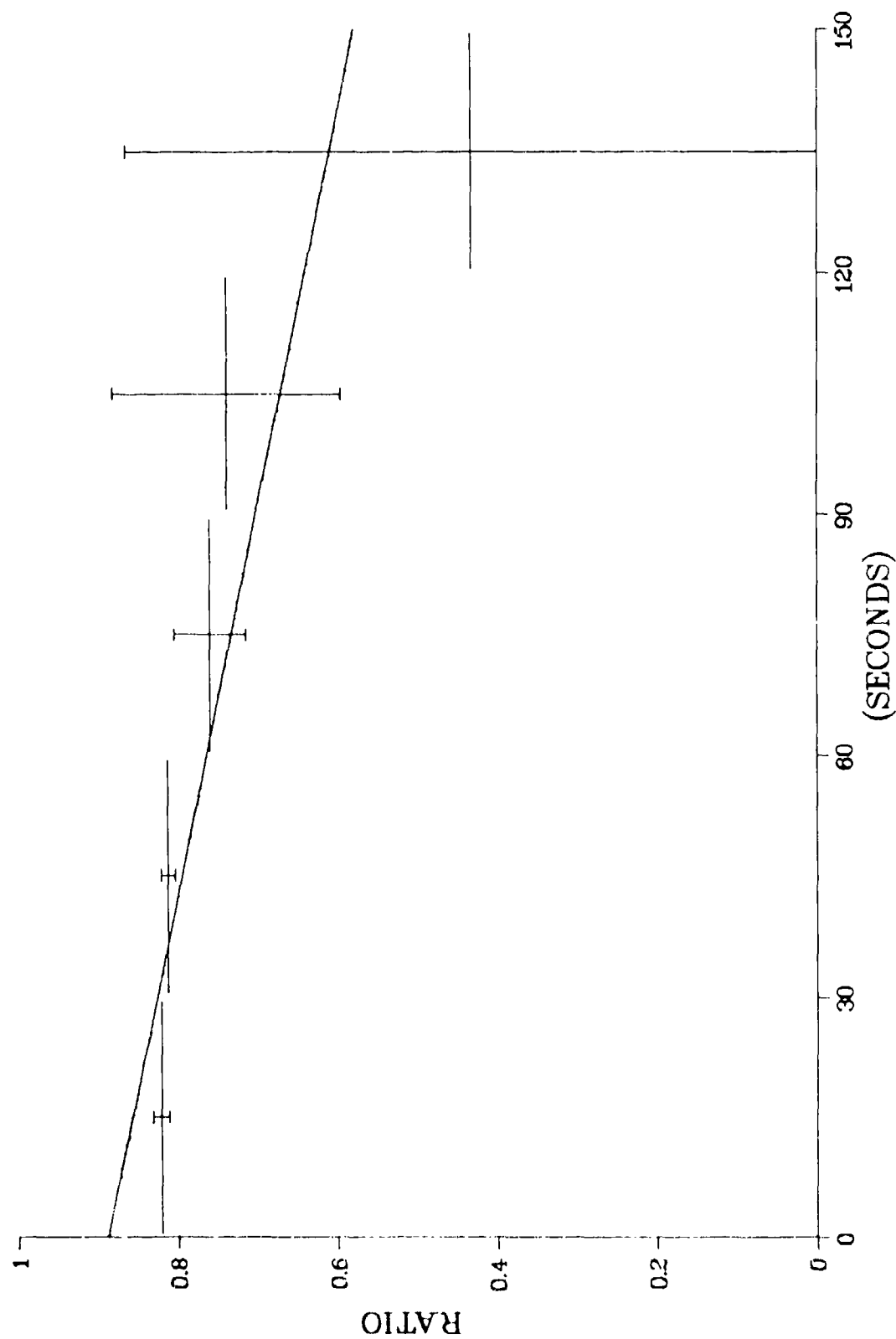


Fig. 3.22. The Mean Hourly Ratio of the Integrated Pulse Concentrations of NO and NO_x Versus Plume Transport Time.

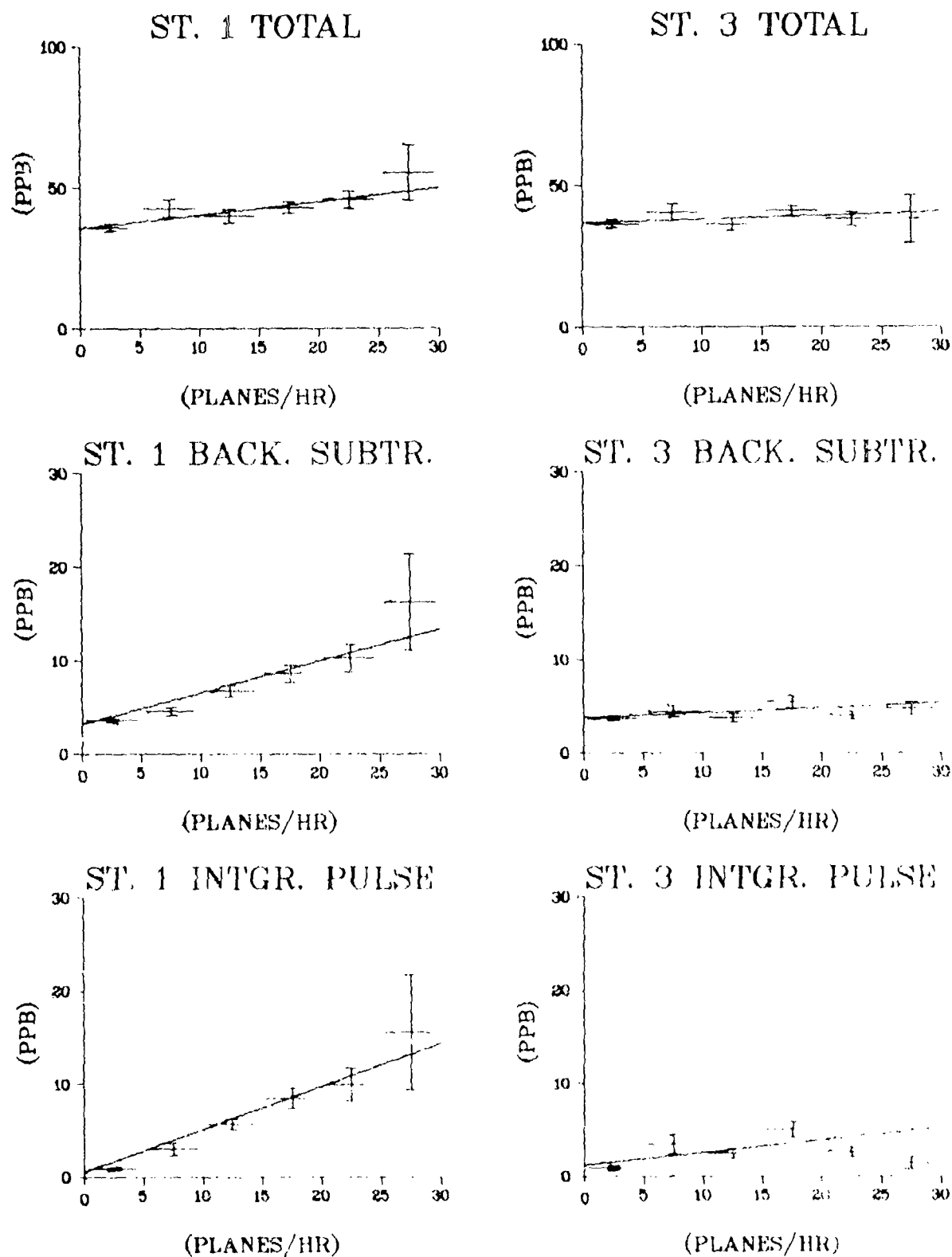


Fig. 3.23. Mean Hourly NO_2 Concentration Versus Aircraft Departure Rate at DCA

Table 3.7. Regressions of Hourly Average Concentrations Vs. Aircraft Departure Rate

	Station 1			Station 3		
	Ave.(ppb)	Intercept(ppb)	Slope (ppb/Departure)	Ave.(ppb)	Intercept(ppb)	Slope (ppb/Departure)
<u>NO_x</u>						
Total	82.7	66.5 ± 5.2	1.60 ± 0.39	90.7	93.8 ± 8.4	-0.35 ± 0.64
Background Subtracted	23.8	11.2 ± 1.3	1.24 ± 0.10	17.5	12.3 ± 1.3	0.52 ± 0.10
Pulse Integrated	16.3	3.4 ± 1.4	1.27 ± 0.11	9.1	4.0 ± 1.5	0.50 ± 0.11
<u>NO</u>						
Total	42.2	30.7 ± 4.4	1.13 ± 0.33	52.0	56.8 ± 7.9	-0.48 ± 0.60
Background Subtracted	17.8	8.2 ± 1.5	0.95 ± 0.11	14.4	10.5 ± 1.4	0.39 ± 0.11
Pulse Integrated	11.6	3.1 ± 1.6	0.84 ± 0.12	7.3	4.2 ± 1.6	0.31 ± 0.12
<u>NO₂</u>						
Total	40.5	35.7 ± 1.5	0.47 ± 0.11	38.3	37.0 ± 1.4	0.13 ± 0.11
Background Subtracted	6.5	3.2 ± 0.5	0.34 ± 0.04	4.3	3.8 ± 0.4	0.05 ± 0.03
Pulse Integrated	5.2	0.6 ± 0.6	0.46 ± 0.05	2.6	1.2 ± 0.4	0.14 ± 0.03

Based on 295 hours obtained during February 1979

Average Departure Rate of 10.1 Aircraft/hr (primarily B727, B737, DC-9)

Pulse integrated data for Station 3 is somewhat questionable

similarly obtained parameters for NO and NO_x. Aircraft impacts, as indicated by the slope parameter, are seen to be substantially smaller at station 3 than at station 1, but some of this may be due to the greater difficulty of separating background and aircraft pulse contributions at station 3. The fact that the intercept parameter is generally consistent with zero (i.e., that in the limit of zero aircraft there is no remaining background pollution) for pulse integrated concentration regressions strongly suggests that the pulse integrated concentration represents a good estimate of the actual aircraft impact. Also, the fact that the three slope estimates for a given station and species are consistent with one another indicates that the regression estimated impact is, as expected, independent of the assumed background. Thus, using the station 1, NO₂ slope parameter and the observed monthly averaged departure rate of 10.1 aircraft per hour, one projects an annual average aircraft impact of about 0.005 ppm (5 ppb). Even allowing an additional factor of two for preferred, seasonal wind direction effects, these levels are small compared with the 0.05 ppm NAAQS. In addition the observed 0.005 ppm impact of aircraft is in approximate agreement with the difference in NO₂ seen between DCA and other Washington area locations. Table 3.8 further suggests that use of the DCA data, acquired during February, will lead to, if anything, a slight overestimate of annual NO₂ at DCA. Hence, one concludes that at DCA, aircraft account for only about one-sixth of the estimated NO₂ annual average of 0.030 ppm.

Table 3.8. Annual NO₂ Levels at Various Washington Area Locations

Location	Annual Average (ppm)	February/Annual
Lewinsville*	0.028	1.2
Seven Corners*	0.023	1.1
Massey Building*	0.020	2.6
DCA (Feb. only)	0.030	---

*data of 1977 from local pollution control agencies

3.5 SUMMARY AND CONCLUSIONS BASED ON THE HOURLY AVERAGE CONCENTRATIONS

Results of CO monitoring near an aircraft queueing area at DCA suggest that observed worst-case, aircraft contributions to hourly CO concentrations on the order of 10 ppm are not unexpected at distances of 500 ft from the aircraft. These highest observed concentrations decrease to about 5 ppm at a distance of 1000 ft., a minimum distance where public exposure might normally be anticipated and in good agreement with worst-case modeling results for LAX. No violations of the 35 ppm hourly standard were observed even as close as 500 ft from the aircraft and the single observed violation of the 8 hr standard is thought to be primarily related to high observed CO values throughout the D.C. area and augmented by intensive operations of airport snowplows very near the monitoring stations.

Preliminary results of CO monitoring at DCA suggest that violation of the hourly NAAQS CO standard, in areas accessible to the general public and by aircraft alone, is highly improbable.

Results of NO, NO_x monitoring indicate that NO, NO_x, and NO₂ concentration distributions are nearly independent of station location (i.e., within the limited spatial regime of monitoring). Worst case NO_x concentrations of ~1 ppm are consistent with modeling predictions for LAX.

No NO₂ concentrations in excess of 0.1 ppm were observed though a conservative extrapolation to once a year probability yields a concentration (i.e., ~0.3 ppm) in the same range as possible short-term standards. Regressions of the NO₂ hourly average data against aircraft departure rate suggests that aircraft are responsible for only about 0.005 ppm of the estimated annual average NO₂ of 0.03 ppm seen near the runway at DCA. This projected annual average aircraft impact of 0.005 ppm is small compared to the 0.05 ppm NAAQS and is in agreement with the concentration differential observed between DCA and other Washington area monitors.

3.6 ANALYSIS OF SINGLE EVENT DATA

The locations of the monitors with respect to takoffs and landings on Runway 36 and the terminal area at DCA allow the impact of airport operations to be measured in several different ways. In addition to the hourly average analysis, pollution from take-off events may be evaluated by subjective analysis of single events or by use of an objective single event evaluation

method. The complexity of the concentration patterns at the various sites makes the formulation of a completely general event finding program most difficult. The results presented here are based on subjective analysis of NO_x peak concentrations and dosages due to single events.

The monitors are positioned such that for a northerly to easterly wind direction, the highest possible instantaneous ambient ground level concentrations of NO_x due to single aircraft sources should be experienced. Within the measurement range, the exhaust plume is likely to behave initially like a momentum jet in a cross flow as discussed in Section 4.5. After this initial phase, the jet momentum is depleted sufficiently for buoyancy forces to take effect and yield an initial plume rise. The ambient surface layer turbulent flow then becomes the dominant plume transport and dispersion mechanism during this jet to plume transition. The nature and magnitude of the ambient turbulence in the near field due to wakes from nearby aircraft in various modes of operation is expected to produce enhanced mixing. The detailed analysis of this unique data set should improve our knowledge of the "effective dispersion" in the initial mixing zone, though the absence of monitors in the vertical plane imposes clear limitations and renders some plume rise/dilution ambiguities unresolvable.

3.6.1 Subjectively Analyzed Single-Event Data

As was seen qualitatively from Figure 3.3, it is possible to extract information about the dispersion of the takeoff plume through examination of the NO_x concentration time histories recorded at the four NO_x instrumented stations. However, the interpretation of the single event peak concentrations and dosages in terms of typical Gaussian dispersion parameters is not completely straightforward. The parametric Gaussian formulation requires that the turbulent elements have temporal and spatial scales much smaller than the observed events which in this case are jet exhaust plumes generated on takeoff. At airports, surface layer turbulence is enhanced by aircraft wakes and trailing vortices. Therefore, especially when conditions are far from neutral, the scale separation is insufficient to analyze each event with a simple Gaussian model. However, a large ensemble of events may more appropriately be approached with this methodology.

With this objective in mind, approximately 120 individual aircraft departure events were measured through digitization of the concentration time histories. Peak concentration, time from peak noise to peak concentration, full width at half maximum above background, and background concentration were extracted for subsequent input into the ensemble research model for the takeoff mode, described in Section 3.6.3. The data extraction technique is referred to as the "subjective" approach primarily because of the element of judgment involved in the estimation of background levels.

3.6.2 DCA Single Event Finding Program

An attempt has been made to develop an objective algorithm to extract peak concentrations and dosages from the month of high sampling rate data gathered at DCA. After the measurements had been transferred to a master archive tape, calibrated in a preliminary fashion, and edited to minimize inclusion of periods of uncertain data, the following procedure was adopted to isolate and quantify events associated with individual aircraft departures.

1. Period of interest is specified such that periods of missing data, zero airport activity, non-optimal wind direction, etc. may be avoided. Only wind directions between 10 and 80° were selected since, for other directions, the plume is transported away from the monitoring sites.
2. The search for a usable event occurs as follows: a noise pulse is searched for that is sufficiently separated from other pulses to allow transport to the furthest receptor before the next aircraft's plume impacts the closest receptor. An event pulse is defined by an 80 dB noise threshold. When runway 18 is in use the noise spikes are similar but the wind is from the south! The screening in step 1 then becomes important to avoid the possibility of erroneous results. The transport time is defined as D/u where D is the along wind distance from station 3 to the runway. Five minute average wind speed (u) and direction values are utilized. If the transport time exceeds the noise event separation the event is skipped.
3. Once a noise event is identified as giving rise to an analyzable "dose event", 3-minute averages, background values, σ_a , and σ_b are evaluated (1 min prior to noise pulse, 2 min after noise pulse). Missing data or data exceeding 0.5 ppm will cause the event to abort.

4. The peak concentrations, triangular doses, and numerically integrated doses are now found by subtracting out the background values of the 3 minute period.
 - a. For each receptor the search for the event begins after a delay time equal to the time of transport from the runway. A window the size of the minimum pulse separation used in step 2 is searched for a maximum.
 - b. The times of half-maximum (above background) are determined, to calculate the triangular dose.
 - c. The endpoints of the numerical dose integration are defined as follows:
 The starting point is the time where the search for the maximum begins. The end point the time at which the concentration becomes smaller than $(1.1 \times \text{background})$ or $(\text{background} + 10 \text{ ppb})$, whichever is greater, or the end of the window in (a), whichever comes first. For a weak pulse above a high background at station 3 the size of the integration interval may be underestimated. Early versions use Simpson's rule but later attempts employ a Gaussian quadrature technique.

Application and limitations of the above described technique include:

1. Care must be taken to specify periods with the proper wind direction or for each 5 minute period the average wind direction must be screened to insure acceptable events (i.e., $10^\circ \leq \theta \leq 80^\circ$ only).
2. Priority should be given to the subset of hours when onsite observations are available because noise network printouts of runway activity are not entirely reliable.
3. The dose of NO sometimes exceeds that of NO_x : this is most likely due to a calibration problem and not inherent in the method. The same problem is evident in the subjectively analyzed single events.
4. The specification of the "window" to search for an event is subject to further experimentation and refinement. A better way to find the endpoints for the integration may be required.
5. The temporal spacing requirements will cause many legitimate events to be skipped. However, with the data base provided, the present program should provide an adequate cross-section of "well defined" single events.

Though the above described approach had yielded a data base consisting of several hundred NO_x plumes from departing aircraft, subsequent analysis of these objectively obtained events has indicated the model's inability to deal with numerous pathological situations. Research model results using these single events as input thus remain high suspect.

3.6.3 DCA Research Model Results

The DCA research model basically considers the aircraft to undergo uniform linear acceleration down the runway while emitting pollutant at a uniform rate from a tail of length L attached directly behind the aircraft. The initial transverse and vertical extent of the plume is specified by parameters $\sigma_x(0)$ and $\sigma_z(0)$ respectively and subsequent plume growth is assumed to be governed by the equations

$$\sigma_x = \sigma_y = \sigma_x(0) + b_x \sigma_{yT}(x)$$

and

$$\sigma_z = \sigma_z(0) + b_z \sigma_{zT}(x)$$

where $\sigma_{yT}(x)$ and $\sigma_{zT}(x)$ are the dispersion coefficients taken from Turner's Workbook and $b_x = b_z = 0.7$ is a correction for averaging time. Unfortunately, the fact that all receptors are near ground-level prevents independent determination of plume center line height (assumed to be at $H_0 \equiv 1.2 \sigma_z(0)$), so that effects of plume rise are erroneously incorporated into the available parameters.

Minimization of the chisquare between predicted and observed peak concentrations and pulse durations yields the parameters

$$\sigma_x(0) = 21.1 \text{ m},$$

$$\sigma_z(0) = 25.7 \text{ m},$$

and

$$L = 52 \text{ m}$$

One notes that the tail length parameter L is unreasonably small and probably is related to simplifying assumptions made in this research model. Nevertheless, the research model algorithm matches the AVAP line source model very well so that reasonable concentration predictions should be expected from AVAP despite the small tail length.

Figure 3.24 shows a scatter plot of observed and research model predicted peak concentrations. Because of an approximation which assumes that the peak concentration is primarily determined by pollution coming from the region of the intersection of the wind direction and the runway, the full range of peak concentrations is not reproduced. An approach is currently under development that will avoid this problem while maintaining maximal overlap with the AVAP method so that research model determined parameters may confidently be used in AVAP. However, it should be pointed out that the present model does indicate the gross error associated with neglect of the initial turbulent mixing: assumption of an initial accelerating point source leads to a theory/observation regression slope of ~ 30 .

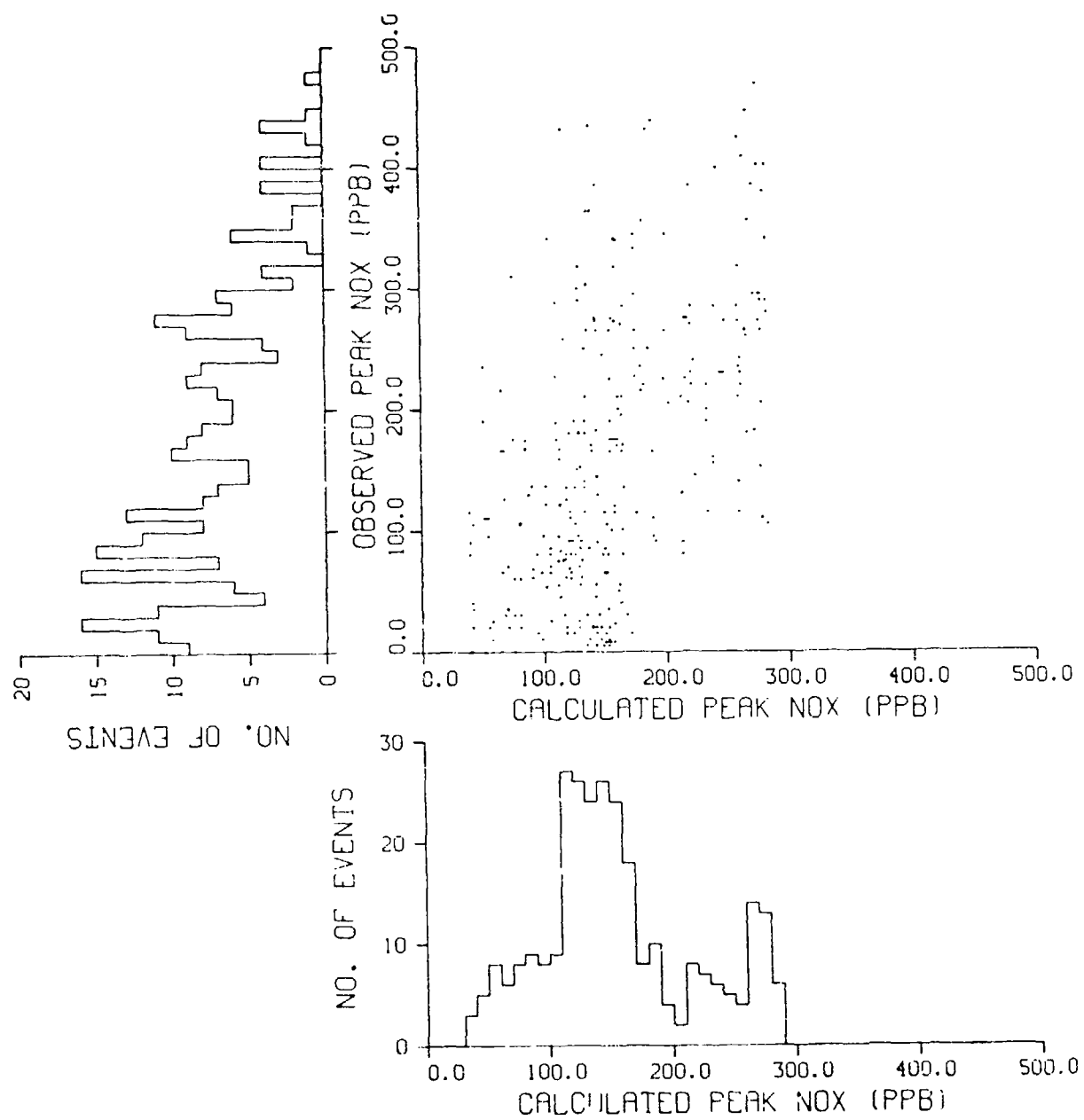


Fig. 3.24. Observed versus Predicted Peak NO_x Concentrations at DCA.

4 ANALYSIS OF EXPERIMENTS AT DULLES INTERNATIONAL AIRPORT

4.1 INTRODUCTION

The measurement program at Dulles International Airport was initiated in 1976 in response to an order by the Secretary of Transportation to monitor pollutant emissions and noise levels associated with Concorde aircraft operations. Three pollutants for which there are engine emission standards (carbon monoxides (CO), nitrogen oxides (NO_x), and hydrocarbons (HC)) were monitored. Measurements were obtained at nearby regional monitoring stations, and these data were analyzed using statistical inference techniques as well as by means of a source finding algorithm; a method designed to locate sources and assess source culpability based on observed concentrations.

Principal effort, both during the experimental program and in subsequent analysis efforts, was devoted to arrays of sensors placed at the airport in the vicinity of aircraft operations. The locations and periods of use for these arrays are detailed elsewhere by Smith et al. (1977)

Early measurements indicated low concentrations that would not be explicable with many conventional airport models, apparently because previous models developed specifically for airports have generally ignored plume rise and initial plume dilution. Although many model applications are not severely limited by this omission, when conservative estimates of airport impact at distances of 2 to 10 miles are at issue, it is essential to consider both the direct and indirect (augmentation of σ_z) effects of plume rise for validating model predictions at closer distances. Thus, the early results led to a design of a progressively more sophisticated experiment, using first one, then two, and finally three towers instrumented at three to five levels with CO sensor probes. Meteorological data included two levels of wind direction and speed and temperature and its gradient. These data have been analyzed in detail to provide information on jet plume rise, actual atmospheric dispersion parameters, and vertical and horizontal "profiles" of exhaust-plume pollutant concentrations for individual aircraft in actual service.

4.2 REGIONAL MEASUREMENTS

As previously mentioned, the monitoring program at Dulles initially consisted of a network of stations located in and around the airport. These stations recorded the concentrations of various pollutants and relevant meteorological data during the time period from May to September, 1976.

The locations of these stations are shown in Fig. 4.1, and the parameters measured at each site are tabulated in Fig. 4.2. Two stations, South Ramp and Sterling Park, were especially important to the monitoring program because of their proximity to the airport and the amount of data recorded at each site. The South Ramp site was located approximately 200 ft south of the jet taxi ramp, and the Sterling Park station was located 3 miles north-northeast of Dulles in the community of Sterling Park.

The data at these two sites was recorded on strip charts which were later digitized and processed by computer to yield hourly averaged concentration and meteorological values. Most of the data in the Dulles regional data base consists of measurements made at those two sites.

4.3 SOURCE FINDING APPLICATION AT DULLES

4.3.1 Introduction

The increasing number and complexity of air quality monitoring networks in operation throughout the world coupled with the greatly increased quantity of data such networks generate, suggests the need for innovative data analysis techniques.

Many analysis tools (such as the use of frequency and cumulative frequency distributions, time series analysis, and factor analysis), while well suited for understanding the significance of data from a single receptor, become somewhat unwieldy when applied to data from a network of receptors. Ideally, one might hope that the data from an n-station array would result in more, and not less, information than obtainable from n-stations considered individually.

The capability of utilizing observed meteorological and pollutant concentration data to determine the location and strength of those sources having the greatest influence on measured concentrations is such a tool, having potential applications which include:

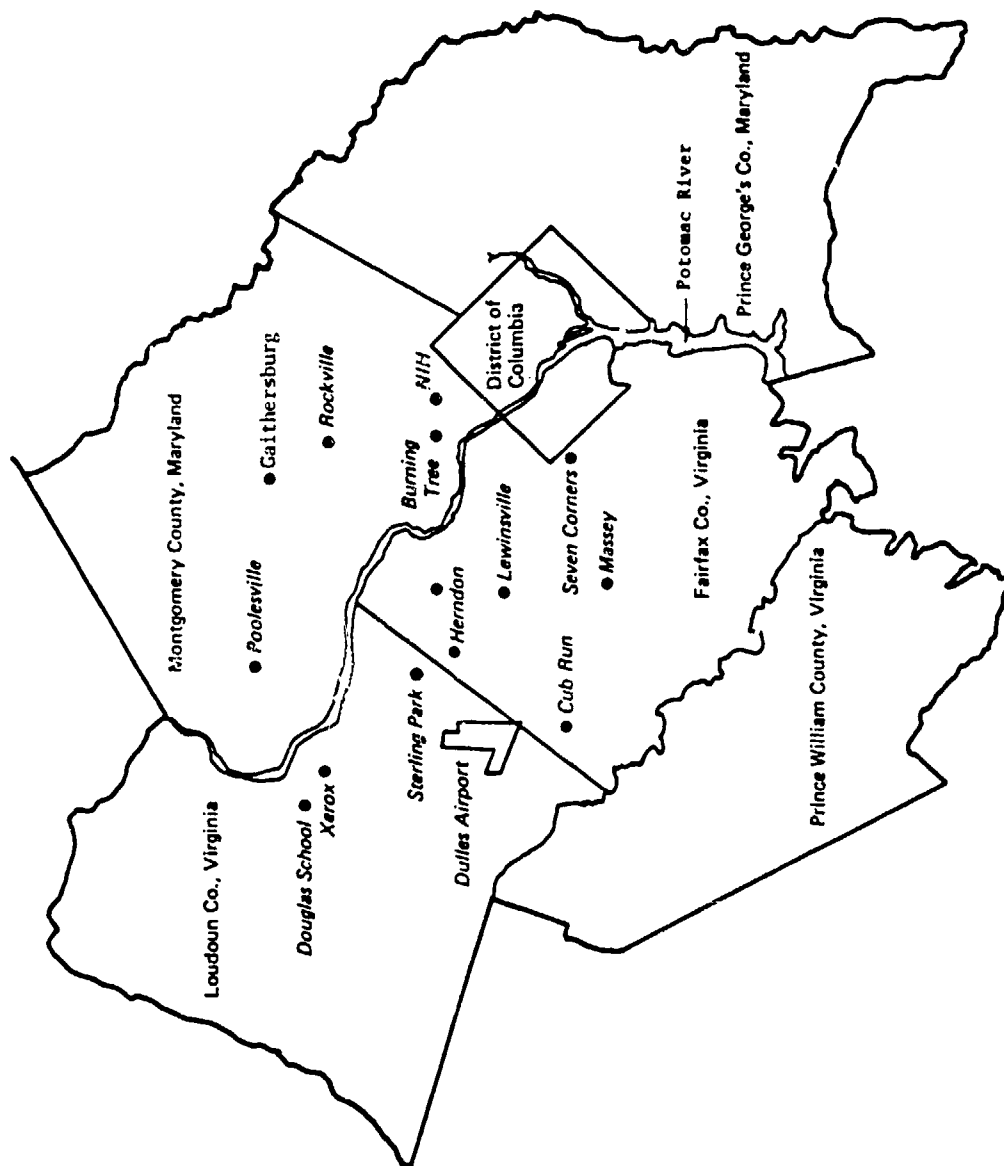


Fig. 4.1. Regional Air Quality Monitoring Stations

PARAMETER STATION	Wind Direction WD	Wind Speed WS	Carbon Monoxide CO	Nitrogen Dioxide NO ₂	Nitric Oxide NO	Ozone O ₂	Total Hydrocarbons THC	Methane CH ₄	Total Suspended Particulates TSP*	Sulphur Dioxide
Station #1 Sterling Park	✓	✓	✓	✓	✓	✓	✓	✓	✓	
Station #6 South Ramp	✓	✓	✓	✓	✓	✓	✓	✓	✓	
Massey			✓	✓	✓	✓			✓	
Lewinsville			✓	✓	✓	✓			✓	
Seven Corners			✓	✓	✓	✓	✓			
NIH Bethesda			✓	✓	✓	✓			✓	✓
Herndon									✓	
Cub Run									✓	
Douglas Elem. School									✓	
Xerox Training School									✓	
Burning Tree									✓	
Galthersburg H.S.									✓	
Poolesville Elem. School									✓	
Rockville									✓	

*TSP values are not reported on an hourly basis but are reported as daily (24) hour values.

Fig. 4.2. Background Stations

- a) an independent means of checking source inventories and determining source culpability,
- b) the ability to locate inadvertent leaks of hazardous effluents into the atmosphere, and
- c) as an enforcement tool for air pollution regulatory agencies.

One possible approach to this problem is to develop a technique for relating the aerometric data obtained from a monitoring network under a wide range of meteorological conditions to the spatial distribution and strengths of emissions sources via the use of existing air quality dispersion algorithms. The approach may be envisioned, quite literally, as the running of an air quality dispersion model "in reverse"; where an effective emission density map is determined from knowledge of the concentrations at the receptors of a network and the values of a few relevant meteorological parameters over the area of interest.

The regional data base available from the Dulles monitoring program can, therefore, be used as input to this source finding algorithm in an attempt to determine the significance of local or on-site sources on the overall measured concentrations.

4.3.2 Model Development

Air quality dispersion models are most often concerned with the determination of pollutant concentrations at a receptor given known source strengths and locations. Assuming steady state conditions have been achieved, the concentration, C_{kt} , at the k^{th} receptor during the t^{th} time interval can be expressed as

$$C_{kt} = \sum_j R_{jkt} Q_j ,$$

where Q_j is the time independent strength of the j^{th} source and R_{jkt} is the transport coupling coefficient between the j^{th} source and k^{th} receptor for the meteorological conditions existent during the t^{th} time interval. The solution of the simple inverse problem

$$Q_j = \sum_k^{-1} R_{jkt}^{-1} C_{kt}$$

is not of particular interest as a unique solution might exist only if the number of receptors, K , equalled the number of source candidates, J . A

more reasonable problem would consist of determining the set of Q_j values leading to the minimization of the quantity χ^2 , defined as

$$\chi^2 = \sum_{t,k} \frac{\left(C_{kt} - \sum_{i=1}^J R_{ikt} Q_i \right)^2}{(\Delta C_{kt})^2} \quad (1)$$

where ΔC_{kt} is the uncertainty in C_{kt} , i is a dummy index, and a summation over both t and k is required. This problem will generally lead to a unique set of J source strengths provided the number of measurements M (nominally KT , where T is the number of time periods of data available) exceeds J , and secondly, that the sources Q_j of interest actually couple to the data in hand (i.e., $R_{jkt} \neq 0$ for all j and some k, t). Given these conditions, one may write down the set of J equations generated by the relations

$$\frac{\partial \chi^2}{\partial Q_j} = 0.$$

These equations are of the form:

$$\sum_j A_{ij} Q_j = B_i \quad (2)$$

where

$$A_{ij} \equiv \sum_{t,k} \frac{R_{ikt} R_{jkt}}{(\Delta C_{kt})^2}$$

and

$$B_i \equiv \sum_{t,k} \frac{C_{kt} R_{ikt}}{(\Delta C_{kt})^2}$$

and upon obtaining the inverse A^{-1} of the positive definite matrix A , one arrives at the solution

$$Q_j = \sum_i A_{ji}^{-1} B_i \quad (3)$$

This approach, with no constraint on the Q_j , is quite acceptable provided the number of candidate source locations J is small (e.g., $J < 100$) and source candidate locations are well separated; however, if nothing is known about the source locations, and instead, an array of point or area sources is conjectured to exist on an X - Y grid of size $n \times m$, then one must

contend with a matrix A of order $(n \times m)$ by $(n \times m)$, which, in turn demands a minimum of $n \times m$ concentration measurements. In addition, the solution Q_j may be quite unstable, with adjacent grid point Q_j values oscillating wildly positive and negative in a region known to be source free. Fortunately the availability of a non-negative least squares algorithm, developed by Lawson and Hanson (1974), enables one to solve equation (2) subject to the physically reasonable requirement that all source strengths Q_j be positive (i.e., $Q_j \geq 0$). Further theoretical developments are presented by Yamartino and Lamich (1979).

4.3.3 Model Application

In order to apply the source finding algorithm to the regional Dulles data, the coupling coefficients, and a source grid must be defined.

Computation of R_{jkt} . The coupling coefficients, R_{jkt} , were computed via the Gaussian plume formalism; however, due to the apriori unknown nature of the sources, the calculations were performed as if each source were a ground-level, square, area source of length ΔX ($\Delta X = 320$ meters - 0.2 miles) so that the array of source candidates is contiguous. Plume rise, which also must be assumed to be unknown in any "source-finding" program, has been neglected, and it should be noted that this highly source oriented, yet meteorologically dependent, variable represents the major stumbling block in the otherwise trivial extension of this two-dimensional "source-finding" theory to three dimensions. This neglect of plume rise limits the usefulness of this approach with the Dulles data since the South Ramp station is close enough to the aircraft for concentrations there to be strongly affected by jet plume rise.

Computational Grid and Receptors. In Fig. 4.3 the computational grid used by the source finding algorithm is shown superimposed on a map of the airport. Also shown are the locations of the two receptors which gathered the concentration data.

Only two of the receptors from the regional monitoring network were used initially because of the steady-state requirement in the original source finding algorithm. The assumption of steady-state conditions in the computation of the coupling coefficients (R_{jkt}) means that the sources must couple to each receptor during the time interval that the computations are being done.

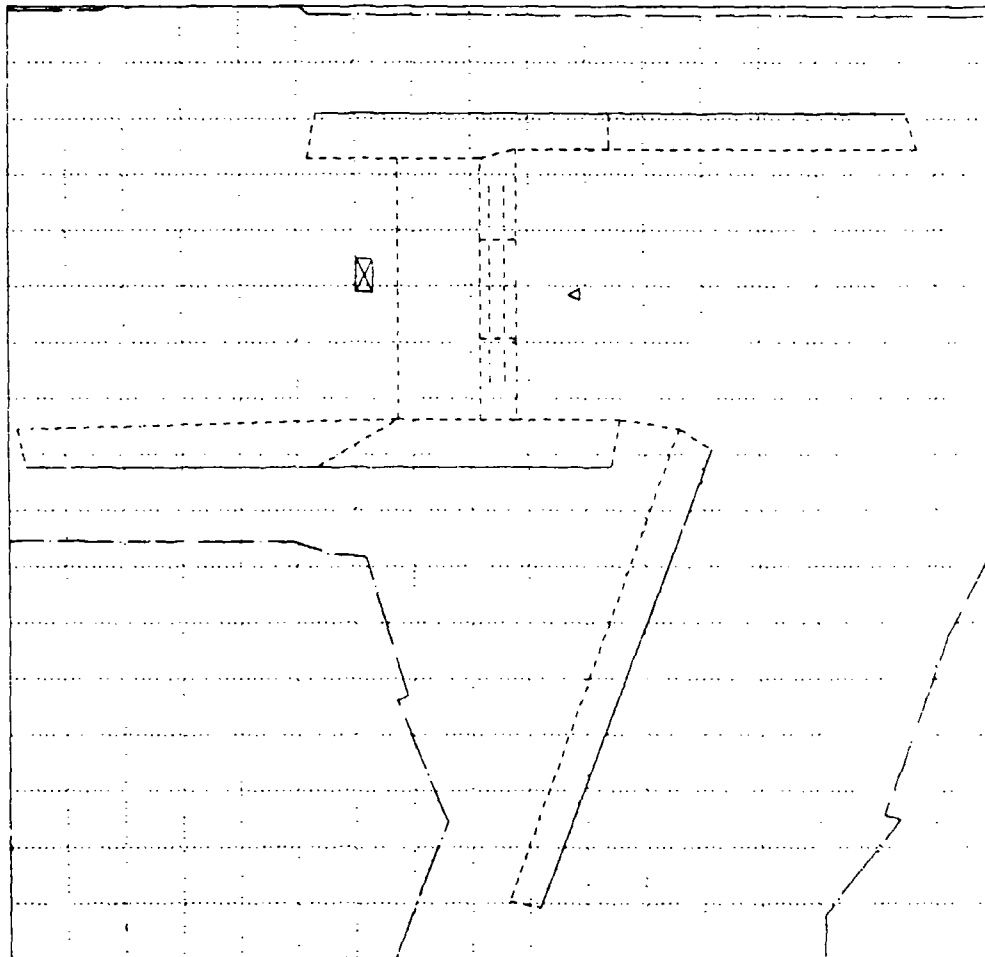


Fig. 4.3. Computational Grid Superimposed
on Map of Dulles International
Airport

⊠ Terminal

△ South Ramp Monitoring Station

— runway

- - - taxiway

- . - airport property line

Hence, there is a cutoff distance around the airport; any receptors lying outside this area cannot be used because the pollutants emitted from airport sources during some time interval will not arrive at those receptors until a later time interval. The only two receptors that were close enough to Dulles to be suitable for such source finding application were the Sterling Park and South Ramp stations. Taking into account network sensitivity and resolving power, it was expected that using only two receptors would not result in a very accurate picture of the significant sources. A subsequent version of the source finding model circumvented this limitation through the use of backward trajectories, which allowed for up to six hours of pollutant transport.

Each mesh point of the computational grid is treated by the algorithm as a potential area source. Minimization of the z value produces an optimal set of relative source strengths, where each member of this set corresponds to an area source located on the grid. When each relative source strength is plotted on a map in its proper location, the resulting picture ideally will show the locations and strengths of the actual sources inside the area covered by the grid.

4.3.4 Model Results

Contours proportional to \log_{10} of CO emission density are plotted in Fig. 4.4. Despite the use of additional data through application of the trajectory method, the solution is nearly identical with that obtained (not shown) using only the Sterling Park and South Ramp data. In essence these are the only stations close enough to the airport to be influenced by it.

The presence of strong sources at the edges of the computational grid is an indication that much of the observed CO actually originates from points outside of the grid. One notes further that the strength of these outside sources is as much as two orders of magnitude greater than CO emission densities found on the airport, and, in particular, in the vicinity of the South Ramp where a major fraction of the aircraft CO would originate.

4.3.5 Conclusions

A formalism has been developed for utilizing data obtained from an air quality monitoring network to determine the locations and strengths of those sources contributing most significantly to the observed concentrations. The

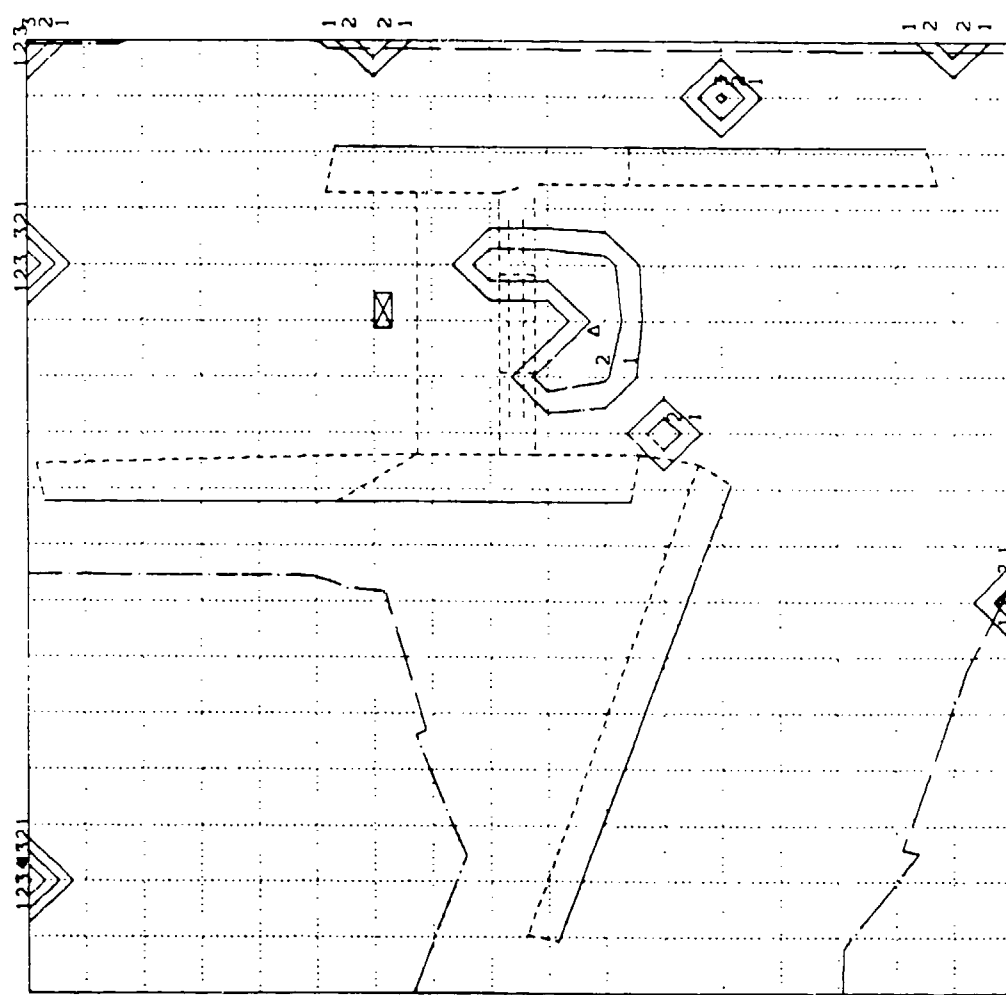


Fig. 4.4. Source Finding Solution Contours for CO. Isopleths are proportional to the \log_{10} of the CO emission density function found to give a best χ^2 fit to observed concentrations.

problem is best treated exactly for the case of J source candidates via solution of the coupled equations

$$\sum_j A_{ij} Q_j = B_i$$

subject to the condition $Q_j \geq 0$ for all j.

Application of this source finding algorithm to the CO data obtained from the regional network at and around Dulles International Airport, correctly locates the leading aircraft CO emission zone but further indicates the presence of substantially stronger off-airport sources.

4.4 THREE TOWER MEASUREMENTS OF CO

The Concorde air quality monitoring and analysis program conducted at Dulles International Airport during 1976-77 provided a unique opportunity to measure CO plumes from taxiing aircraft. The transport and dispersion of these CO plumes was monitored at 13 points on the three tower array shown in Fig. 4.5, measured with Ecolyzers, and recorded on high-speed strip chart recorders. CO values were extracted from measurements of strip chart records. A sample set of CO traces is also seen in Fig. 4.5. Wind speed and direction were measured at the 80' and 14' levels on the first tower. Temperature gradient was measured between 67' and 14' on the same tower. Several hundred plumes were observed under neutral/unstable daytime conditions during the one-, two-, and three-tower phases of the experiment. Commercial aircraft types monitored included the Concorde, 707, 727, 737, 747, DC8, DC9, DC10, and L1011. Though peak instantaneous CO levels reached 10 ppm at the first tower (only 215 ft from the taxiway centerline), maximum aircraft contribution to the hourly average, ground level, CO concentration remained below 0.06 ppm per aircraft. Extrapolations to 1000 ft from the taxiway indicate a maximum hourly average concentration of 0.03 ppm CO per aircraft. Thus, hourly concentrations in excess of several ppm, adjacent to a busy taxiway, would be unlikely to occur.

Though maximum CO impacts are expected from queueing operations rather than taxi, the data from the taxi mode provide interesting information on initial plume dimensions and buoyant plume rise. These plume parameters may then be used in airport air quality models to increase their accuracy and predictive power.

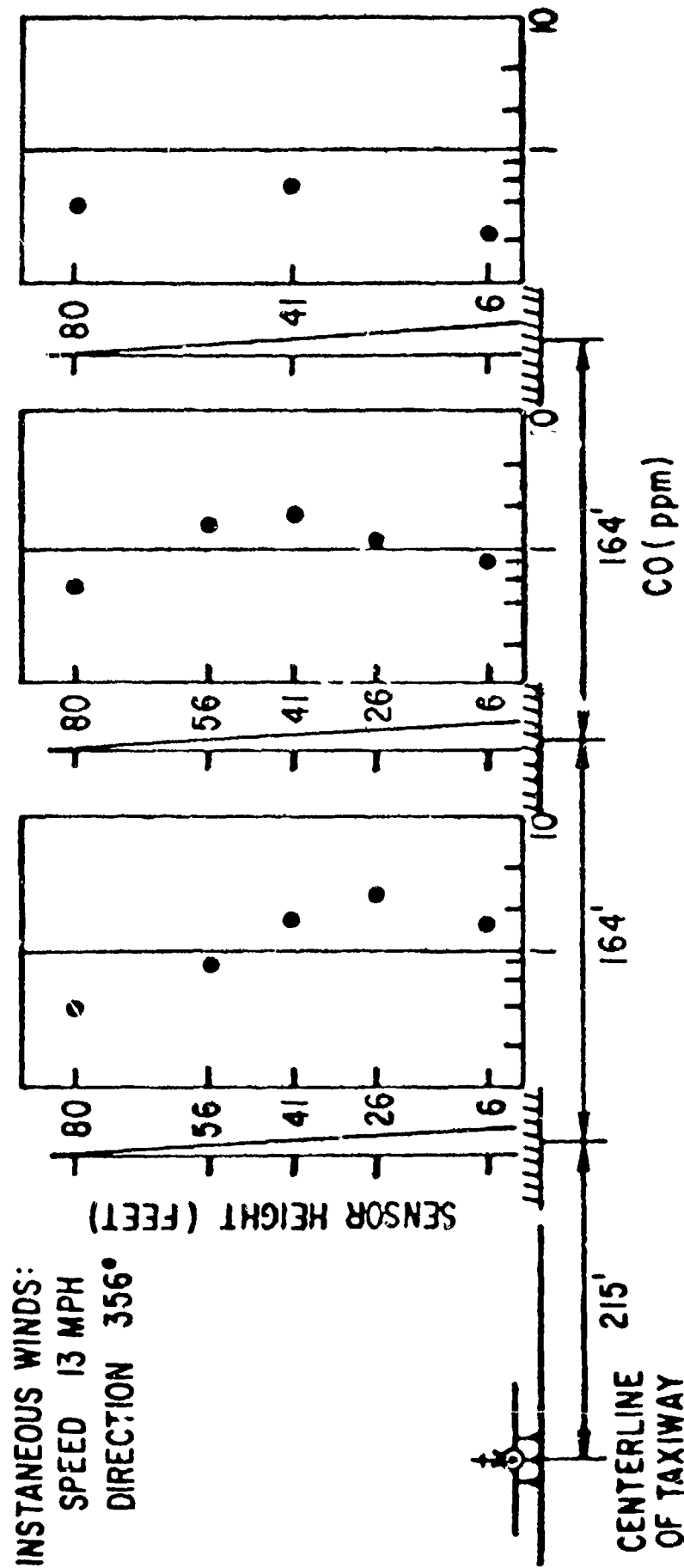


Fig. 4.5. Peak CO Concentration Vs. Sensor Intake Position

As indicated in Fig. 4.5, CO was measured by pumping air samples continuously through identical volume sampling lines into individual Ecolyzer units. These units were housed in an air conditioned shelter. They were periodically calibrated by sequential switching of the intakes to the same 18 ppm concentration. The calibration system was designed to allow precise timing of sensor exposure to calibration gases of different concentrations so that response time constraints and linearity of signal amplitude could be determined. Since an aircraft passage "event" was expected to produce a pulse representing concentration versus time (as shown in Fig. 4.6), the measurement of sensor system time characteristics was deemed important. The time constant of the Ecolyzers averaged 12 seconds, and their threshold sensitivity averaged 0.25 ppm.

The concentration shown in Fig. 4.5 represent the instantaneous peak values from the relatively high speed chart records. Figure 4.6 is idealized in the sense that the skew (to the right) observed as a result of the time response, and potentially the pollutant distribution, is not shown. When the data was reduced, both the time-to-peak and the time-to-half-peak were recorded in addition to the peak CO value, the full-width-at-half-maximum time, and the background CO so that skewness could be accounted for in future modeling. Details of the method for correcting the peak concentrations when one uses an event modeling technique are given by Smith (1977).

In addition to concentration measurements, documentation for each event included event time, direction of aircraft travel, departure or arrival made, time to travel 50 m, and meteorological conditions. Wind direction and speed were averaged over three minutes. The value of σ_0 for the same averaging time was found from 30 six-second samples for each event, commencing at the recorded event time. The specific ranges of meteorological conditions are given with the results below. All selected tests were conducted in the daytime and had winds between 290° and 70°. The taxiing activity pattern, the orientation of the towers at Dulles, and simplicity for modeling were factors leading to this selection.

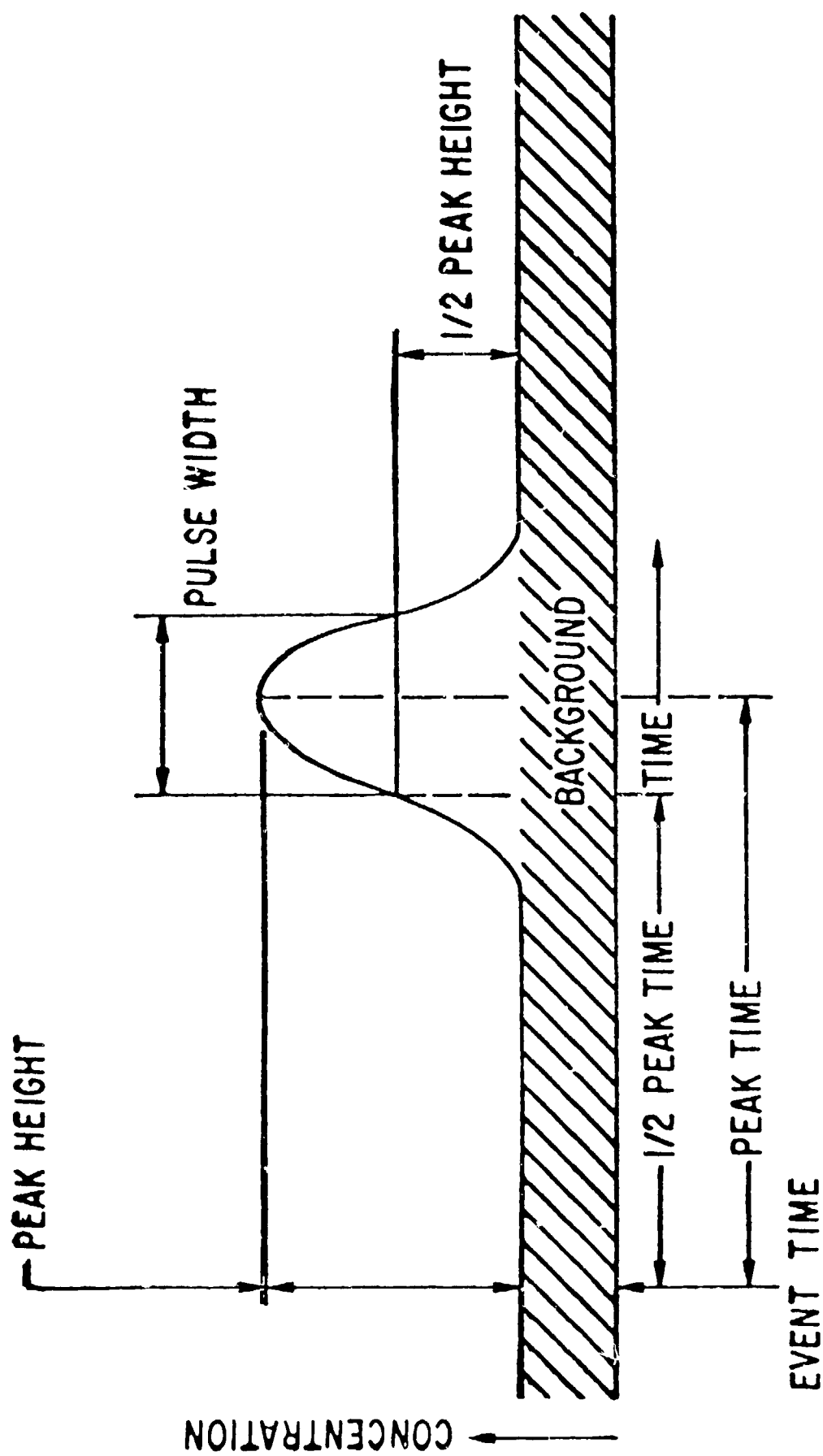


Fig. 4.6. Concentration Measurement Parameters

4.5 PLUME RISE FROM JET AIRCRAFT DURING THE TAXI MODE

4.5.1 Introduction

This section discusses the results of an investigation of the behavior of buoyant jet engine exhaust plumes in a crosswind; it attempts to identify the degree to which the plume rise can be described by relationships developed for other types of sources.

At least four factors affecting the rate of dilution of jet exhaust before it reaches receptor adjacent to taxi-ways or runways have been previously identified [Heywood et al. (1971)]:

1. turbulent mixing of the jet exhaust at the engine exit
2. buoyant plume rise
3. advective dilution
4. dispersion by ambient turbulence

Observational studies of plumes generally allow only one or two separate processes to be measured (plume rise and total dispersion rate). Although the bending of an exhaust plume from its original release axis until it is aligned with the prevailing wind direction is also observable (particularly from above). This change in orientation or "bending" may also be viewed as the transition from plume dilution dominated by the first mechanism to dilution controlled by the latter three. For this reason, the maximum length of the highly turbulent jet trail as a function of wind speed is of interest.

The assumption is made that the two phenomena, plume bending and plume rise, can be treated independently as a first approach. Both theoretical and empirical models are available to describe plume bending in a perpendicular wind [e.g. Abramovich (1963)]. Estimates of the maximum distances of dominance of jet exhaust mechanical turbulence are made for taxiing aircraft. The estimates here are restricted to perpendicular winds for simplicity.

Analysis of the experimental data revealed that the precision of measurement of the initiation time of each aircraft passage "event" was not adequate for analysis of differences between expected arrival times for CO at the first tower under alternate plume bending hypothesis. Thus, although

these alternative descriptions of aircraft plume bending are given, the present comparisons with experimental evidence are restricted to the phenomenon of plume rise. It is this mechanism for aircraft plume dilution that was of primary concern in the Dulles experiments [Smith (1977)], although the other three mechanisms listed were also considered.

4.5.2 Modeling Turbulent Jet Exhausts without Plume Rise

Aircraft jet exhausts discharged horizontally into a uniform crosswind may be described in two stages: the momentum-dominant stage and the buoyancy-dominant stage. In the momentum-dominant stage, the horizontal velocity of the jet plume decays through turbulent mixing with ambient air, and plume rise is suppressed. In the buoyancy-dominant stage, the plume rises and is entrained by the vertical motion. If it is assumed that there are no interactions between adjacent engine plumes and plume rise ignored, the bending path of a nonbuoyant momentum jet in a crosswind may be estimated from Eq. (1):

$$\hat{y} = 1.5 V_r^{2/3} \hat{x}^{1/3} \quad (1)$$

where the coordinate system is that shown in Fig. 4.7, with B (angle between the y-axis and aircraft path) equal to zero [see Briggs (1969)].

$$V_r = V_e/u$$

$$V_e = \text{exhaust velocity}$$

$$u = \text{windspeed}$$

$$\hat{y} \equiv y/D$$

$$\hat{x} \equiv x/D$$

$$D = \text{exit diameter}$$

the maximum penetration length of the exhaust plume behind the aircraft can be estimated from:

$$\hat{y}_{\max} = 3V_r \text{ and } \hat{x}_{\max} = 8V_r \quad (2)$$

At this y_{\max} distance behind the aircraft, the angle between the plume centerline and the y-axis may be found from Eq. (3):

$$\theta = \tan(dy/dx) = \tan^{-1} \left[1/2 \left(\frac{V_r}{x} \right)^{2/3} \right] \quad (3)$$

therefore, $\theta_{\max} = 7^\circ$.

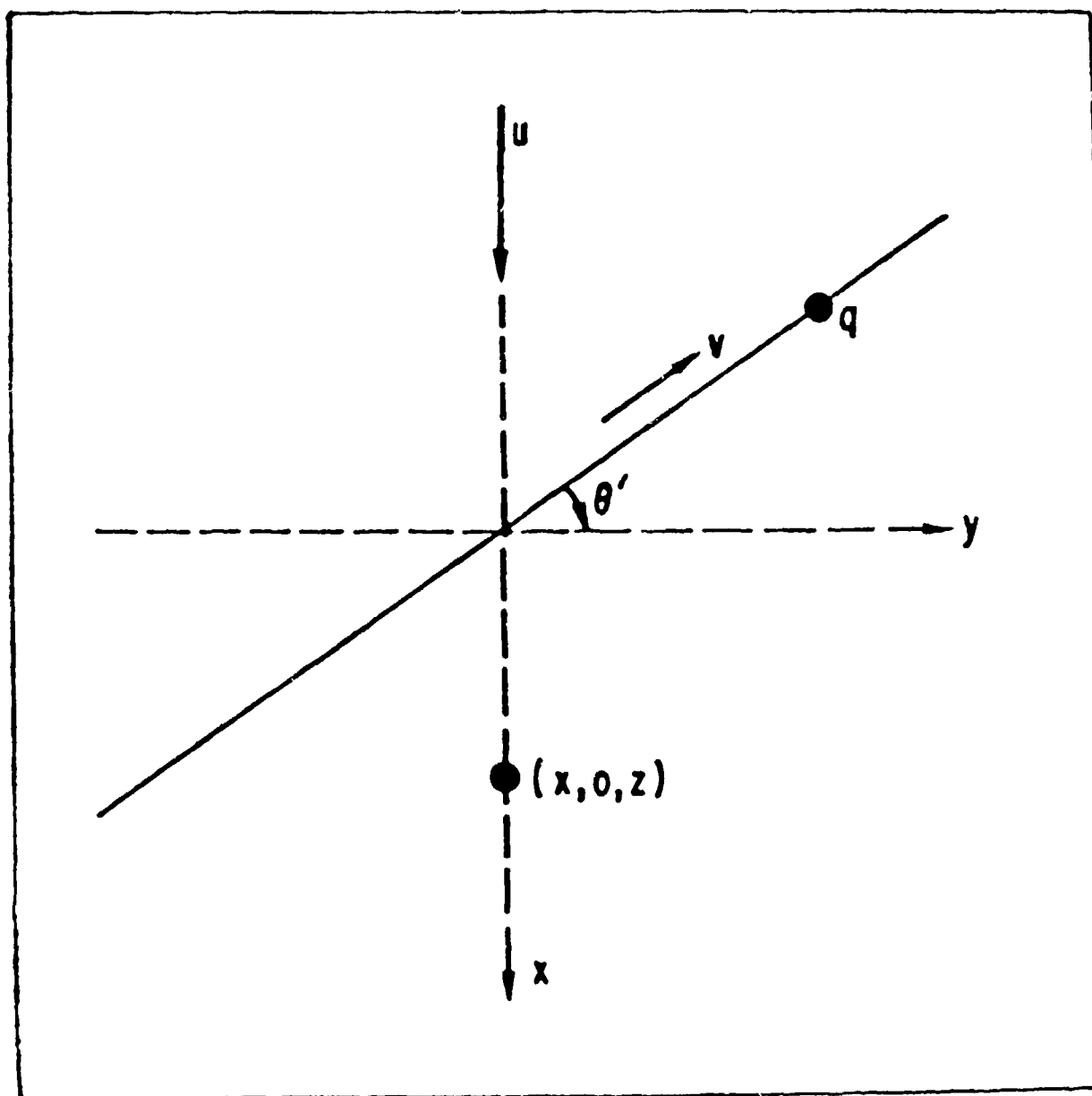


Fig. 4.7. Coordinate System for Model

To evaluate \hat{y}_{\max} and \hat{x}_{\max} for engines of the specific aircraft, Table 4.1 should be consulted. Also presented in Table 4.1 are appropriate values of the exit velocities and temperatures for calculation of effective velocity ratio:

$$V_r' \equiv \left[\frac{\rho' v_e^2}{\rho u^2} \right]^{1/2} \quad (4)$$

where ρ = density of the ambient air
 ρ' = density of the jet exhaust

It is expected that substitution of V_r' in the Eq. (1) through (3) will yield more accurate estimates for jet exhausts. In Table 4.1, the exhaust diameter, exit velocity, and exit temperature is given for the JT-3 and JT-8 engine during taxi/idle mode operation. Thrust values and mass emission rates are also given for comparison. For average surface winds of 5 m/sec, V_r' would range from 15 for the JT3s to 23 for the JT-8s during taxiing operations. For the range of $8 < V_r' < 54$ and $x \leq 34$, experimental evidence [Patrick (1967)] indicates:

$$\hat{y} = (V_r')^{0.85} (x)^{0.38} \text{ and } y_{\max} = 2.3 (V_r')^{1.37} \quad (5)$$

These relationships yield similar results to those obtained from Eqs. (1) and (2). Thus, for taxiing B707s, $y_{\max} \approx 40$ m and for B727s $y_{\max} \approx 53$ m, and corresponding x_{\max} values of 108 m and 138 m (with wind speeds of 5 m/sec). For sensors near the edge of the taxiway, the value of x_{\max} would determine whether dilution of the plume reaching those sensors was dominated by jet trail turbulence or ambient turbulence.

Table 4.1. Aircraft Engine Emission Parameters

Aircraft Type	B707	B727
Engine Type	JT-3	JT-8
Diameter, Exit (m)	0.9	0.75
Ve (m/sec)	76	114
Te (°K)	386	440
Mass Rate (Kg/sec)	45	40
Thrust (Nt)	270	250

Source: Goldberg (1978)

4.5.3 Plume Rise Modeling

To obtain a simple plume rise equation for a buoyant plume it is necessary to make some basic assumptions:

1. The flow is fully turbulent, thus the effect of molecular viscosity or Reynolds number is negligible.
2. Boussinesq approximation is valid, i.e., local density variations are neglected except when multiplying by gravity.
3. The buoyancy is assumed to be conserved.
4. The fluids are quasi-incompressible.

This theory or the 2/3 power relation was obtained by Slawson and Csanady (1967) and substantiated by Briggs (1969) and Hoult, Fay and Forney (1969).

Using the entrainment hypothesis given by Morton, Taylor, and Turner (1956), one may express the rise of the buoyant plume from jet aircraft as:

$$z - z_0 = \left[\frac{3}{2\alpha^2} \right]^{1/3} F^{1/3} u^{-1} (x - x_0)^{2/3} \quad (6)$$

where

- z_0 = initial height
- x_0 = initial downwind distance
- F = bouyancy flux
- α = entrainment constant
- u = windspeed

Although this 2/3 power law relation was developed originally for stationary sources with lower exit plumes than jet exhaust, its use as a first estimate for the present application is encouraged two factors:

1. The heat flux from a jet engine is similar in magnitude to a small stationary source ($F \approx 10^2 \text{ m}^4/\text{sec}^3$).
2. This same power law has been successful in describing plumes from high temperature gas turbine stacks located in a region of high ambient turbulence [Hoult (1975) and Egan (1975)].

4.5.4 Event Modeling

Several distinct approaches were attempted in the analysis of the Dulles three-tower data. The most straight-forward involved fitting a gaussian vertical profile, plus ground reflection term to the concentration measurements at each tower to obtain the plume's centerline location and vertical spread for each event. After this individual fitting, the dynamical plume rise and growth equations were fitted to the earlier obtained values for the plume centerline and σ_z . The advantage of this approach was that plume successful for the first tower (i.e., closest to the taxiway), but it proved unreliable at the more distant towers where plume centerlines were often above the highest receptor and/ or where rapid vertical dispersion produced nearly uniform vertical concentration profiles.

At the other extreme lies the ensemble-fit method, where the entire set of observations of a single aircraft type under the full range of meteorological conditions is applied to a single comprehensive theory containing a number of adjustable parameters. This method provides a starting point for investigating single event deviations from the ensemble predictions but may obscure interesting dynamical effects not built explicitly into the model. This method was chosen above the single event method because of the fact that many events had a "non-ideal" distribution where a centerline maximum was not observable at even the first tower. Figure illustrates the plume rise at tower 1.

Other methods like alternate multiparameter schemes for assessing individual events were considered but abandoned as their numerous parameters could not be adequately determined by the data accompanying each event.

4.5.5 The Ensemble Model

Consider the case of a source with emission rate q moving at velocity V along an infinite line orientated at an angle θ' with respect to the positive y direction (see Fig. 4.7). If the wind, u , defines the positive x direction, the receptor is located at $(x, 0, z)$ and $t = 0$ corresponds to the source position $(0,0)$, then the instantaneous concentration at the receptor is given by Eq. 7.

$$c(t) = \frac{q \exp \left\{ -\frac{1}{2} \left(\frac{x - ut}{\sigma} \right)^2 - \left(\frac{V \cos \theta'}{V_e} \right)^2 \right\} S(z, H, z)}{2 \pi \sigma^2 z V_e} \quad (7)$$

where

$$S(z, H, \sigma_z) \equiv \exp \left\{ -\frac{1}{2} \left(\frac{z - H}{\sigma_z} \right)^2 \right\} + \exp \left\{ -\frac{1}{2} \left(\frac{z + H}{\sigma_z} \right)^2 \right\}$$

$$V_e \equiv |\vec{u} - \vec{v}|$$

and assuming $\sigma_x = \sigma_y = \sigma$ does not vary significantly over the time interval:

$$\frac{x - \sigma}{u} < t < \frac{x + \sigma}{u}$$

While several assumptions involved may be avoided by a more tedious calculation, they do not appear in conflict with the experimental situation at hand. This simple formulation then leads directly to the expressions:

$$C_{\text{peak}} = \frac{qS(z, H, \sigma_z)}{2\pi\sigma\sigma_z V_e} \quad (10)$$

and

$$\Gamma = \sqrt{8\ln 2} \frac{\sigma}{u} \left(\frac{V_e}{V \cos \theta'} \right) \quad (11)$$

which, with minor corrections for Ecolyzer response (Smith, 1977) correspond to the measured peak concentration above background and the pulse duration at 50% of peak concentration, respectively.

The dynamic behavior of the plume was assumed to be described by the equations:

$$\sigma = \sigma_x(0) + b_x ut \sin \sigma_\theta \quad (12)$$

$$\sigma_z^2 = [\sigma_z(0) + b_z ut \sin \sigma_\theta]^2 + \frac{(H - H_0)^2}{10} \quad (13)$$

$$H = H_0 + h(x - ut_0)^p / u^q \quad (14)$$

$$H_0 = 1.2 \sigma_z(0) \quad (15)$$

where

σ_θ = 3 min average measurement of the standard deviation of wind direction,

$\sigma_x(0)$ = initial along-wing plume spread,

$\sigma_z(0)$ = initial vertical plume spread,

b_x, b_z = plume growth parameters. They describe the growth of the plume relative to σ_θ ,

H = plume centerline height at distance x ,

H_0 = initial plume centerline height.

The addition of the term $\frac{(H - H_0)^2}{10}$ is suggested by Pasquill.

The Eq. (14) used for plume rise is somewhat more general than the equation suggested theoretically in that the powers p and q are free parameters. Fits were done with p and q free and with these parameters fixed at $p = 2/3$ and $q = 1$ as given by the $2/3$ power law relation.

Equation 15, $H_0 = 1.2 \sigma_z(0)$ is dictated by the assumption of zero vertical concentration gradient which causes an uniform concentration profile near the ground.

With these Eq. (9-14) we can define a measure of "goodness-of-fit" χ^2 and via minimization of χ^2 the eight free parameters $\sigma_x(0)$, $\sigma_z(0)$, b_x , b_z , h , t_0 , p , and q are to be determined. The equation for χ^2 is given by:

$$\chi^2 = \frac{1}{(\delta C)^2} \sum \left(C_{\text{peak}}^T - C_{\text{peak}}^M \right)^2 + \frac{1}{(\delta \Gamma)^2} \sum \left(\Gamma^T - \Gamma^M \right)^2 \quad (16)$$

where ΓC and $\delta \Gamma$ denote the approximate measurement errors of 0.25 ppm and 10 seconds. The superscripts T and M denote theory and measurement respectively. The indicated summation is over all measurements for a single aircraft type.

The preceding expression for χ^2 should actually be normalized by the total expected variances in C_{peak} and (i.e., the statistical plus the measurement component) and not merely by the measurement variances. However, the statistical variances are not determinable from these data alone. This shortcoming preclude determination of overall model confidence level and parameter errors. Some additional insight into potential model improvements is provided by alternate consideration of the linear correlation coef-

ficients, for predicted versus observed C_{peak} and Γ , and the associated confidence bounds on these correlations.

4.5.6 Results

Table 4.2 shows the number of events for the different aircraft types. The results are based on a somewhat smaller selection because of the constraint that the wind direction was within 70° of being perpendicular to the taxiway. All events were observed under near neutral to unstable atmospheric conditions, with bulk Richardson numbers ranging from -1.0×10^{-4} to -0.02 , windspeeds in the range from 1.2 to 13.4 m/sec, and 3-minute σ_θ from 4.7 to 37.0 degrees. Average taxi speeds ranged from 7.6 to 11.8 m/sec.

Fixing the values of p and q as $2/3$ and 1 respectively, the ensemble fit yields the parameters given in Table 4.3. The correlation values for the concentration values and their 95% confidence limits are also given.

The correlation values for the pulse duration is not given. The theory is quite poor in predicting Γ , the pulse duration. This is partially attributable to the fact that Γ is predicted to be independent of height but considerable fluctuation is observed experimentally. Another factor contributing to this poor correlation is that, contrary to theoretical expectations, the observed pulse duration increases very little between the first and third tower and is, in fact, consistent with zero along wind plume growth (i.e., $b_x = 0$). Thus, the differences in horizontal growth rate factor b_x between aircraft types cannot be considered significant. The value of b_z is found to be highly correlated with the H parameter, which establishes the rate of plume rise and the associated vertical dispersion due to entrainment. In addition, despite significant differences in engine placement on the B707, B727, and DC8 aircraft, the initial along wind and vertical plume dimensions are nearly identical.

The rather poor value of the correlation coefficient r is thought to be due to large variations in ambient air stratification and its effect on buoyancy. Evidence for this is obtained when each event is optimized separately with h , the parameter which describes the buoyancy, as the only free parameter. The other parameters were fixed to their values, found in the ensemble fit. Figure 4.8 shows the wide variety of h values for the B707 when calculated as described above. Significant variations about the ensemble

Table 4.2. Number of Events per Aircraft Type

A/C TYPE	EVENTS
B707	48
B727	25
B737	4
B747	7
DC8	12
DC9	3
DC10	17
A37	7
L1011	15
SST	10
CESSNA	3
TURBO	1

Table 4.3. Ensemble Fit Parameters

AIRCRAFT TYPE	$\sigma_x(0)$	$\sigma_z(0)(ft)$	b_x	b_z	h	$t_0(sec)$	$r(95\% C.L.)$
B707	73.7	10.7	0.13	0.67	16.0	8.45	0.53 $\begin{pmatrix} 0.47 \\ 0.59 \end{pmatrix}$
B727	65.4	11.5	0.45	0.26	11.9	8.89	0.24 $\begin{pmatrix} 0.14 \\ 0.34 \end{pmatrix}$
B737/DC9	75.6	18.1	0.55	0.19	5.1	9.67	0.51 $\begin{pmatrix} 0.33 \\ 0.65 \end{pmatrix}$
B747	97.6	0.03	0.76	2.13	26.2	15.8	0.49 $\begin{pmatrix} 0.30 \\ 0.64 \end{pmatrix}$
DC8	79.8	10.9	0.08	1.26	1.3	60.0	0.64 $\begin{pmatrix} 0.53 \\ 0.73 \end{pmatrix}$
DC10	43.9	15.5	0.49	0.35	14.8	12.8	0.44 $\begin{pmatrix} 0.32 \\ 0.54 \end{pmatrix}$
L1011	117.4	11.8	0.08	0.29	9.8	10.3	0.60 $\begin{pmatrix} 0.50 \\ 0.68 \end{pmatrix}$
A37	5.0	14.1	0.33	0.08	8.6	12.0	0.37 $\begin{pmatrix} 0.15 \\ 0.55 \end{pmatrix}$

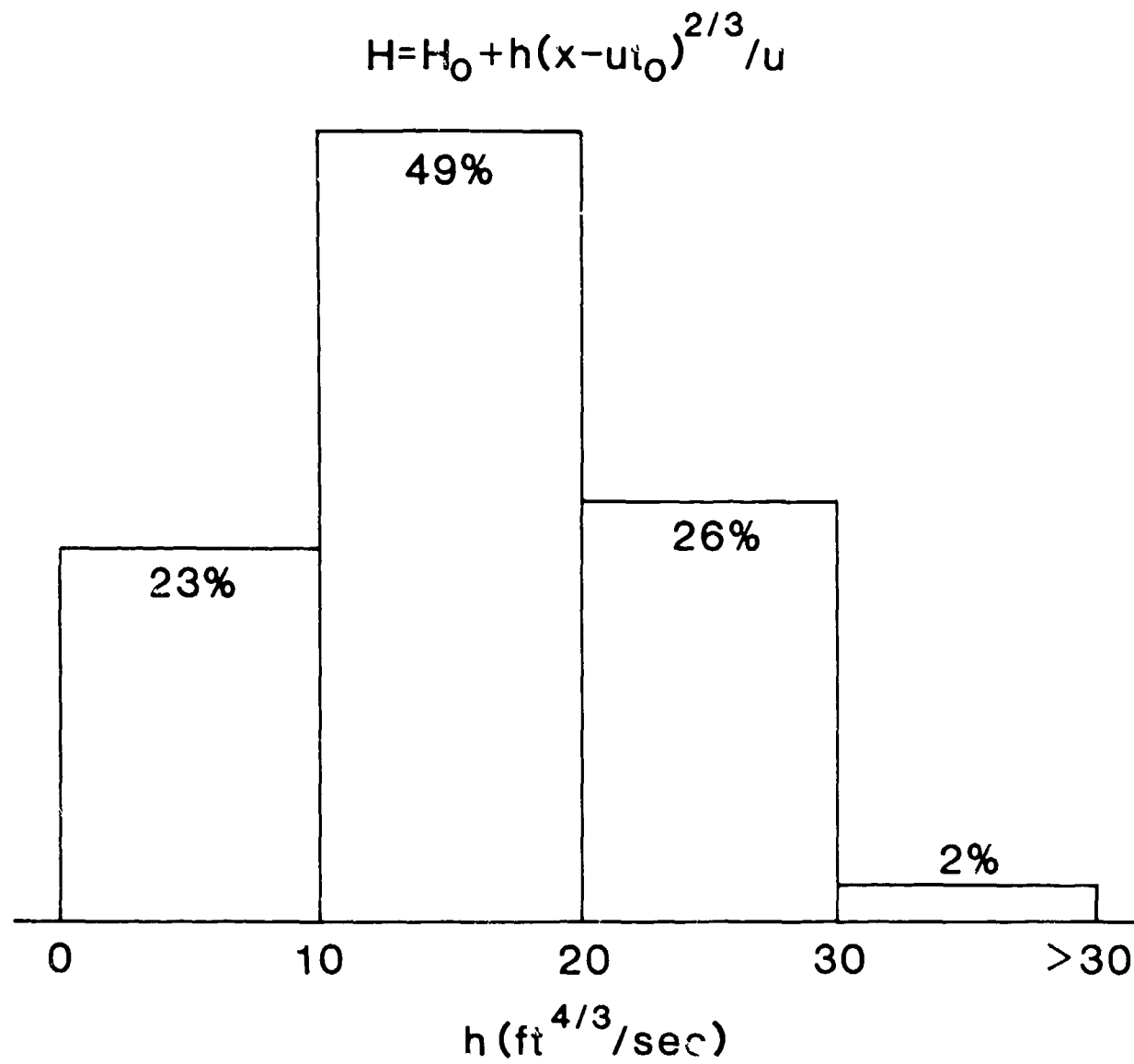


Fig. 4.8. Frequency Distribution of Plume Rise Coefficient

value of 16 are seen. The correlation coefficient of jumps from 0.53 to 0.81 when this event-by-event freedom is permitted.

Another insight into event-by-event deviation from the predicted $x^{2/3}$ plume rise behavior can be seen in Fig. 4.9. It shows the wide variety of p-values (the plume rise trajectories) one obtains when p is determined on an event-by-event basis. Ensemble optimizations in which p and q were allowed to be free indicated somewhat higher values for p and q of 1.25 and 1.75, respectively; however, the resulting improvements in r were insignificant.

The plume rise equation used in the above analysis does not predict final plume height and thus is of limited usefulness in terms of airport air quality models. A simpler model, described briefly below has been applied to the 3-tower data and the results indicate the importance of initial plume dilution and rise on observed concentrations.

Assume that plume growth is governed by the equations

$$\sigma_x = \sigma_y = \sigma_x(0) + b_x \sigma_{yT}(x) \quad (17)$$

and

$$\sigma_z = \left[\left(\sigma_z(0) + b_z \sigma_{zT}(x) \right)^2 + 0.1 (H - H_0)^2 \right]^{1/2}, \quad (18)$$

where $\sigma_x(0)$ and $\sigma_z(0)$ are the initial horizontal and vertical plume dimensions, $\sigma_{yT}(x)$ and $\sigma_{zT}(x)$ are the dispersion coefficients taken from Turner (1970) and $b_x = b_z = 0.7$ is a correction for averaging time. Further assume that the final plume rise is given by the equation

$$H = H_0 + h/u, \quad \text{where } H_0 = 1.2 \sigma_z(0) \quad (19)$$

u is the wind speed, and h is the plume rise factor to be determined. Taking the dynamical behavior of the plume rise into account and applying these equations to a sample of 121 cases, encompassing all the aforementioned aircraft types except Concorde, one obtains the optimized parameters

$$\sigma_x(0) = 60 \text{ ft}$$

$$\sigma_z(0) = 26 \text{ ft}$$

$$h = 386 \text{ ft}^2/\text{sec}$$

For ground level data points ($z = 6 \text{ ft}$) the regression equation

$$C_{\text{OBSERVED}} = m C_{\text{THEORY}} + b$$

$$H = H_0 + h(x - u) \gamma_0)^p / u^q$$

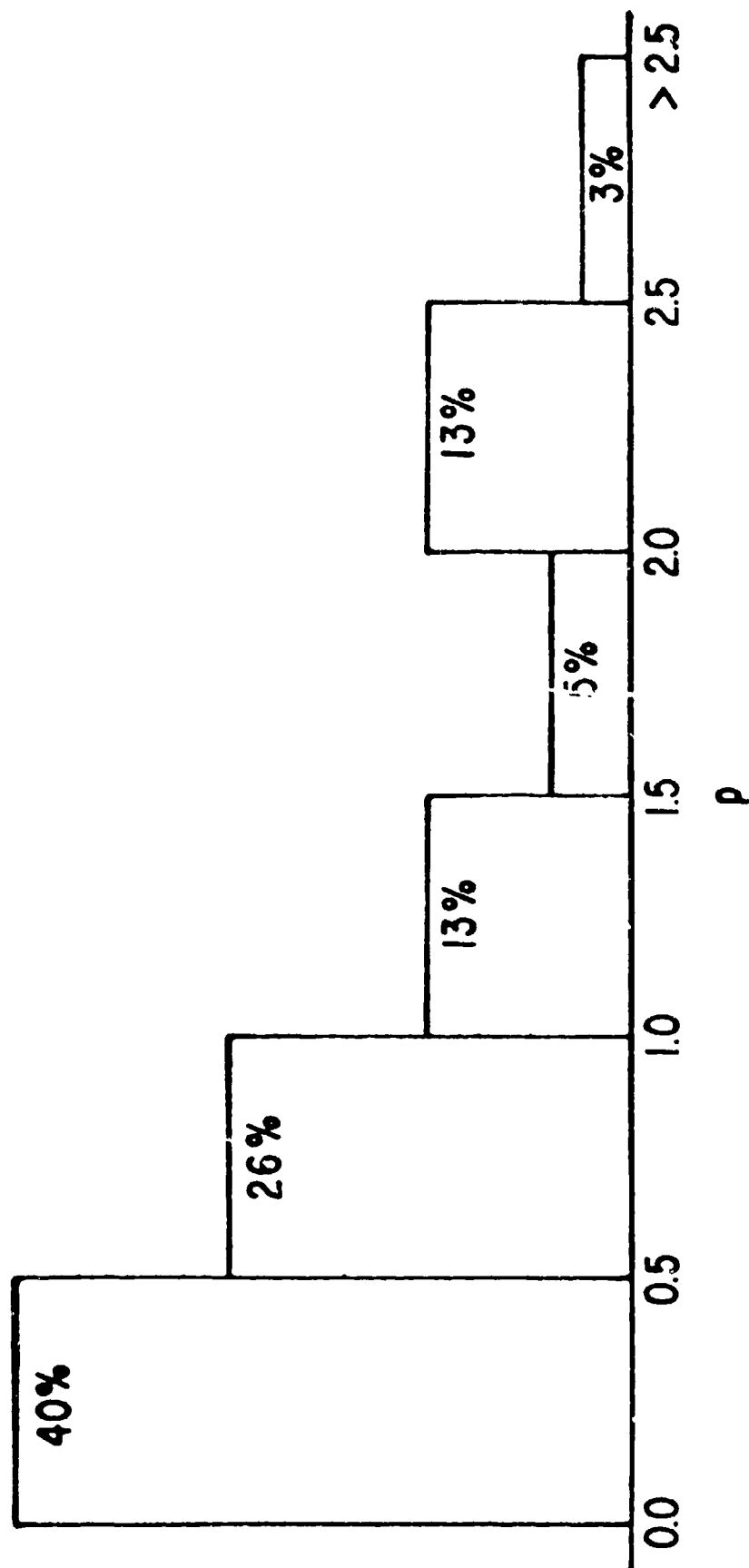


Fig. 4.9. Frequency Distribution of Power Law for Distance Dependence

fit to the peak concentrations yields a correlation coefficient of 0.56, a slope of $m = 0.96$, and an intercept of $b = 0.11$ ppm. A scatter plot of observed versus peak concentrations is shown in Fig. 4.10.

If the parameters describing the initial plume dimensions and plume rise are instead taken as $\sigma_x(0) = \sigma_z(0) = h = 0$, the resulting regression parameters are $m = 0.11$ and $b = 0.52$, which implies that for the highest observed concentrations, the theory is overpredicting by a factor of 9. Hence the assumptions about initial plume size and rise can have serious air quality modeling consequences. For example, the initial vertical dispersion of 26 ft is equivalent to the amount of dispersion realized by 1500 ft of downwind transport under F stability conditions.

4.5.7 Conclusions

Preliminary analysis of measurements of the CO exhaust plume from taxiing aircraft suggest that the rise of these horizontally injected, buoyant plumes is not inconsistent with the $2/3$ power law relation over the distance range of 65 m to 165 m, but large event-by-event fluctuations from this average behavior lead to rather mediocre correlations between theoretically predicted and observed pollutant concentrations.

There is an evidence for about a 10 second delay in plume rise. The present analysis suggests that the plume rise delay time, t_0 is significant and at the highest wind speed has the effect of suppressing plume rise at the first tower.

Recalling the comparison between the B707, B727, and DC8, the initial plume rise during taxi was found to be characteristic of aircraft dimensions. The significance of engine geometry one might expect was not observed.

The average value of h , which describes the buoyancy, determined here is about equal to one-half the value found from

$$\left(\frac{3}{2\alpha^2}\right)^{1/3} F^{1/3},$$

where the total buoyancy flux F for the B707 and B727 aircraft types while taxiing is about $150 \text{ m}^4/\text{sec}^3$ [Goldberg (1978)]. A value of 0.6 for α was used in this calculation. In the case of jet aircraft plumes a larger value for the entrainment constant might be expected.

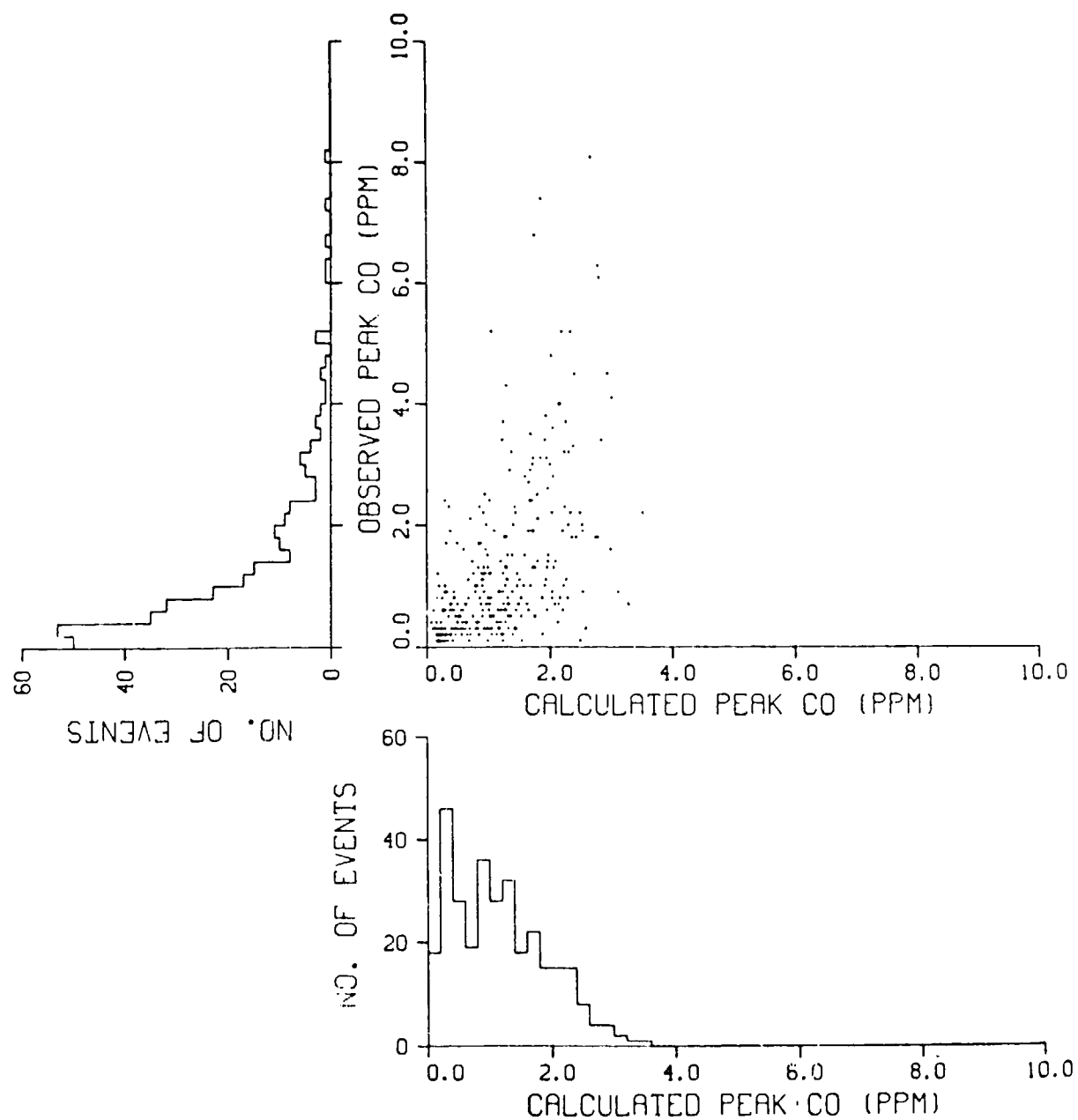


Fig. 4.10. Scatter Plot Plus Projection Histograms for Observed Versus Calculated Peak CO at Ground Level Receptors ($z = 6$ ft.). The calculation uses equations 17-19 and the optimal parameters given in the text.

Dulles measurements indicate that aircraft contributions to hourly CO concentrations do not exceed 0.06 ppm per aircraft at a distance of 200 ft from the taxiway centerline. Thus, concentrations adjacent to a busy taxiway accommodating 100 aircraft per hour should not exceed 6 ppm. The Dulles data also permits determination of initial plume dimensions and plume rise for subsequent use in airport air quality models, and further indicate that failure to consider these initial plume parameters can lead to order-of-magnitude overpredictions of local concentrations.

4.6 RE-EXAMINATION OF DULLES SINGLE EVENTS (THC VS CO)

Although hydrocarbons (HC) are not the main impetus of this program, they are perceived to be a major component of the air quality deterioration experienced at airports. In this regard, simultaneous measurements of HC and CO from taxiing aircraft at Dulles have shown a high degree of correlation. The THC measurements at Dulles must be treated with the same reservations concerning the separation of reactive and non-reactive species. However, when dosages due to single aircraft are considered, the methane fraction may most likely be ignored. The peak THC concentrations above background due to the passage of an aircraft average 1.48 ppm. With an average THC dose per aircraft of 32 ppm-sec, it will require 84 aircraft operations between 6 to 9 A.M. to reach 0.25 ppm. The THC is measured at a height of 6 ft, 215 ft from the taxiway, with C stability as an average. Adjusting these measurements to reflect worst case conditions suggests that 0.25 ppm may be approached at Dulles with ~40 operations per 3 hours under such adverse conditions.

In order to evaluate indirectly the decrease in THC with distance due to turbulent dispersion, coincidentally measured concentrations of THC and CO are compared. According to published emission factors for the taxi/idle mode, the CO/THC emission ratio varies from 1.1 to ~4 depending on aircraft type. A scatter plot (Fig. 4.11) of peak concentrations of CO versus THC for taxiing aircraft events exhibits significant correlation ($r = 0.72$) and a CO/THC ratio of mean peak concentrations of 1.26. A similar analysis of the mean doses gives a ratio of 2.1. As peak concentrations are a function of instrument response time, the dose ratio represents the more useful figure. The dose ratios, found to vary more between individual events than between aircraft

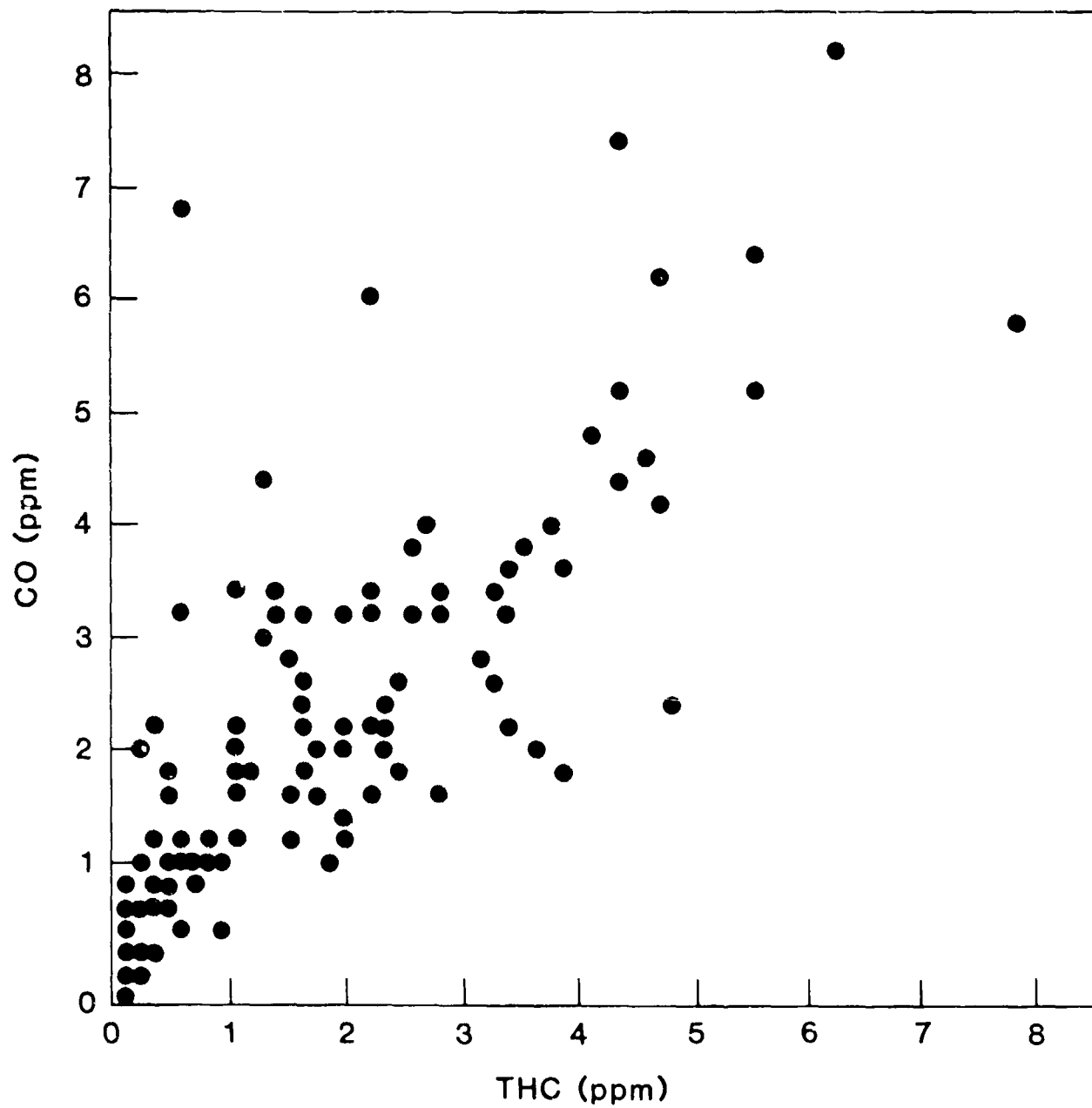


Fig. 4.11. Concentration Crossplot of CO vs THC from Taxiing Aircraft

(i.e., engine) types, are seen to agree in the mean with the engine emission ratios of CO to THC. From these single station comparisons it appears that estimation of THC through scaling of CO concentrations is viable for such near-field experiments where the background may be separately identified.

5 CARBON MONOXIDE MEASUREMENTS AT A HIGH ACTIVITY FLY-IN AT LAKELAND AIRPORT, FLORIDA⁺

5.1 INTRODUCTION

Carbon Monoxide (CO) concentrations were measured during a major fly-in of general aviation (GA) and experimental aircraft at Lakeland Airport, Florida from January 23 thru 29, 1978. Over 3000 aircraft participated in this fly-in, where in excess of 250 aircraft operations per hour were experienced. The purpose of the measurements was to quantify the effect of emissions from GA aircraft on air quality under extreme conditions of airport activity. The Federal Aviation Administration (FAA), in conjunction with the Environmental Protection Agency (EPA), planned the measurement activity. Three FAA-owned Energetic Sciences "Ecolysers" (CO monitors) were used. EPA personnel participated in the field program and assisted in data gathering.

Figure 5.1 is an aerial view of the airport and the lightly populated surrounding countryside and Figures 5.2 and 5.3 show the operating pattern at the airport during easterly and westerly winds, respectively. Figure 5.4 shows the location of the 25 monitoring sites used at one time or another in the course of the data gathering. Measurements were made during aircraft landing, takeoff and taxi modes. Additionally, an instrument was set up in an auto which was periodically driven around the entire airfield at the periphery, in attempts to detect gross airport contributions to the local CO "background." Within the discriminating capability of the equipment this was not possible, nor were significant observable levels of CO measured during any of some 50 observed landings.

From all these measurements taken under a variety of airplane activity, and meteorological conditions, the maximum projected one-hour average concentration measured at positions where people might be expected to be located was less than 2 parts per million (ppm) by volume. This concentration is insignificant (Federal Register, June 19, 1978) when compared to the one-hour National Ambient Air Quality Standard (NAAQS) of 35 ppm. These measurements constituted one consideration in the formal recommendation by the EPA to withdraw GA engine emission standards (Federal Register, March 24, 1978).

⁺Adapted from "Pollution Dispersion Measurements at High-Activity Fly-In of General Aviation, Military, and Antique Aircraft" by H.M. Segal, 1978

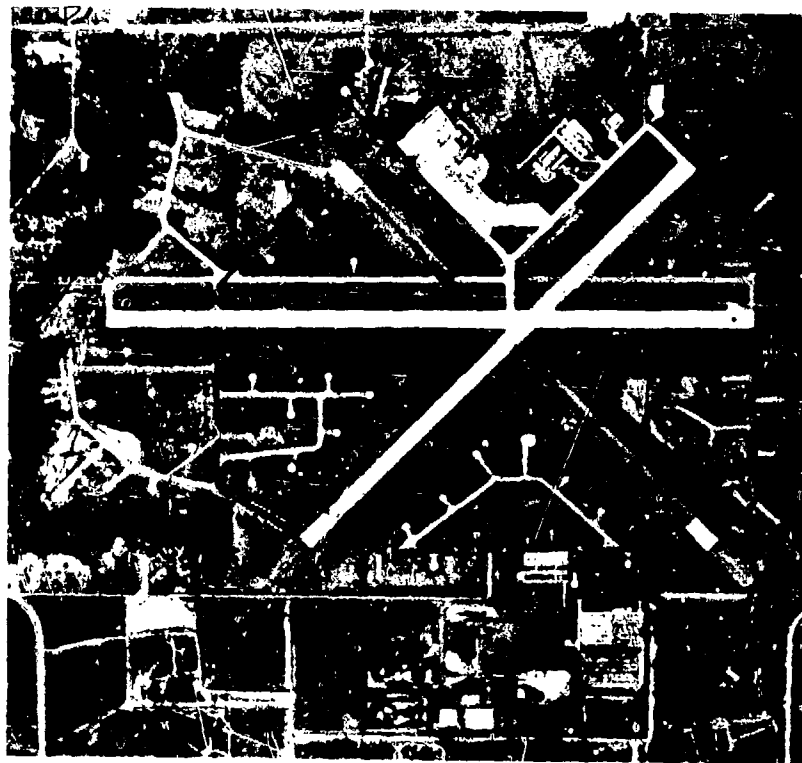


FIG. 5.1. Aerial View of Lakeland Airport, Fla.

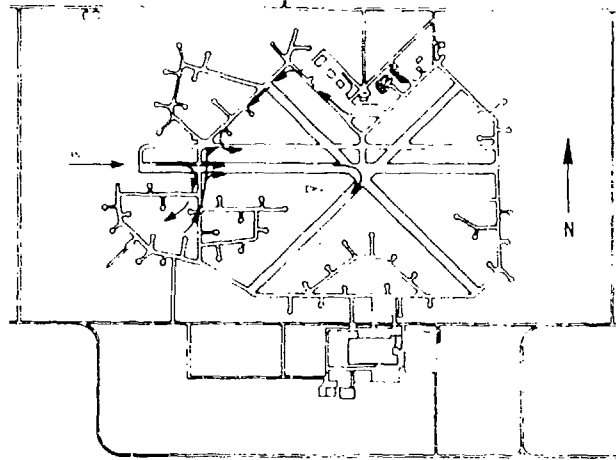


Fig. 5.2. Airport Operations During Easterly Winds - Lakeland Airport

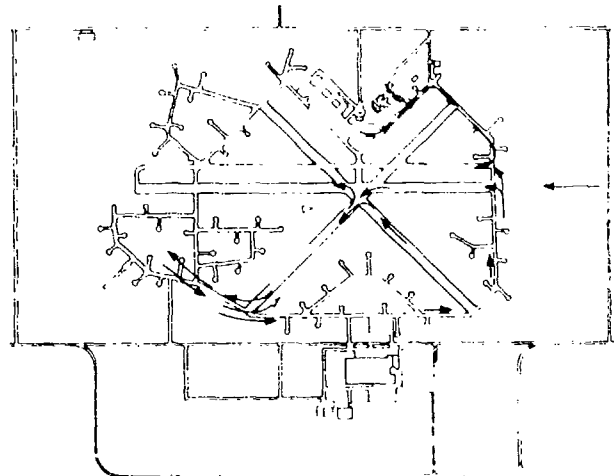


Fig. 5.3. Airport Operations During Westerly Winds - Lakeland Airport

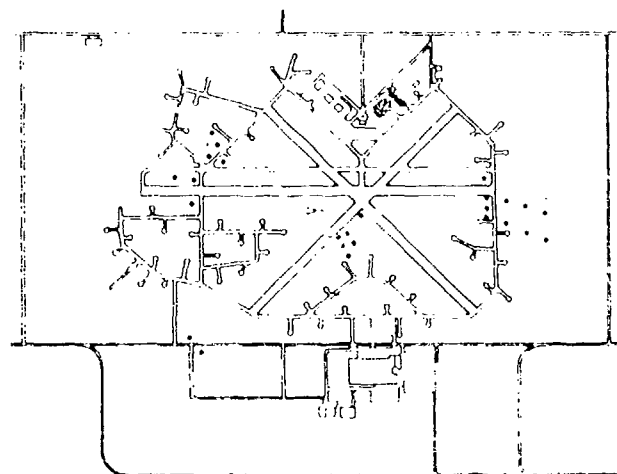


Fig. 5.4. Monitoring Sites - Lakeland Airport January 23-30, 1978

Analysis of these measurements not only showed the small influence of GA aircraft on air quality but also for the first time quantified the dispersion rate from individual and groups of GA aircraft that were landing, taxiing and taking-off. Comparison of these measurements with theory indicated that some models may not account for the unique dispersion characteristics of the hot, turbulent airplane emission source.

5.2 APPROACH

To fulfill the need for mobile monitoring, Ecolysers and associated strip chart recorders were placed in the two automobiles used in this monitoring effort. By reinforcing the radio antenna with a dowel, an effective mobil air sampling system was devised. Figures 5.5 and 5.6 show this installation with the instruments placed inside and outside the automobile. Where a third monitoring site was required the installation shown in Figure 5.7 was used. Instruments were calibrated with 20 ppm calibration gas twice per day and before and after each major series of measurements.

The monitoring procedure was similar to the one used at Dulles International Airport to monitor Concorde emissions (Segal, 1977 and Smith et al, 1977). Three monitors were placed in a line abeam to the path of a taking-off or taxiing aircraft so that these instruments could sequentially detect the exhaust plume of aircraft emissions as the plume was transported by the wind over the three stations. In addition, as mentioned above, a car instrumented with an Ecolyser was periodically driven around the entire airport in attempts to detect the gross airport contribution to the local vicinity CO background.

Measurements were also taken during landing, takeoff and taxi. Taxi measurements were made at both (multiple event) and low (single event) activity times.

5.3 RESULTS

Landing Measurements - On January 27, emissions from over 50 landing aircraft were measured at site 20. (Figure 5.4). Winds were from the north at 18 mph and "C" stability was estimated.

No concentration above background level was recorded at this site, located 450 ft. from the runway.



Fig. 5.5. Monitoring Installation - Inside Automobile

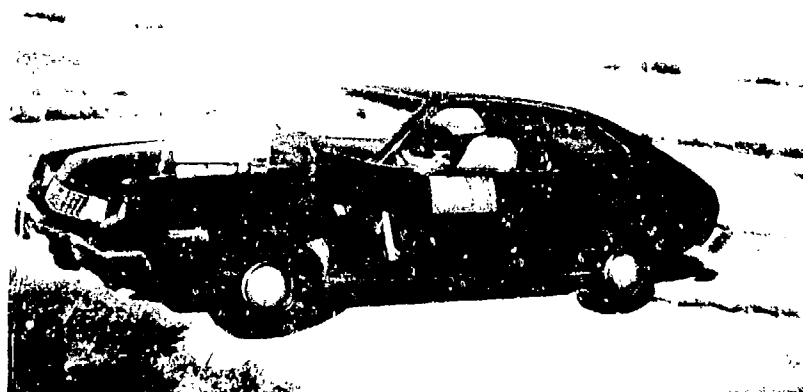


Fig. 5.6. Monitoring Installation - Outside Automobile



Fig. 5.7. Monitoring Installation - Non-vehicle

Takeoff Measurements - On January 29, emissions from over 30 taking-off aircraft were measured at sites 20, 21, and 22. (Figure 5.4). Wind was from 330° at 12 mph and a "B" stability was estimated.

The strip chart trace from a typical taking-off GA aircraft is shown in Figure 5.8. Emissions from this modern GA aircraft are quite low.

However, at sites 20, 21, and 22, the highest pollution levels of the entire week was also recorded. This occurred when a World War II vintage B-25 took off. The CO strip chart trace of this take-off is shown in Figure 5.9. The high emission levels from this aircraft's large radial engines, characteristic of both military and commercial aircraft engines of that time period are to be compared with the almost undetectable pollution produced by the turbine engines used in present day commercial aircraft (Segal, 1977 and Smith et al, 1977). This comparison indicates that pollutant emissions have been drastically reduced by the aircraft industry in developing the gas turbine engine technology of the present era.

Dispersion measurements permit determination of a power law exponent by which atmospheric dispersion may be parameterized. This dispersion rate exponent has been measured during airplane taxi and takeoff assuming that the relationship between concentration and downwind distance can be expressed as:

$$C = X^{-K} \quad (1)$$

where C is the concentration at downwind distance X. The rate exponent at which the pollutant disperses is defined as K. Peak concentrations of those takeoff events having adequate signal to background ratio were averaged and were found to disperse as $X^{-1.9}$ in the power law expression listed above. This exponent which is derived from measurement data will be compared with the theoretical value of this exponent in Section 5.4.

Taxi Measurements (Low Activity) - On January 26, emissions from over 40 taxiing aircraft were recorded. Wind was from 340° at 15 mph and a "C" stability was estimated. Pollution from this mode dispersed as $X^{-1.0}$ in the previously mentioned power law relationship.

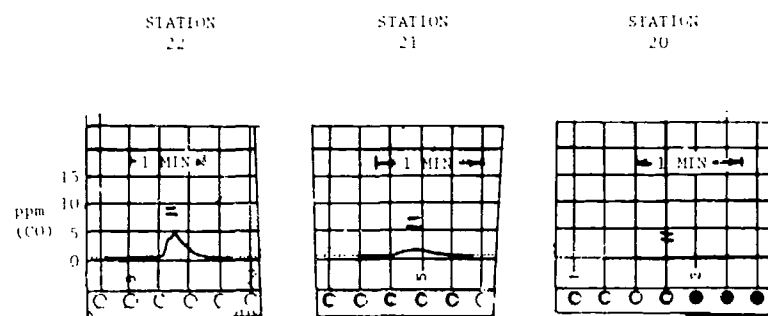


Fig. 5.8. Trace of General Aviation Takeoff

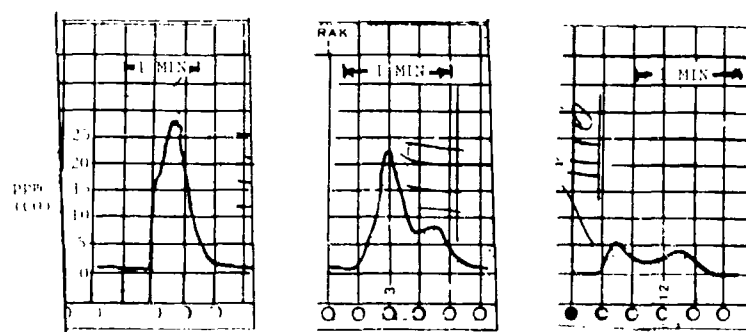


Fig. 5.9. Trace of B-25 Takeoff

Taxi Measurements (High Activity) - The most note-worthy data were obtained at station 17, 18 and 19 between 1700 and 1740 hours on January 28, when a continuous queue of over 30 aircraft stretched down the taxiway for more than 1/2 mile. Wind was from 345° at 12 mph and "D" stability was estimated. During peak activity one airplane taxied by the monitoring station every ten seconds. As they approached the end of the taxiway, these aircraft were almost continuously dispatched down the two takeoff runways at the rate of 278 aircraft per hour.

Because both taxi and takeoff emissions impacted at the three monitoring stations downwind of the taxiing aircraft, it was necessary to devise a method for measuring emissions from the taking-off aircraft only. This was accomplished by moving the instrumented auto at site 18 to site 20 which is directly upwind of the taxiing aircraft. Takeoff concentrations were measured at this location. This move was made after sufficient data had been collected at site 18.

The contribution of takeoff emissions to concentrations at sites 17, 18, 19, and 20 was modeled and calibrated with measurements taken at site 20. This takeoff contribution was then subtracted from the total concentrations measured at sites 17, 18, and 19 to identify concentrations directly attributable to the taxiing aircraft. These data are plotted in Figure 5.10. These multiple event taxi emissions are found to disperse as $X^{-0.4}$ in the power law relationship $C \propto X^{-K}$.

5.4 CONCLUSIONS

The following conclusions may be drawn from the concentration summary of Table 5.1:

1. From all measurements taken under extreme aircraft activity conditions, the maximum recorded concentration for CO at the closest position where people might be expected to be located, was less than 2 ppm for a projected one-hour time period. This concentration is insignificant when compared to the one-hour NAAQS of 35 ppm.
2. The highest CO concentration ever recorded of the dispersing plumes of a taking-off airplane (22 ppm at 335 ft. from the runway centerline) was measured at Lakeland Airport on January 29, 1978. This measurement, which was from a World War II vintage B-25, indicates that airplanes have been significant sources of CO pollution in the past.

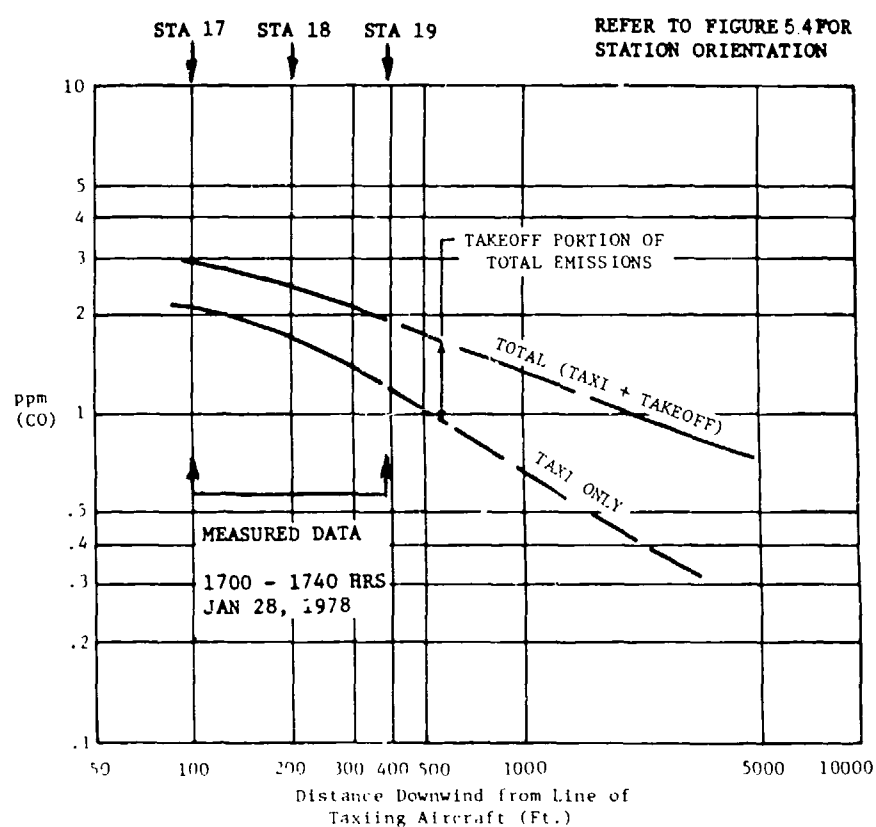


Fig. 5.10. Dispersion of Carbon Monoxide During Taxi and Takeoff - Lakeland Airport, Florida

Table 5.1. Carbon Monoxide Concentrations During Different Operational Modes

MODE	STABILITY CLASS	WIND SPEED (MPH)	CHARACTERISTICS PEAK CONCENTRATIONS PPM ABOVE BACKGROUND		
			SINGLE EVENT		1 HOUR AVERAGE
			DIST. 450 FT.	DIST. 335 FT.	DISTANCE 385 FT.
LANDING (SINGLE EVENT)	C	18	<1 PPM		
TAKEOFF (SINGLE EVENT)	B	12	<1 PPM*	23 PPM (B-25) 2 PPM (GA)	
TAXI (SINGLE EVENT)	C	15		< 1 PPM	
TAXI (DURING QUEUE)	D	12			~2 PPM

* Commercial Jet from Dulles Data, Ref. Smith et al, 1977)

The measured dispersion rate exponents during taxi and takeoff in some cases do not coincide with expectations based on dispersion rate curves (Turner, 1970) that are used in most airport models. This inconsistency is important to recognize, since it may contribute to errors in receptor concentrations calculated from airport pollution models. While this short term measurement program was not designed to develop a large data base or to explain dispersion inconsistencies (m.b., that no measurements of the vertical dispersion of the emission plume were made), the listing of the dispersion parameters in Table 5.2 represents an initial quantification of previously unmeasured dispersion characteristics of several types of aircraft exhaust plumes.

Factors contributing to the inconsistency between measurement and theory may be traced to the inability of the theory to effectively account for:

- a. Plume rise
- b. Extensive initial dispersion related to the turbulence field created by the high velocity fan action of the propeller. (The extent and duration of this turbulent field is unknown at the present time.)
- c. Different emission densities and turbulence intensity along the takeoff path of an accelerating aircraft.

Table 5.2. Measured versus Theoretical Aircraft Plume Dispersion Rates

Mode	Approximate Aircraft Speed	Propeller Speed	Measured Power Law Exponent, K.	Theoretical* Power Law Exponent, K.
Taxi (Single Event)	15 MPH (Constant)	Low	1.0	1.8
Taxi (During Queue)	5 MPH (Constant)	Low	0.4	0.9
Takeoff	25 (Accelerating)	High	1.9	1.8

*Derived from Turner, 1970

6 THE MEASUREMENT OF CO CONCENTRATIONS FROM QUEUING AIRCRAFT AT LOS ANGELES INTERNATIONAL AIRPORT⁺

6.1 INTRODUCTION

Carbon monoxide (CO) emissions from queuing aircraft were monitored at Los Angeles International Airport (LAX) from April 16 to April 20, 1979. Carbon monoxide was selected as the pollutant of concern because it is stable, easily measured and predominant during aircraft queuing. LAX was selected for this experiment because:

1. It is a busy airport.
2. High data accumulation is possible under the influence of the predominant sea breeze which blows emissions directly down the main queueing taxiway.
3. The airport authority was very cooperative and permitted equipment positioning directly on the taxiways.
4. A National Climatic Weather Station which records wind direction, speed and vertical temperature profiles is located within 1500 meters of the monitoring sites.
5. Data from this program could be compared with similar data generated in the early 1970s and which was used as a justification for the aircraft engine emission standards.

6.2 APPROACH

The approach of this program is to measure and model the emissions of aircraft that are lined up (or queued) along a taxiway just prior to takeoff. Queuing was measured at both the north and south runway complexes (Figure 6.1) from April 16 to April 20, 1979. Monitoring and wind measurement equipment were positioned directly downwind of the queuing aircraft.

Two Energetic Sciences Model 2000 "Ecolysers" were employed in this program. These instruments were calibrated with 20 parts per million (ppm) calibration gas before and after each intensive measurement period.

Equipment was placed in a Federal Aviation Administration vehicle with the pollution sampling tube extending outside the vehicle where it was attached to a vertical probe. Air intake height was 1.7 meters. A second

⁺Adapted from "Emissions from Queuing Aircraft" by H.M. Segal, 1980.

monitoring instrument was located 50 meters downwind from the first monitoring location. Its air intake tube was attached to a tripod and elevated to a height of 1.7 meters. (Results from this second monitoring location are not reported.) Figure 6.2 shows instrument layout. Equipment was lined up in the direction of the prevailing wind which, because of its westerly direction, transported a line of aircraft emissions directly over the receptors. This arrangement provided the desired worst case pollution geometry. Wind velocity was measured every 15 minutes at the monitoring sites.

Air quality was recorded during 162 minutes of aircraft activity during a five-day time period. Queue lengths varied from 1 to 8 aircraft. (Figure 3 shows the configuration of one 7 aircraft queue that was monitored.) Distance from the first queuing aircraft to the nearest receptor was 220 meters from the south runway and 320 meters for the north runway. Air quality was recorded for wind speeds of 2.8 to 8.6 meters per second under Pasquill-Gifford stability classes of B, C, D, and E. Airplane entrance to and exit from the various queue positions was recorded to the nearest second. This precise recording of the time when each aircraft entered and left its queue position and the simultaneous recording of pollutant concentrations at the downwind receptors were essential portions of this program. One person was assigned full time to accomplish these tasks.

Upon completing the monitoring program, the 162 minutes of data were stratified according to wind speed, stability class, and queue length, and a flow diagram such as the one shown in Figure 6.4 was prepared for each of eight different queuing conditions. These conditions reflected measurements taken during different days, wind speeds, and stability conditions. Emissions dispersion during transport to the monitoring sites was then modeled for comparison with measurements. Each airplane was positioned on the taxiway in accordance with its observed location. Data from Tank and Hodder (1978) were used to determine the height of the plume centerline and the initial size of the plume. Pollutant transport times from queue to the receptor location were determined by dividing each source-to-receptor distance by the measured wind speed.

6.3 ANALYSIS

Two types of analysis were performed. First, emissions from a number of short-duration queue events that occurred during the entire monitoring period were analyzed separately. This ensemble of measurements was then used to verify the model. Then, the single longest queueing event of 19 minutes duration, which occurred on April 18, was analyzed in detail. Emissions from this event were also summed with emissions from all other aircraft activity during a 70 minute time period surrounding the event. This longer averaging time calculation permitted model performance to be determined for the longer averaging time (1 hr) considered in the National Ambient Air Quality Standard (NAAQS) for carbon monoxide (CO).

Three types of data were considered. First, measured concentrations were averaged over the short duration of a queue event. Secondly, model estimates of concentrations were made corresponding to the meteorological conditions and averaging times of these measurements. Thirdly, model estimates were made to reflect worst case meteorology for comparison with the NAAQS. The NAAQS limit of 35 ppm is not to be exceeded more than once per year (approximately one time in 10,000 or the 99.99th percentile) and the meteorology accompanying such a violation usually consists of stable air and low wind speeds. (These conditions may be conservative since they often do not coincide with peak aircraft activity (i.e., longest queues).) The receptor for this latter calculation was also relocated to reflect a characteristic location where public exposure might be expected.

6.4 MODELING CONSIDERATIONS

The FAA Simplex model (Segal, 1979) was used in this study. The more complex airport models were not employed because of their spatial and temporal averaging assumptions. The Simplex model employs a simple point source algorithm with provisions for selecting a particular plume height and initial plume dilution box size for each aircraft being analyzed. It employs the classical Gaussian point source equation and the Pasquill-Gifford curves from Turner (1968). For consistency, the same sampling times were used in all cases. A power law expression for the standard deviation of plume size

$$\sigma_z = K_z x^{0.9}, \sigma_y = K_y x^{0.9} \text{ was assumed,}$$

where K_y , K_z were chosen to match the P-G curves at $x = 1.0$ km.

This functional form was used in all calculations which encompassed stability classes B thru E. Such an approximation greatly facilitated calculations and differed negligibly from the P-G-T predictions even at the shortest distances used in this study.

6.5 RESULTS

The results are displayed in Figures 6.5 and 6.6. Figure 6.6 shows the comparison of estimated and measured concentrations during the variety of wind and stability conditions experienced over the entire monitoring period. The average ratio of estimated to measured concentrations for the ensemble of measurement events reduces substantially when finite values for plume height and initial plume size are used. The ratio of 1.7 for the latter condition is within the factor-of-two considered in determining an acceptable level of model performance.

Measurements performed during the longest queue were analyzed separately. The results of this analysis are shown in Figure 6.5. The horizontal bars represent the times during which each airplane occupied a particular queue position. The queue length at any time is determined by summing the number of horizontal bars crossed at any particular time. Between 1742 and 1801 hours on April 18 the queue length increased to eight airplanes. During this time period estimated concentrations were 3 ppm while measured (average) concentrations were 1.5 ppm. A second comparison was then made for the extended averaging time period (70 minutes). Under these conditions, the estimated concentration was 1.3 ppm and the measured concentration was 0.9 ppm. Both of these model test conditions fall within the factor-of-two criteria for determining model performance.

A final model calculation was performed to reflect worst case meteorological conditions for comparison to the NAAQS. Worst case conditions of "E" stability and one meter per second wind speed were assumed. The receptor was relocated 750 meters downwind from the end of the taxiway, a distance which is characteristic of where people might first experience aircraft emissions. The uppermost curve in Figure 6.5 is a plot of these conditions. When this curve

is averaged over the entire 70 minute period, an estimated concentration of 4 ppm results.

6.6 CONCLUSIONS

The model appears to reflect measured concentrations quite well under both the short averaging times of specific queue events and the longer averaging times associated with all types of airplane activity at the end of the taxiway.

It is interesting to note the ability of the model to track the pollution peaks and valleys during the period from 1742 to 1801. This capability is quite impressive considering the number of times the airplane changes its queue position. The time shift between the two curves is in the expected direction and is probably related to the time taken for the high velocity engine exhaust to slow down to ambient conditions prior to atmospheric transport and to the actual slowing down of the ambient wind field by a line of queuing aircraft. (This latter condition has been observed at Washington National Airport).

When the verified Simplex model is used to estimate concentrations at expected populated locations during the highest activity hour monitored, concentrations of only 4 ppm from aircraft alone result. This value is small when compared to the NAAQS limit value of 35 ppm.

This assessment indicates that a simple point source algorithm can successfully accomplish the "verification by parts" procedure suggested by Turner (1979). Parameterizations from this verified model may subsequently be incorporated into a number of more complex models if validation efforts at other airports confirm these results.

The results of this study should apply to other engine exhaust gases and should be particularly useful in defining the queuing concentrations of engine NO_x (NO_2 under a high ozone environment). This can be accomplished by merely changing the model inputs to reflect NO_x rather than CO emissions.



Fig. 6.1. Monitoring Site Locations

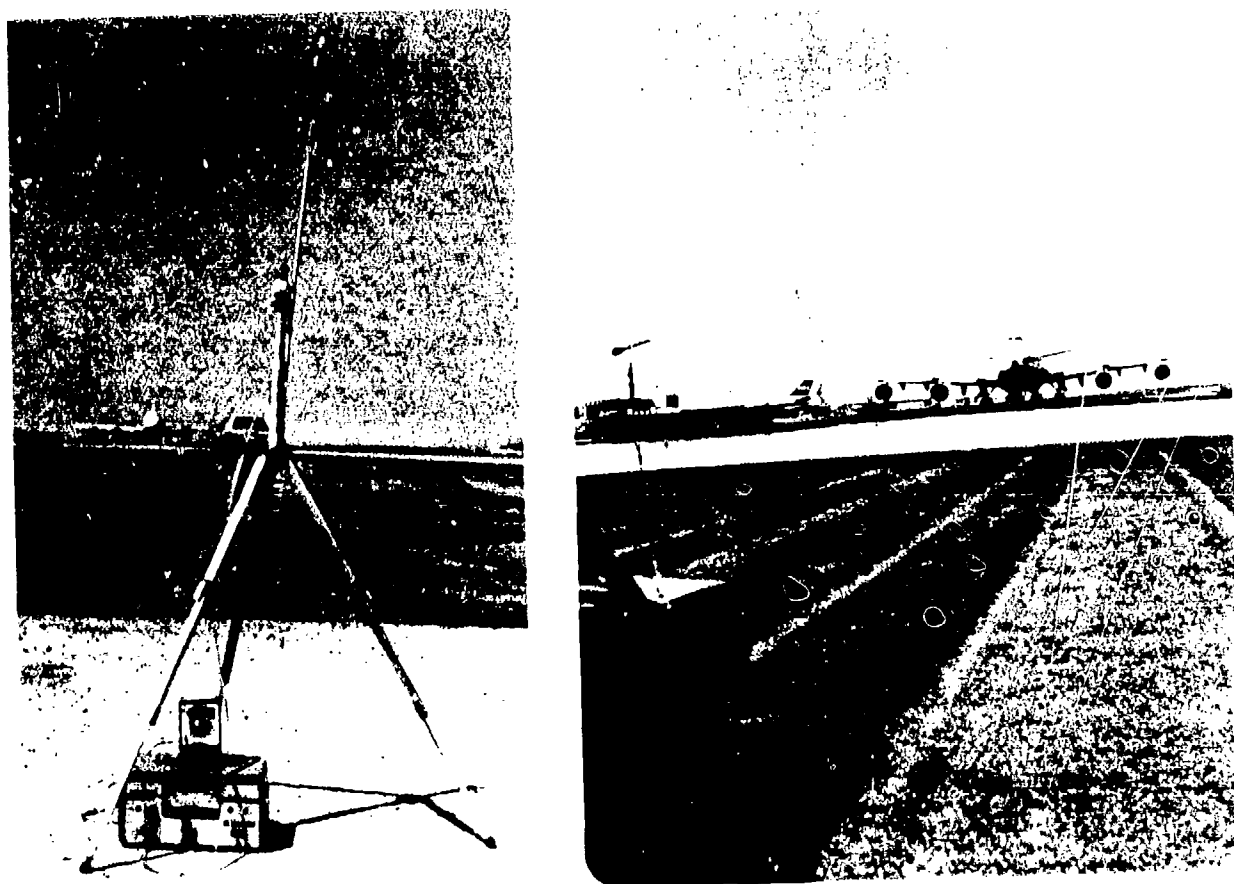


Fig. 6.2. Monitoring Equipment

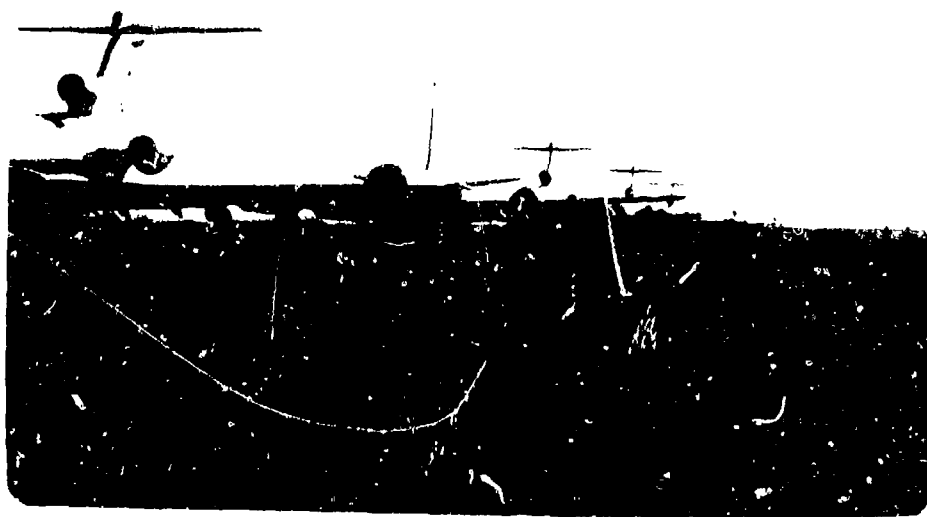


Fig. 6.3. Seven airplane Queue

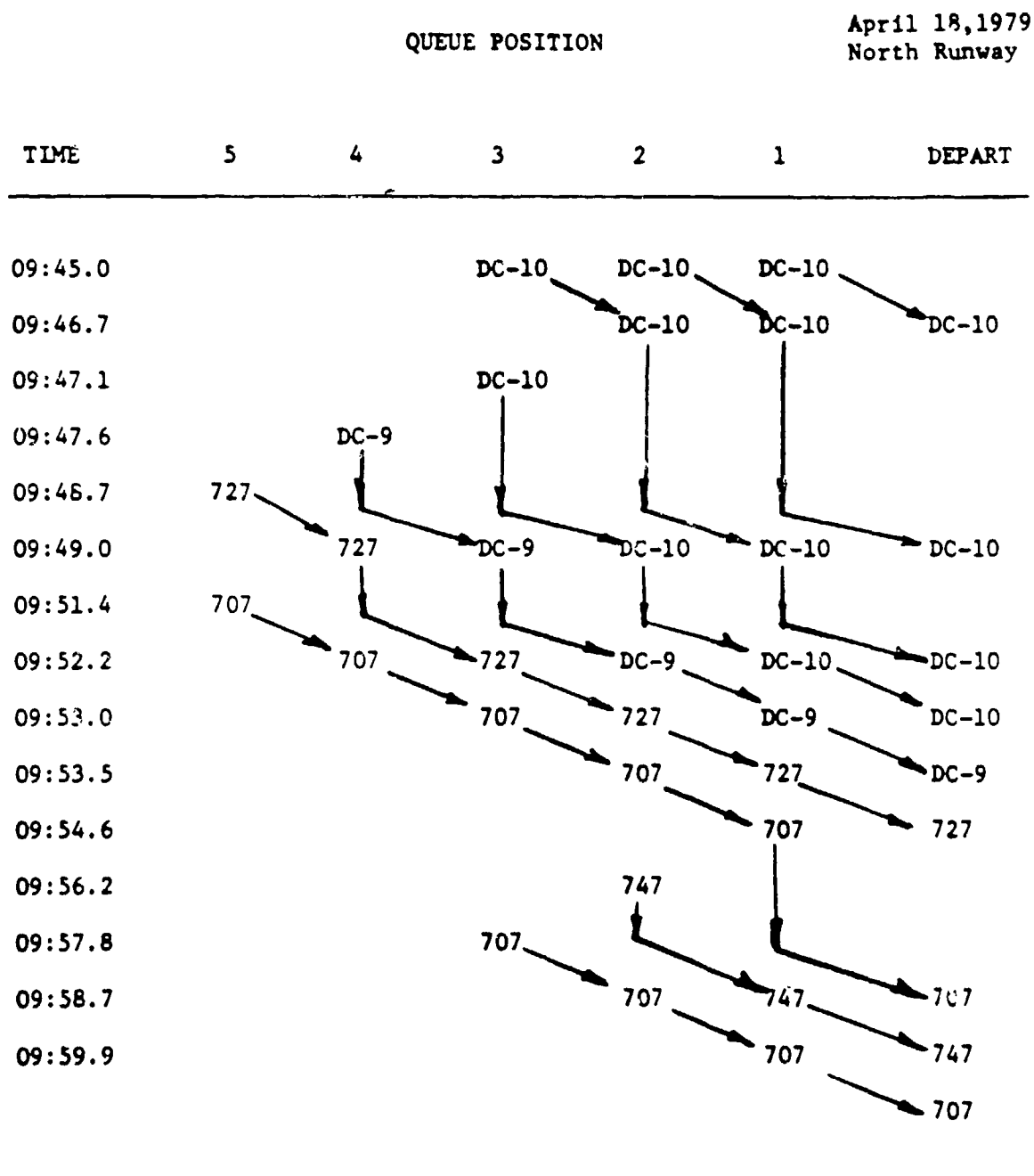


Fig. 6.4. Airplane Flow Diagram

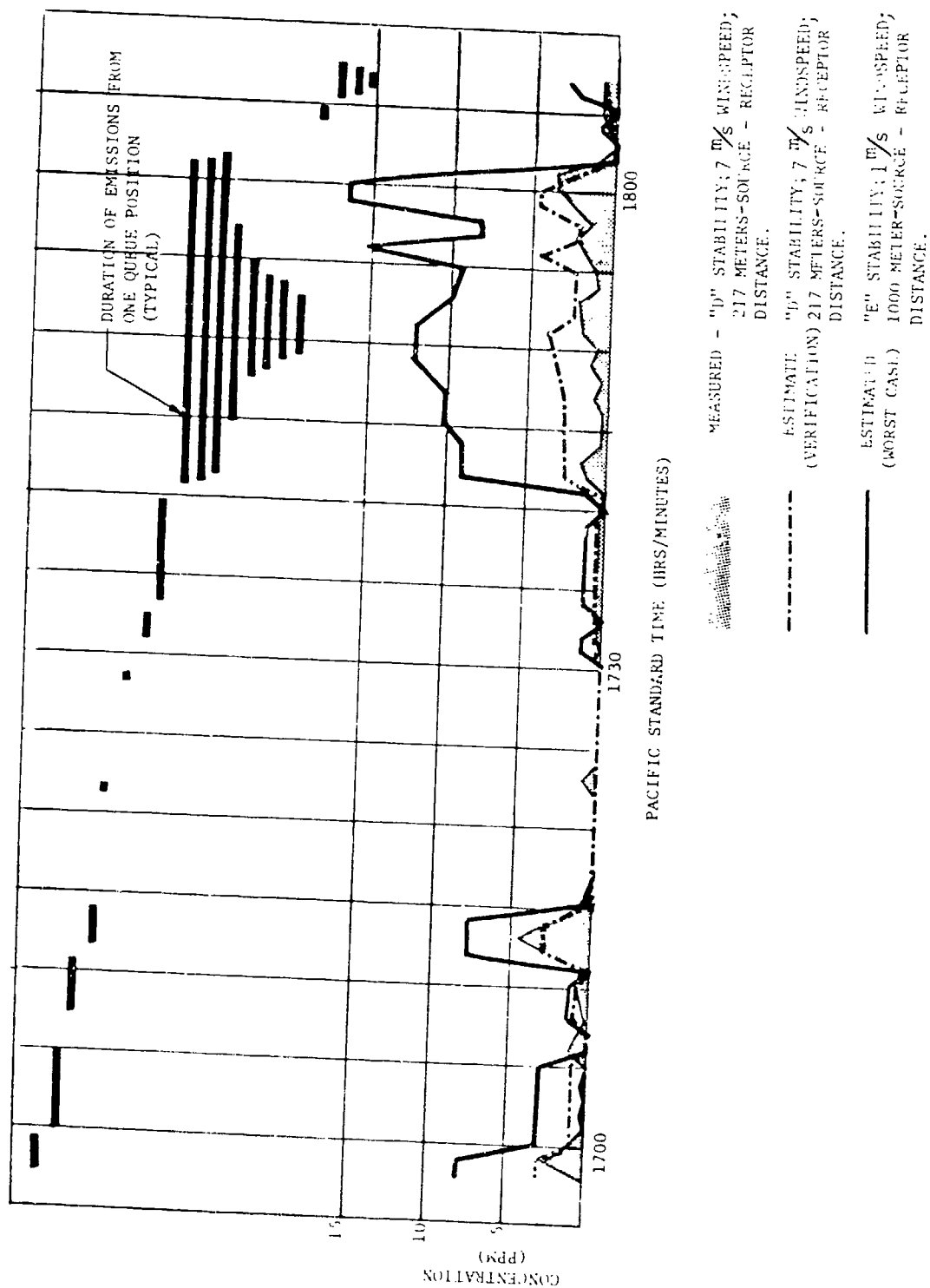


Fig. 6.5. Concentrations and Times in Queue (April 18, 1979)

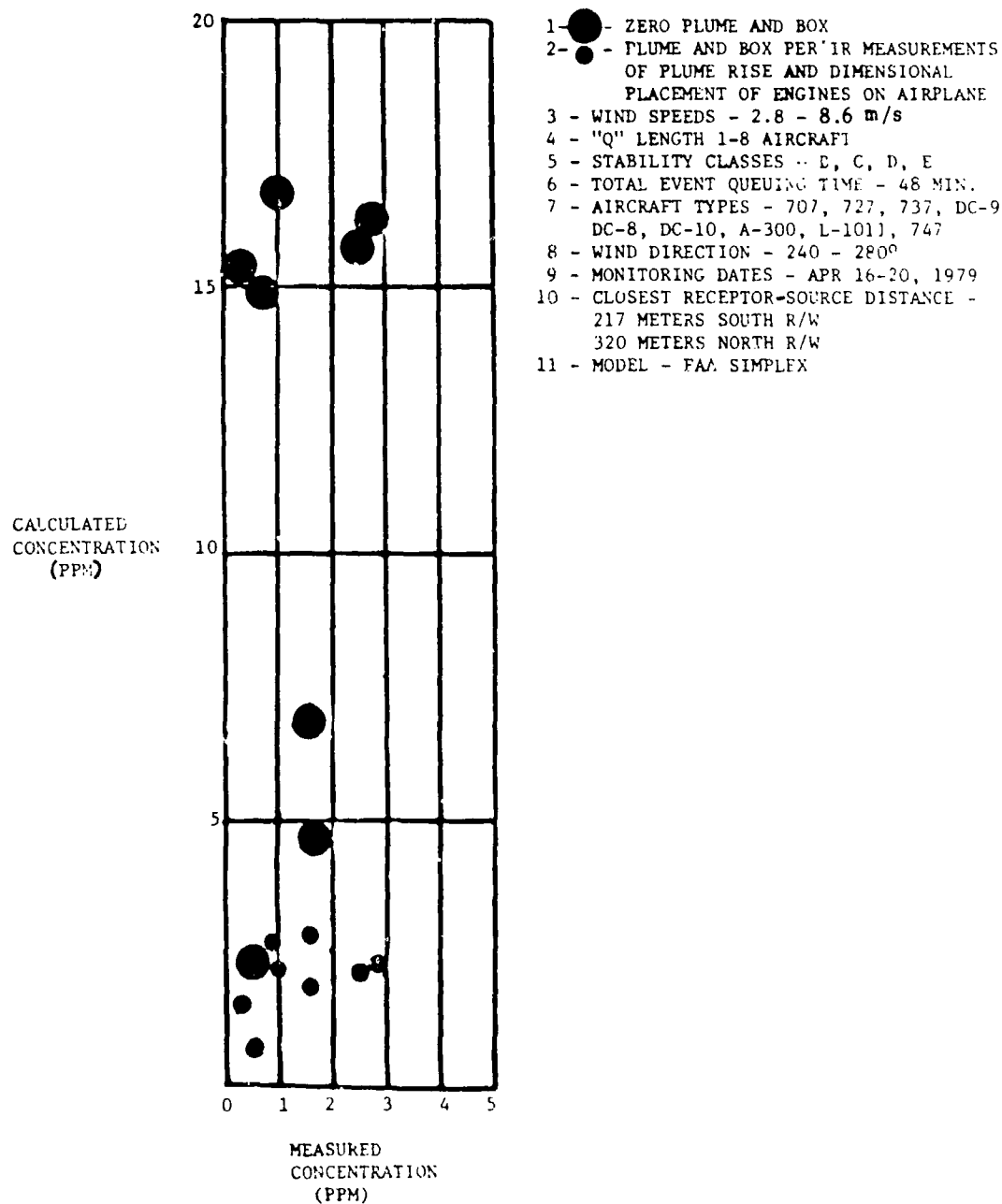


Fig. 6.6. Reconciliation of Measured with Estimated Carbon Monoxide Concentrations During Aircraft Queuing at Los Angeles International Airport (LAX)

7 ACCURACY DEFINITION OF THE AIR QUALITY ASSESSMENT MODEL (AQAM) AT WILLIAMS AIR FORCE BASE⁺

7.1 OBJECTIVES

The U.S. Air Force must have an analytical tool which can reliably predict the impact of their airbases on air quality. Such a tool is essential for assessing the significance of existing airbase emissions in relation to National Ambient Air Quality Standards (NAAQS) and for estimating the impact of proposed facilities and missions changes as is required by federal, state and local laws. The Air Quality Assessment Model (AQAM), developed by ANL for the Air Force is such a tool that meets these air quality impact assessment requirements. The AQAM model treats airbase emissions in sufficiently great detail and incorporates a state-of-the-art treatment of pollutant transport and diffusion. However, until now, a suitable data base has not been available for determining the accuracy limits of this mathematical computer-based model.

Ambient air quality measurements of CO, NO, NO_x, THC, and CH₄, and visibility were made at Williams AFB, near Phoenix from June 1976 to June 1977. The objectives were (1) to determine the effects of local aircraft operations on air quality and (2) to provide a data base for evaluation of AQAM. In this report model independent statistical analyses of the data and comparisons of AQAM predicted and observed concentrations are performed to determine the accuracy limits of AQAM.

7.2 APPROACH

The AQAM is designed to predict the impact of airbase operations, including aircraft, on the air quality in the vicinity of the airbase. It does not predict background concentrations as such. Hence, it is important from a model evaluation point of view that the influence of the local, modeled sources dominate the measured pollutant levels. Spatial and temporal dependences of these local sources must also be well described. These considera-

⁺From "Analyses for the Accuracy Definition of the Air Quality Assessment Model (AQAM) at Williams Air Force Base" by Yamartino, et al, 1980.

tions played a significant role in the selection of Williams AFB at the site meeting these requirements for this model validation effort. Williams AFB had a high volume aircraft operations and is relatively remote from an urban area.

Thirteen months of hourly average concentrations of CO, NMHC, and NO_x monitored at the five-station network, shown in Fig. 7.1, constitutes the data base used for assessing the predictive capabilities of AQAM. Parallel data bases of hour-by-hour meteorology and aircraft activity were utilized, in conjunction with the standard emissions inventory input to AQAM, to compute pollutant concentrations at the locations of interest. To define the incremental AQAM predictive power obtained through the use of higher time resolution aircraft data, AQAM predictions were made based on both the standard AQAM input of annual total aircraft operations (referred to as AQAM I predictions) and on the hour-by-hour aircraft operations mentioned above (referred to as AQAM II predictions).

7.3 IMPACT OF AIRCRAFT ON LOCAL AIR QUALITY

As seen in Table 7.1, pollutant levels at several receptors are found to depend in a significant way on aircraft emissions though the average concentration impacts are small relative to the National Ambient Air Quality Standards (NAAQS). In all cases AQAM overpredicts the percentage role of aircraft emissions but much of this is simply due to the background levels not accounted for in AQAM. The fact that AQAM overpredicts the absolute role of aircraft at most stations is thought to be related to the model's neglect of plume rise and plume turbulence enhanced dispersion: two mechanisms which act to reduce concentrations nearby the aircraft. The largest observed average daytime impact of aircraft occurs at station 4 where, on the average, aircraft account for 36% of the CO, 28% of the NMHC and 24% of the NO_x.

Both AQAM predictions and measurements agree that station 4, atypical in the sense of its close proximity to buildings, trees, and automobiles, sees the highest concentrations: a factor of 2-3 higher than station 1, 2, 3, and 5 collectively in the cumulative frequency distribution (CFD) sense. The failure of the AQAM to correctly reproduce the observed rank ordering among stations 1, 2, 3, and 5 is also thought to be due to dynamical factors such as the neglect of aircraft plume rise (which clearly leads to overprediction of

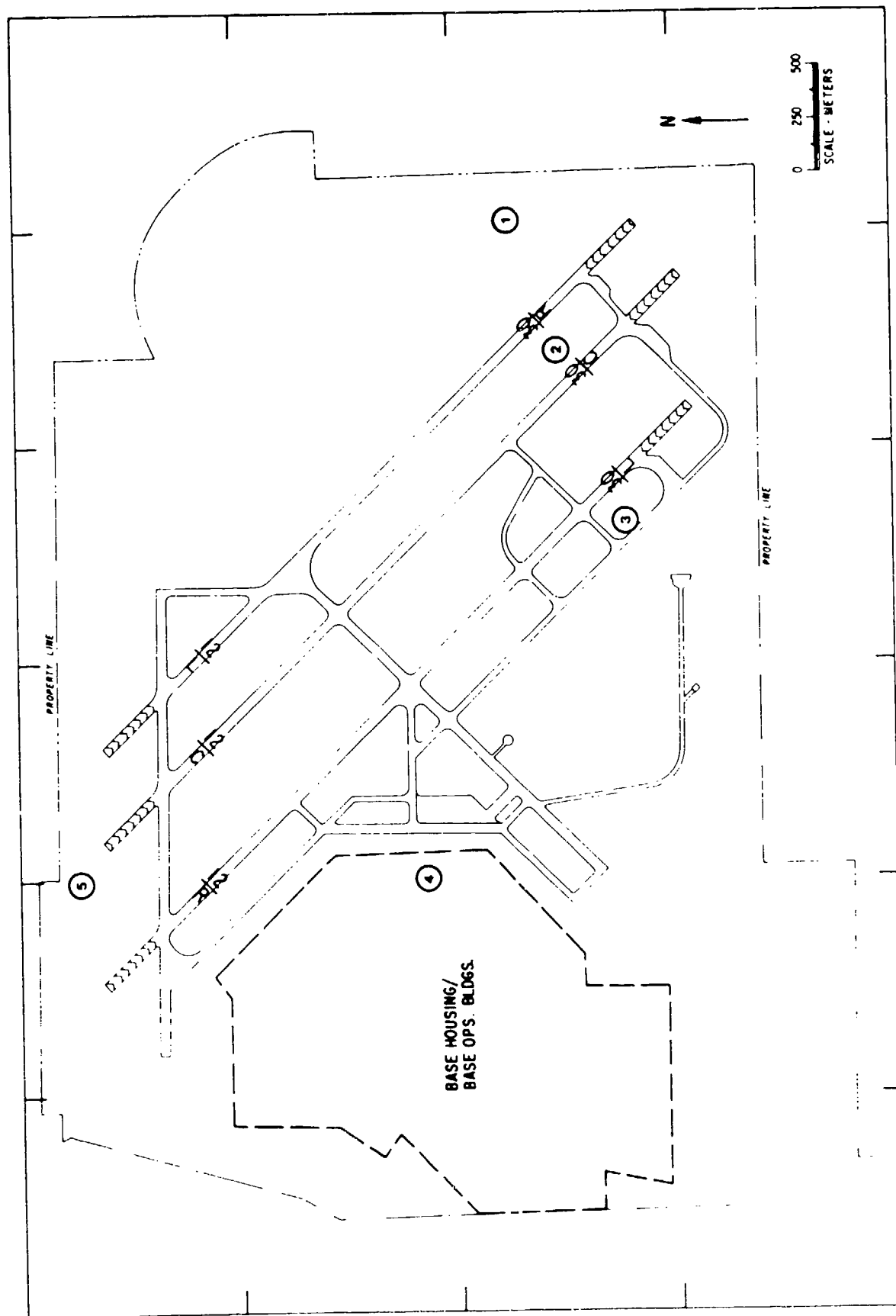


Fig. 7.1. Locations of the Five Ambient Air Quality Monitoring Trailers

Table 7.1. Williams AFB Aircraft Emissions Impact on Annual Average Hourly 6AM-6PM Concentrations

	Total Concentration (ppm)	Concentration Without Aircraft* (ppm)	Aircraft Contribution (ppm)	Percent Aircraft Contribution
<u>CO</u>				
Station 1				
Observed	0.114	0.105	0.009	8
AQAM II	0.071	0.040	0.031	44
Station 2				
Observed	0.134	0.119	0.015	11
AQAM II	0.106	0.039	0.067	63
Station 3				
Observed	0.108	0.093	0.015	14
AQAM II	0.195	0.064	0.131	67
Station 4				
Observed	0.362	0.230	0.132	36
AQAM II	0.345	0.168	0.177	51
Station 5				
Observed	0.156	0.136	0.020	13
AQAM II	0.099	0.046	0.053	54
<u>NMHC</u>				
Station 2				
Observed	0.123	0.128	-0.005	consistent with zero
AQAM II	0.039	0.019	0.020	51
Station 4				
Observed	0.215	0.155	0.060	28
AQAM II	0.209	0.071	0.138	66
<u>NO_x</u> (concentrations in ppb)				
Station 2				
Observed	9.44	8.98	0.46	5
AQAM II	3.68	2.15	1.53	42
Station 4				
Observed	15.1	11.5	3.6	24
AQAM II	8.4	6.6	1.8	41

*Based on regression of pollutant vs AQAM II estimated aircraft emissions on ground level line sources.

CO and NMHC at station 3). Finally, using the computed CFDs for off-base populated areas and allowing for possible underprediction by a factor of 2-3, one concludes that, with the exception of the 6-9 AM National ambient guideline concentration for reactive hydrocarbons, the airbase impact is negligible relative to existing NAAQS.

No significant difference in predictive power between the AQAM I and AQAM II has been found, thus extremely detailed time histories of aircraft operations do not have a significant effect on the model's accuracy (predictive power) and the standard AQAM input of an average diurnal distribution of aircraft operations appears adequate.

7.4 PERFORMANCE OF THE MODEL

In the CFD sense, the AQAM predictions for the upper percentile concentration range agree reasonably well in magnitude and slope with the observed concentration distributions (sample case seen in Fig. 7.2), suggesting that the model simulation encompasses a range of emission and dispersion conditions comparable with reality. At the lower concentration percentile levels, the CFDs are often orders-of-magnitude different, reflecting the problem of absence of background levels in the AQAM computations. CFD estimates of the 99.99 percentile concentrations (i.e., highest hourly average concentration per year) of ≈ 3 ppm CO, 1-3 ppm NMHC, and 0.1-0.3 ppm NO_x agree surprisingly well with observed values of 2-4 ppm CO, 1-3 ppm NMHC, and 0.08-0.15 ppm NO_x if stations 1, 2, 3, and 5 are considered collectively; however, such estimates for any single station may underpredict the once per year high by as much as a factor of 1.7 for CO and NMHC and 3 for NO_x . The fact that the CFDs of observed concentrations at the different stations converge at the upper percentiles while the individual station curves diverge slightly for the AQAM predictions, suggests that the most severe pollution episodes actually exist over a spatial domain much larger than the airbase and thus are probably not solely due to specific local sources such as aircraft, as suggested by the model.

In examining the performance of AQAM on an hour-by-hour basis one encounters shortcomings common to Gaussian plume models in general. If no accounting of background pollutant levels is made, hour-by-hour comparisons of AQAM with observations indicate severe underprediction for all three

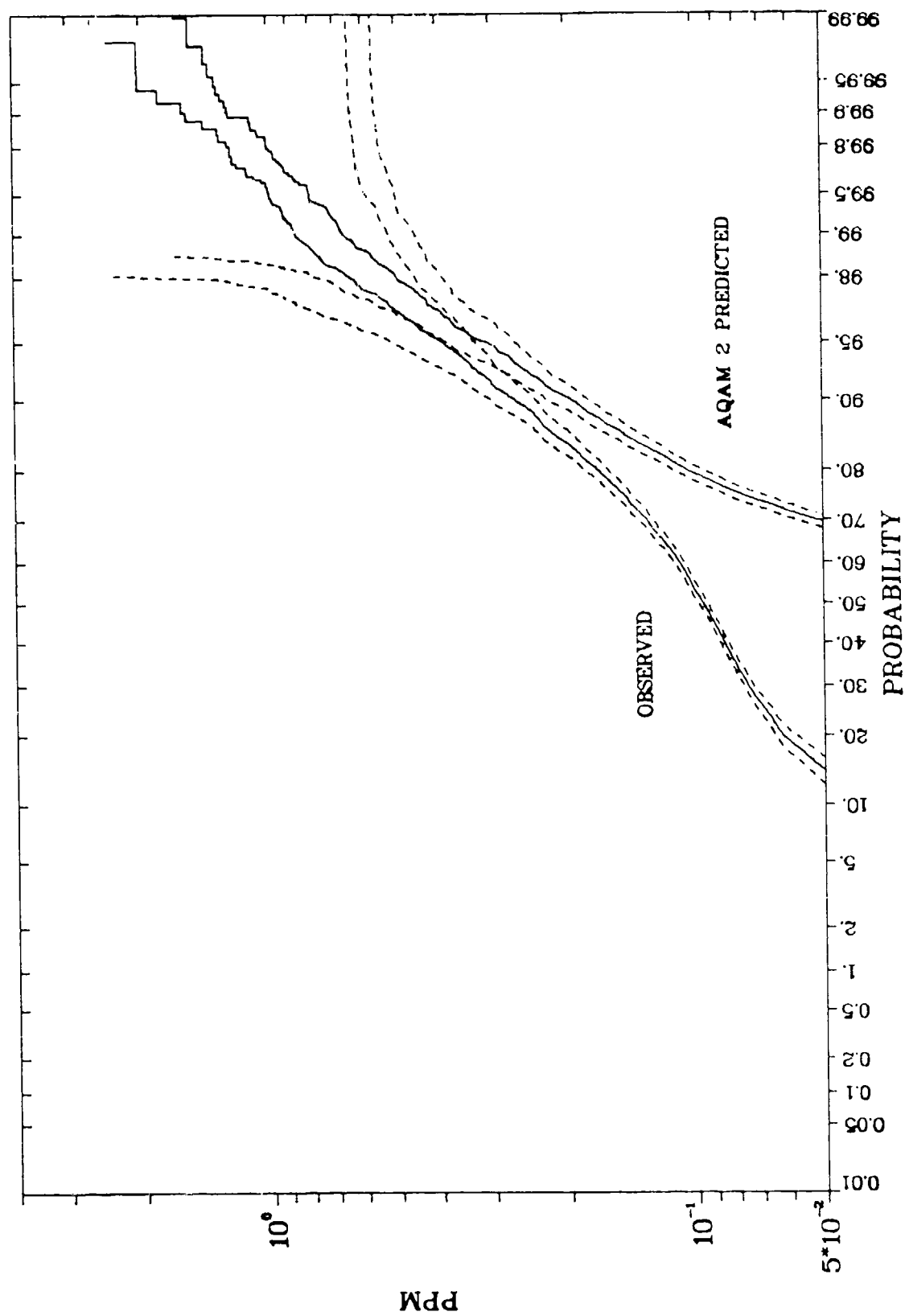


Fig. 7.2. Cumulative Frequency Distribution for Observed and AQAM II Predicted CO at Station 1 -- 95% Confidence Bounds are Indicated

pollutants (a mean factor of 3 for CO and NMHC and a factor of 5 for NO_x). In addition, the standard deviations of these distributions indicate that the unadjusted model falls short of the "50-percent within a factor-of-two" criteria for Gaussian models. However, addition of a modest annual mean background (0.09 ppm for CO, 0.08 ppm for NMHC, and 7 ppb for NO_x) leads to a dramatic improvement in predictive power. The background adjusted model yields predictions with a factor-of-two of observation in excess of 65% of the time, while errors in excess of factor-of-ten occur at a tolerable $\approx 1\%$ level. The reason such order of magnitude discrepancies exist lies with the fundamental limitations of modeling a stochastic process with a deterministic model.

7.5 DIFFICULTIES WITH THE THEORY VERSUS OBSERVATION COMPARISON

At the time the experiment was being planned (circa 1975), Williams Air had the highest level of aircraft operations of any airbase in the U.S., and, as Williams is a training base, it was expected that records of aircraft activity would be more accurately maintained than at other bases. While accurate records were available during normal training operations periods, documentation of off-hours activity (e.g. weekends) was incomplete. In addition, as most of the operations involved small twin-engine aircraft (i.e. T37, T38, and F5), selection of the airbase having the highest traffic count was not necessarily compatible with a choice based on highest aircraft pollutant emissions.

It was also thought that the remoteness of the base from other significant sources would render the resolution of airbase and aircraft generated pollution from background levels straightforward. Unfortunately, Phoenix, though some 50 km to the Northwest, contributed high background levels to the measured air quality particularly at night. These so-called background levels often exceeded the local pollutant levels, resulting in a poor signal-to-noise ratio and greatly reducing the effectiveness of the receptor network in sensing local source (i.e., airbase) created pollutant gradients. In addition, the entire Valley of the Sun appears at times to exhibit pollution reservoir characteristics which can not be predicted by a short-range Gaussian plume model such as AQAM. Even the several hour transport and dispersion of pollutant from Phoenix, though included in the AQAM inventory of environ sources, is not adequately treated due to total reliance on the

stationary state assumption. Such multihour transport could have been more realistically modeled using a backward trajectory technique, which would select the emission rate for the time period presently impacting the receptors and allow for varying dispersion rates over the trajectory of the plume, but such is not the case in the present AQAM, designed for short-range pollutant transport and dispersion calculations. Thus, it was necessary to attempt to validate the model under conditions where a major portion of the aerometric signal was related to distant, background sources not adequately treated by the model. The presence of five monitors on the base could have been useful in subtracting out these unwanted and poorly described components of the observed concentrations. However, two factors limited the effectiveness of this latter approach to investigating the local (i.e., airbase) contribution to the observed pollutant levels. First, noise in the form of spatial inhomogeneities of the background and, second, inter-instrument random and systematic errors which tended to wash out many of the more subtle effects since local signal components were often small compared to the accuracy limits of the instruments.

All of the studies of model predictive power versus meteorological parameters or time of day suggest that time of day is the most significant variable affecting AQAM performance in that AQAM reproduces the major trends in daytime observed concentrations when local sources dominate but seriously underpredicts at night when more distant sources contribute. This deficiency is probably due to an underestimate of vehicle activity between midnight and 5 a.m. and to a breakdown of the steady-state Gaussian plume assumption used in the model. Major revision of the model to incorporate backward trajectories would probably be required to rectify this latter problem; however, such a revision is perhaps of only academic interest at present since the AQAM is most successful in simulating the potential "worst case" airbase impact situations associated with morning, low wind speed, stable or low inversion height conditions coincident with the commencement of high airbase emissions.

7.6 CONCLUSIONS

In final summary, we note the major findings of this study as

- the upper concentration-percentile range of the CFD of AQAM predictions agrees well enough with observation to make this a valuable tool for predicting rare worst case situations. As at William AFB, the estimate of worst case (e.g., highest hourly per annum) concentrations at a particular station may be underpredicted by a factor of two or three so that complementary monitoring (for perhaps a few hundred hours) should be performed in questionable situations when concentrations approach 50% of NAAQS.
- the AQAM, adjusted for background levels, provides a predictive tool for hourly average concentrations commensurate in ability (i.e., greater than 50% of predictions within a factor of two of observed concentrations) with well calibrated Gaussian plume models applied to urban areas.
- Without adjustment for background levels, most AQAM results underpredict by more than a factor of two and often by as much as 10 to 100. Without background compensation, AQAM results should be interpreted with caution. Air quality monitoring data sampled in the Air Quality Control Region should be considered when analyzing AQAM results.
- The present AQAM, unadjusted for jet plume rise or other jet plume dynamical factors, tends to overpredict the near field air quality impact of aircraft. Studies at commercial airports suggest that this overprediction becomes negligible beyond a few hundred meters from the aircraft.
- The highest predicted, average hourly aircraft impact of 0.18 ppm CO (51% of total CO) at station 4 only slightly overpredicts the observed impact of 0.13 ppm CO (36% of total CO). [Special instances do exist, however, where aircraft contribute nearly 100% of observed and predicted concentrations.]

- The ability of the AQAM to accurately predict inter-station concentration differences is only weakly confirmed because of large measurement errors relative to these observed concentration differences and because of the unexpectedly high background concentrations.
- The AQAM could benefit from minor revisions such as the incorporation of jet plume rise and turbulence enhanced dispersion and from major revisions such as a backward trajectory calculation for more realistic assessment of the impact from distant sources.
- AQAM is ready for acceptance under EPA Guidelines on Air Quality Modeling.

8 REFERENCES

- Abramovich, G.N., 1963. *The Theory of Turbulent Jets*. Cambridge, MA, MIT Press.
- Arey, F.K., R.W. Murdoch, and F. Smith, 1979, *Audit of the Washington, D.C. National Airport Air Monitoring Sites*. Research Triangle Institute Report 43U/1487/92-01F.
- Bastress, E., R. Baker, C. Robertson, R. Siegel, and G. Smith, 1971. *Assessment of Aircraft Emission Control Technology*. Northern Research and Engineering Corp. Report 1168-1.
- Breuer, W., 1965. *Die Aussagekraft kontinuierlicher Immissionsmessungen*. IWL. Institut fuer Gewerbliche Wasserwirtschaft und Luftreinhaltung E. V. Forum 65, Band 3.
- Briggs, G.A., 1969. *Plume Rise*. USAEC, TID-25075, Springfield, Virginia.
- Cirillo, R.R., J.F. Tschanz, and J.E. Camaioni, 1975. *An Evaluation of Strategies for Airport Air Pollution Control*. Argonne National Laboratory, Argonne, IL, Report No. ANL/ES-45.
- Coordinating Research Council, 1960. *Report of the Program Study Group on Aircraft Exhaust*. CRC Inc.
- Daley, P. and D. Naugle, 1978. *Measurement and Analysis of Airport Emissions*. Proceedings, Air Quality and Aviation: An International Conference, Federal Aviation Administration Report No. FAA-EE-78-26 pp. 2-9. Also published in J. Air Pollution Control Assoc., 29, pp. 113-116, February 1979.
- Duewer, W.H. and J.J. Walton, 1978. *Potential Effects of Commercial Aviation on Region-wide Air Quality in the San Francisco Bay Area*. Proceedings, Air Quality and Aviation: An International Conference, Federal Aviation Administration, Report No. FAA-EE-78-26, pp. 88-101.
- Egan, B.A. et al., 1975. *The ESEERCO Model for the Prediction of Plume Rise and Dispersion from Gas Turbine Engines*. Air Pollution Control Association 68th Annual Meeting Session 49.
- EPA, 1972. *Aircraft Emissions: Impact on Air Quality and Feasibility of Control*. U.S. Environmental Protection Agency, Office of Air Quality Planning and Standards, Research Triangle Park, NC.
- EPA, 1980. *Washington National Airport Air Quality Study*. Source Receptor Analysis Branch, MDAD, OAQPS Report.
- Federal Register*, June 19, 1978, Part V, Environmental Protection Agency, 1977 Clean Air Act; Prevention of Significant Air Quality Deterioration.
- Federal Register*, March 24, 1978, Part III, Environmental Protection Agency, Control of Air Pollution from Aircraft and Aircraft Engines, Proposed Amendments to Standards.
- George, R. and R. Burlin, 1960. *Air Pollution from Commercial Jet Aircraft*. L.A. County Air Pollution Control District, Los Angeles, CA.

Goldberg, P., 1978. Pratt and Whitney Aircraft, E. Hartford, Connecticut, personal communication.

Greenberg, C., 1978. *Air Quality in the Vicinity of Airports*. Proceedings, Air Quality and Aviation: An International Conference, Federal Aviation Administration Report No. FAA-EE-78-26, pp 20-26.

Hallanger, N.L., 1974. *Meteorological Factors in Air Quality Evaluation; Environmental Impact Study Los Angeles International Airport, Alheda, California: Meteorological Research, Inc.*

Heywood, J.B., J. A. Fay, and L. H. Linden, 1971. *Jet Aircraft Air Pollutant Production and Dispersion*. AIAA Jour. 9 .

Hogstrom, U., 1975. *Confirming the Local Sources of Observed Air Pollution in Communities*. Atmospheric Environment 9, 923-929.

Hoult, D.P., J. A. Fay, and L. J. Forney, 1979. *A Theory of Plume Rise Compared with Field Observations*, J. Air Pollution Control Association 19:585-590.

Hoult, D.P., et al., 1975. *Turbulent Plume in a Turbulent Cross Flow; Comparison of Wind Tunnel Tests with Field Observations*, Air Pollution Control Association 68th Annual Meeting Session 49.

Jordan, B.C., 1977a. *An Assessment of the Potential Air Quality Impact of General Aviation Aircraft Emissions*. U.S. Environmental Protection Agency, Office of Air Quality Planning and Standards, Research Triangle Park, NC (June 27, 1977).

Jordan, B.C., 1977b. *Potential Impact of NO_x Emissions from Commercial Aircraft on NO₂ Air Quality*. U.S. Environmental Protection Agency, Office of Air Quality Planning and Standards, Research Triangle Park, NC (Nov. 15, 1977).

Jordan, B.C. and A.J. Broderick, 1978. *Emissions of Oxides of Nitrogen from Aircraft*. Proceedings, Air Quality and Aviation: An International Conference, Federal Aviation Administration, Report No. FAA-EE-78-26, pp. 10-19. Also published in J. Air Pollution Control Assoc., 29, pp. 119-124 February 1979.

Junge, Christian, 1963. *Air Chemistry and Radioactivity*. Academic Press, 382 pp.

LAAPCD, 1971. *Study of Jet Aircraft Emissions and Air Quality in the Vicinity of Los Angeles International Airport*. Air Pollution Control District, County of Los Angeles, Calif. NTIS-PB-193-699.

Lawson, C.L. and R. J. Hanson, 1974. *Solving Least Squares Problems*, Englewood Cliffs, New Jersey, Prentice-Hall, Inc.

Lemke, E., N. Shaffer, and J. Verssen, 1965. *Air Pollution from Jet Aircraft in Los Angeles County*. L.A. Air Pollution Control District, Los Angeles, CA.

Lloyd, A.C., F.W. Lurmann, D.G. Godden, J.F. Hutchins, A.Q. Eschenroeder, and R.A. Nordsieck, 1979. *Development of the ELSTAR Photochemical Air Quality Simulation Model and Its Evaluation Relative to the LARPP Data Base*. ERT Westlake Village, CA, Document No. P-5287.

- Lorang, P., 1978. *Review of Past Studies Addressing the Potential Impact of CO, HC, and NO_x Emissions from Commercial Aircraft on Air Quality*. U.S. Environmental Protection Agency, Standards Development and Support Branch, Document No. AC-78-03.
- Morton, B.R., G.T. Taylor, and J. S. Turner, 1956. *Turbulent Gravitational Convection from Maintained and Instantaneous Sources*, Proc. Roy Soc. A., 234:1-23.
- Single, D., B. Grems, and P. Daley, 1978. *Air Quality Impact of Aircraft at Ten U.S. Air Force Bases*. J. Air Pollution Control Assoc., 28, pp 370-373.
- Norco, J.E., R.R. Cirillo, T.E. Baldwin, and J.W. Gudenas, 1973. *An Air Pollution Impact Methodology for Airports and Attendant Land Use - Phase I*. Argonne National Laboratory, Argonne, IL, Report No. APTD-1470.
- Oliver, R.C., E. Bauer, H. Hidalgo, K.A. Gardner, and W. Wasyliwskyj, 1977. *Aircraft Emissions: Potential Effects on Ozone and Climate - A Review and Progress Report*. U.S. Department of Transportation, Federal Aviation Administration, Report No. FAA-EQ-77-3.
- Pace, R.G., 1977. Technical Support Report -- *Aircraft Emissions Factors*, U.S. EPA Report.
- Patrick, H.A., 1967. *Experimental Investigation of the Mixing and Penetration of a Round Turbulent Jet Injected Perpendicularly into a Traverse Stream*, Trans. Inst. Chem. Eng. 45:16-31.
- Platt, M., R. Baker, E. Bastress, K. Chng, and R. Siegel, 1971. *The Potential Impact of Aircraft Emissions on Air Quality*. Northern Research and Engineering Corp. Report 1167-1.
- Pratt and Whitney, 1972. *Collection and Assessment of Aircraft Emissions Baseline Data - Turbine Engines*. Pratt and Whitney Aircraft Group, East Hartford, CT, Report No. P&WA 4339.
- Rote, D., I. Wang, L. Wangen, R. Hecht, R. Cirillo, and J. Pratapas, 1973. *Airport Vicinity Air Pollution Study*. Report No. FAA-RD-73-113.
- Rote, D.M. and L. E. Wangen, 1975. *A Generalized Air Quality Assessment Model for Air Force Operations*, Technical Report AFWL-TR-74-304.
- Schewe, G., L. Budney, and B. Jordan, 1978. *CO Impact of General Aviation Aircraft*. Proceedings, Air Quality and Aviation: An International Conference, Federal Aviation Administration Report No. FAA-EE-78-26, pp 147-152.
- Segal, H.M., 1977. *Monitoring Concorde Emissions*. J. of Air Pollution Control Assoc. 27(7)623.
- Segal, H.M., 1980. *Emissions from Queuing Aircraft*. Air Pollution Control Association 73rd Annual Meeting, Paper 80-3.5.

Segal, H.M., 1978. *Pollution Dispersion Measurements at High Activity Fly-In of General Aviation, Military, and Antique Aircraft*. Proceedings, Air Quality Aviation: An International Conference, Federal Aviation Administration Report No. FAA-EE-78-26, pp 76-80.

Segal, H.M., 1979. *Simplified Modeling and Measurement of Air Quality*. Air Pollution Control Association 72nd Annual Meeting, Paper 79-37.5.

Slawson, P.R., and G.T. Csanady, 1967. *On the Mean Path of Buoyant, Bent-Over Chimney Plumes*, J. Fluid Mech. 23:311-322.

Smith, D.G., R.J. Yamartino, C. Benkley, R. Isaacs, J. Lee, and D. Chang, 1977. *Concorde Air Quality Monitoring and Analysis Program at Dulles International Airport*. U.S. DOT Report No. FAA-AEQ-77-14.

Smith, D. and D. Heinold, 1980. *Logan Airport Air Quality Study*, ERT Final Project Report A-218.

Springer, K. and T. Baines, 1977. *Emissions from Diesel Versions of Production Passenger Cars*. SAE Paper 770818.

Tank, W.G., and B.K. Hodder, 1978. *Engine Exhaust Plume Growth in the Airport Environment*, Proc. International Conference on Air Quality and Aviation, Reston, Va. FAA Report FAA-EE-78-26 pp 153-164.

Thayer, S.D., Pelton, D.J., Stadskleve, G.H., and Weaver, B.D., 1974. *Model Verification - Aircraft Emissions Impact on Air Quality*, Geomet, Inc. EPA-650/4-79-049.

Turner, D.B., 1964. *A Diffusion Model for an Urban Area*. J. Appl. Meteorol., 3, pp 83-91.

Turner, D.B., 1970. *Workbook of Atmospheric Dispersion Estimates*, U.S. Dept. of Health, Education, and Welfare, Public Health Service Publication No. 999-AP-26.

Turner, D.B., 1979. *Atmospheric Dispersion Modeling: A Critical Review*. J. Air Pollution Control Assoc., 29, pp 502-519.

U.S. Congress, 1963. *Clean Air Act*. Public Law 88-206.

U.S. Congress, 1967. *Air Quality Act*. Public Law 90-148, Section 211b.

U.S. Congress, 1970. *Clean Air Amendments of 1970*. Public Law 91-604.

U.S. DHEW, 1968. *Nature and Control of Aircraft Engine Exhaust Emissions*. HEW report to U.S. Congress, Doc. No 91-9, also NTIS-PB187-771, 388 pp.

Wang I. and D. Rote, 1975. *A Finite Line Source Dispersion Model for Mobile Source Air Pollution*. J. Air Pollution Control Assoc., 25, pp 730-733.

Wangen, L. and L. Conley, 1975. *Air Quality Assessment Model Applied to Washington National Airport*. U.S. AFWL Report under Contract AFWL-75-PO-071.

Whitten, G.Z. and H. Hogo, 1976. *Introductory Study of the Chemical Behavior of Jet Emissions in Photochemical Smog - Final Report*. Systems Applications, Inc., San Rafael, CA, Contract No. NAS2-8821.

Yamartino, R.J., 1977. *A Source Finding Algorithm: A Novel Approach for Relating Air Quality Data to Dispersion Models*. Eighth International Technical Meeting on Air Pollution Modeling and its Application, Louvain-La-Neuve, Belgium.

Yamartino, R.J., and D.J. Lamich, 1979a. *The Formulation and Application of a Source Finding Algorithm*. Proc. Fourth Symposium on Turbulence, Diffusion and Air Pollution, Reno, Nevada, pp. 84-88.

Yamartino, R.J. J. Lee, S. Bremer, D. Smith, and J. Calman, 1979b. *Analysis of Plume Rise from Jet Aircraft*. Proc. Fourth Symposium on Turbulence, Diffusion, and Air Pollution, Reno, Nevada, pp 630-635.

Yamartino, R., L. Conley, D. Rote, D. Lamich, E. Dunphy, K. Zeller, D. Naugle, 1980. *Analyses for the Accuracy Definition of the Air Quality Assessment Model (AQAM) at Williams Air Force Base*. AFESC Report, in press.

Yamartino, R.J. and D.M. Rote, 1978. *Updated Model Assessment of Pollution at Major U.S. Airports*. Proceedings, Air Quality and Aviation: An International Conference, Federal Aviation Administration, Report No. FAA-EE-78-26, pp. 170-176. Published in shorted form in J. Air Pollution Control Assoc., 29, pp 128-132, February 1979.